

Original Article

Morphology matters: congruence of morphology and phylogeny in the integrative taxonomy of Clevelandellidae (Ciliophora: Armophorea) with description of six new species

Michael Kotyk^{1,*}, William A. Bourland¹, Matyáš Soviš¹, Daniel Méndez-Sánchez¹, Pavel Škaloud², Zuzana Kotyková Varadínová^{1,3} and Ivan Čepička¹

¹Department of Zoology, Faculty of Science, Charles University, Viničná 7, Prague, 12800, Czech Republic

²Department of Botany, Faculty of Science, Charles University, Benátská 2, Prague, 12800, Czech Republic

³Department of Zoology, National Museum of the Czech Republic, Václavské náměstí 68, Prague, 11579, Czech Republic

*Corresponding author. Department of Zoology, Faculty of Science, Charles University, Viničná 7, Prague, 12800, Czech Republic. E-mail: m.kotyk@seznam.cz

ABSTRACT

Armophorid ciliates of family Clevelandellidae represent ecologically interesting symbionts of ecologically interesting hosts: wood-eating cockroaches of subfamily Panesthiinae unrelated to the termite/*Cryptocercus* lineage. Moreover, these protists exhibit a peculiar morphology, with the posteriorization of oral structures being the most striking of their unique characters. Despite that, the family is relatively understudied, with only a handful of morphologically novel species being described since its erection more than 80 years ago. Recently, however, several clevelandellid species were described solely on the basis of molecular characters and it has been suggested that morphology should be abandoned in favour of purely molecular taxonomy. In our study we report on the diversity of Clevelandellidae from the widest host spectrum assessed so far, characterize a majority of previously described Clevelandellidae species, and describe six new *Clevelandella* species. By applying an integrative taxonomical approach, using molecular and modern morphological methods, we demonstrate the pitfalls of a purely molecular approach and show that morphology still has its place in the taxonomy of Clevelandellidae. Moreover, thanks to a combination of observations of *in vivo* cells, protargol preparations, and scanning electron microscopy (used for the first time in Clevelandellidae), we were able to clarify morphological uncertainties of previous works and discuss various morphological peculiarities of Clevelandellidae.

Keywords: biogeography; Clevelandellida; cockroach; host specificity; Panesthiinae; scanning electron microscopy; symbiont; 18S rRNA gene

INTRODUCTION

Blattodea (cockroaches and termites) are a morphologically and ecologically diverse lineage of insects with significant economic impact. Several globally distributed cockroach species are infamous synanthropic pests and sources of allergens (Cochran 1999). Termites, on the other hand, are the major structural and agricultural pests in tropical and subtropical areas and are also of great ecological importance (Govorushko 2019). Most termite species feed on wood and, since they are unable to completely digest wood particles by themselves, the ancestors of termites and wood-eating Cryptocercidae cockroaches entered into symbioses with various organisms more than 130 million years ago (Evangelista *et al.* 2019). These partners, either alone or as part

of a microbial consortia, are able to degrade cellulose and other compounds of wood, making themselves indispensable for their hosts (Brune 2014, Chouvenec *et al.* 2021). Cryptocercidae, and the so-called lower termites, host in their hindgut endosymbiotic flagellates belonging to Parabasalia and Preaxostyla. These protists are excellent and well-studied examples of coevolution with their hosts and are notable for having evolved into huge and morphologically bizarre forms (Noda *et al.* 2007, Čepička *et al.* 2010, Taerum *et al.* 2018). Additionally, an independent evolution of wood-eating occurred in the distantly related cockroach subfamily Panesthiinae (Blaberoidea: Blaberidae) (Bell *et al.* 2007, Djernæs *et al.* 2020). Similar to the lower termites and cryptocercids, panesthiines also host morphologically unusual

protists in their hindguts. However, these are not metamonad flagellates, but ciliates of the family Clevelandellidae (Armophorea: Clevelandellida). As in the case of termites, several symbiont species are usually found simultaneously in a single host organism (Kidder 1937). Whether Clevelandellidae play any role in the cellulose digestion of panesthiines is unknown. But even if they do, it seems unlikely to be of great benefit to the host, since it has been shown that at least one panesthiine, *Panesthia cribrata* Saussure, 1864, produces endogenous cellulase and can be maintained for at least 12 weeks in the absence of protozoan and most of the bacterial endosymbionts (Scrivener et al. 1989, Slaytor 1992). Moreover, unlike hypermastigotes, which visibly ingest large particles of wood into their cell, members of Clevelandellidae have not been reported to do so.

In contrast to their more or less ovoid nyctotherid relatives, Clevelandellidae are immediately recognizable by their bizarre morphology. The anterior end of the cell is tapered to a rounded point and the oral apparatus is situated at the posterior end of the cell, giving a false impression of the ciliate swimming backwards. In most species, the buccal cavity occupies a posterior extension: the peristomial projection. The distinctive appearance is further accentuated by the conspicuously asymmetric cell shape of most species.

The family Clevelandellidae gave the name to the whole order Clevelandellida, which consists entirely of ciliates living as symbionts of various animals. The endosymbiotic lifestyle has obviously originated in an exclusive common ancestor of Clevelandellida, because the order forms an internal branch of predominantly free-living ciliates of the order Metopida (Lynn and Wright 2013, Rotterová et al. 2018). While representatives of the family Clevelandellidae inhabit only Blattodea, members of the other four families of the order Clevelandellida (Nyctotheridae, Sicutophoridae, Neonyctotheridae, and Inferostomatidae) live as symbionts in a wide variety of both vertebrate and invertebrate animals. Clevelandellidae comprise five genera: *Anteclevelandella* Pecina and Vďačný, 2022, *Clevelandella* Kidder, 1938 (a replacement name for the preoccupied *Clevelandia* Kidder, 1937), *Paraclevelandia* Kidder, 1937, *Metaclevelandella* Uttangi and Desai, 1963, and *Rhynchoclevelandella* Pecina and Vďačný, 2022. Genera *Clevelandella* (with seven species) and *Paraclevelandia* (with two species) were described more than 80 years ago by Kidder (1937) from the cockroaches *Panesthia angustipennis* (Illiger, 1801) (known as *Panesthia javanica* Serville, 1831 at that time) from Philippines and *Panesthia angustipennis spadica* Shiraki, 1906 from Japan, respectively. Yamasaki (1939), apparently unaware of Kidder's work, described the genus *Emmaninius* Yamasaki, 1939, comprising three species, from an unidentified subspecies of *Panesthia angustipennis* (Illiger, 1801) from Japan. However, the genus name *Emmaninius* was unavailable, since Yamasaki (1939) did not designate the type species. Jankowski (2007) made the name available, designating *E. papilloris* as the type species. We consider *Emmaninius* Jankowski, 2007 to be a junior synonym of *Clevelandella* Kidder, 1938 and *E. papilloris*, *E. plantiformis*, and *E. longicollis* to be junior synonyms of *C. panesthiae*, *C. constricta*, and *C. nipponensis*, respectively. Since 1939, only two morphologically described species of *Clevelandella* from host genus *Panesthia* Serville, 1831 have been added (Mandal and

Nair 1974, Pecina and Vďačný 2020a). Recently, Pecina and Vďačný (2022) split the genus *Clevelandella* into three genera: *Clevelandella*, *Anteclevelandella*, and *Rhynchoclevelandella*. They also described eight new species between the three genera; however, the descriptions are based solely on molecular methods and no morphological differences are mentioned. *Metaclevelandella termitis* Uttangi and Desai, 1963, the sole representative of its genus, was, surprisingly, described not from a Panesthiinae cockroach but from a termite, *Dicuspitermes incola* (Wasmann, 1893) (known as *Capritermes longicornis* Wasmann, 1902 at that time) from India (Uttangi and Desai 1963).

Molecular data for Clevelandellidae were unavailable until Lynn and Wright (2013) analyzed the 18S rRNA gene sequences of four species of *Clevelandella* from Australia, all of which they considered to be conspecific with ones previously described by Kidder (1937). It was shown that Clevelandellidae form an internal branch of the genus *Nyctotherus* Leidy, 1849 (Clevelandellida: Nyctotheridae), and that *Clevelandella* is specifically related to *Nyctotherus* lineages from cockroaches, suggesting that the morphologically divergent Clevelandellidae evolved within cockroaches from a ciliate ancestor with a much less derived morphology (Albaret 1975). More recent studies that dealt with additional species and added more molecular markers (Pecina and Vďačný 2020a, b, 2022) were congruous with the findings of Lynn and Wright (2013). Somewhat surprisingly they pointed to a peculiar inconsistency of morphology and genetics in Clevelandellida (Pecina and Vďačný 2020b) leading to a proposal to shift from morphology-based species descriptions in the group to a purely molecular approach (Pecina and Vďačný 2022).

The occurrence of morphologically similar organisms in geographically distant hosts from Philippines, Japan, and Australia suggested a rather cosmopolitan distribution for a number of Clevelandellidae species (Kidder 1937, Yamasaki 1939, Lynn and Wright 2013). More recent works (Pecina and Vďačný 2020b, 2022), on one hand, found similar organisms also in mainland Asia, but, on the other, showed that some of the species or lineages may exhibit some geographical specificity. In regard to host specificity, the diversity of the hosts assessed so far is too low to draw meaningful conclusions as, until now, only five species of the cockroach genus *Panesthia*, one species of *Salganea* Stål, 1877, and one species of *Macropanesthia* Saussure, 1895 were inspected for gut ciliates (Kidder 1937, Yamasaki 1939, Mandal and Nair 1974, Lynn and Wright 2013, Pecina and Vďačný 2020a, b, 2022). This represents only a small fraction of subfamily Panesthiinae (including Geoscapheinae, see: Beasley-Hall et al. 2021), which comprises at least 169 species in 11 genera distributed in Sino-Japanese, Oriental, and Australian regions (Beccaloni 2014).

In this study we report on the diversity of Clevelandellidae from 13 host populations, the widest host spectrum assessed to date. We dissected 104 cockroach specimens and examined the diversity of their Clevelandellidae symbionts based on the morphology and single-cell 18S, ITS, and partial 28S rRNA gene sequences. We report nine previously described species, describe six new species, and report one new, as yet, undescribed species. We combine molecular and morphological methods and show that morphology is important in the taxonomy of

Clevelandellidae, contrary to a previous suggestion to abandon morphology in favour of a purely molecular approach (Pecina and Vďačný 2022). We propose synonymy of eight previously described species. We also discuss numerous morphological peculiarities, the phylogeny, diversity, host specificity, and biogeography of Clevelandellidae.

MATERIALS AND METHODS

Sample collections

To obtain Clevelandellidae symbionts, 104 individuals from 13 Panesthiinae host populations were dissected. *Ancaudellia pygmaea* Roth, 1982 (AP), *Ancaudellia serratissima serratissima* (Brunner von Wattenwyl, 1865) (ASS), *Panesthia angustipennis* (PA), *Panesthia angustipennis angustipennis* (PAA), *Salganea raggei* Roth, 1979 (SR), *Salganea rugulata* Saussure, 1895 (SRU), *Salganea ternatensis hirsuta* Roth, 1979 (STH), and *Salganea taiwanensis ryukyuanus* Asahina, 1988 (STR) were collected from nature. *Ancaudellia hamifera* (Hanitsch, 1930) (AH), *Miopanesthia polita* (Krauss, 1902) (MP), *Panesthia angustipennis cognata* Bey-Bienko, 1969 (PAC), *Panesthia angustipennis angustipennis* 'gold wing' (PGW), and *Panesthia triangulifera* Hanitsch, 1927 (PT) were obtained from hobby cultures. The origin of host cockroaches is summarized in the [Supporting Information, Table S1](#). The cockroach colonies were housed separately in plastic containers filled with decaying wood with appropriate humidity and room temperature. Close attention was paid to avoid any contact of animals and substrate between colonies to prevent symbiont cross-contamination.

The cockroaches were euthanized by ethyl acetate vapors. The hindgut was extracted, freed from the fat body, homogenized in the liquid phase of Dobell and Laidlaw's medium (Dobell and Laidlaw 1926), and stored in 1.5 mL Eppendorf tubes, where the ciliates survived from a few hours to several days at room temperature. Since the high viscosity of the culture medium due to added egg white severely hinders work with micropipettes, aliquots of the gut were transferred to drops of Ringer's solution for manual picking of ciliate cells under the dissecting microscope. The ciliates usually died within 20–40 min after being placed on slides.

Light microscopy

The morphology of live and protargol-impregnated cells was examined with an Olympus BX51 or BX53 microscope equipped with either a DP71 (Olympus, Japan) or Canon EOS 80D camera, and an AE2000 inverted microscope equipped with a BTU10 camera (Motic, Xiamen, China). Protargol (Polysciences Inc., Warrington, PA, no longer commercially available) preparations were done according to Bourland and Wendell (2014). Images of protargol-impregnated specimens were taken under brightfield illumination. Images of live cells were taken using differential interference contrast illumination (DIC). Measurements were performed using calibrated QuickPHOTO CAMERA 2.3 (Promicra) or ImageJ (National Institutes of Health, <https://imagej.nih.gov/ij/index.html>) software. Due to variability in cell orientation, not all characters could be measured in all cells.

Scanning electron microscopy

Ciliates collected as described above were placed in a drop of Ringer's solution on a glass slide, selected with a glass

micropipette, and washed free of detritus by transfer to three successive drops of fresh Ringer's solution. The cells were then placed in 1 mL of 2.5% glutaraldehyde in 1.5-mL Eppendorf tubes for at least 30 min and up to several days. Glutaraldehyde-fixed cells were washed in distilled water under the dissecting microscope, placed in brass sample chambers (Foissner 2014), and dehydrated in the chambers through a graded ethanol series (50%, 70%, 90% for 5 min each, and three exchanges of 100% for 15 min each). Critical point drying was done in a BalTech CPD030 critical point dryer (Leica Microsystems, Vienna, Austria) and dried cells were scattered on adhesive carbon tabs on aluminium specimen stubs and sputter coated with gold (vacuum 0.1 mbar, current 40 mA for 90 s). Observations were done in a JSM-6380 scanning electron microscope (JEOL LV, USA) in secondary electron and back-scattered electron detection modes at an accelerating voltage of 15 kV.

Statistical analyses

All statistical analyses were performed in R 4.2.0 (R Core Team 2023). For the purpose of a detailed morphological investigation of ciliate species, the following features were determined in a total of 455 protargol-stained cells from 33 strains of 16 species ('brevis' and 'simplex' morphs of *Paraclevelandia brevis* were considered as separate species in this analysis): (i) body length, (ii) body width, (iii) the presence of peristomial projection, (iv) peristomial projection length, (v) peristomial opening width, (vi) adoral zone of membranelles length, (vii) adoral membranelles number, (viii) distance from the anterior of the cell to the posterior of macronucleus, (ix) macronucleus length, (x) macronucleus width, (xi) micronucleus length, and (xii) micronucleus width. From 7 to 73 cells (24 in average) were morphologically analyzed per each species. Missing data were imputed with a principal component analysis (PCA) using the 'missMDA' package (Josse and Husson 2016) applying the iterative PCA algorithm. An NMDS (non-parametric multi-dimensional scaling) analysis was carried out with the 'vegan' package (Oksanen et al. 2020), based on the imputed dataset and using a total of 1000 random starts in search of a stable solution. The morphological similarities of analyzed cells were visualized with a scatterplot of the first two axes (stress factor = 0.076).

In addition, we performed a linear discriminant analysis (LDA) using the 'MASS' package (Venables and Ripley 2022) and calculated a classification matrix measuring the performance of the model. This matrix reports the number of cases correctly and incorrectly assigned to each of the groups (species) based on the discriminant analysis of determined morphological traits.

To assess shrinkage of protargol preparations we have compared measurements of the cell size (length or width) for a given species between protargol preparations and *in vivo* measurements. We used a generalized linear model (GLM) model with gamma distribution and link function log to test the effect of species, cell condition (live cell/protargol preparation), and their interaction on the measured cell size. Reduced major axis (RMA) regression from the package 'lmodel2' was used to analyze the effect of species cell size (length or width) on shrinkage.

DNA isolation, amplification, and sequencing

Individual ciliates were handpicked from the gut content with micropipettes, washed three times in Ringer's solution, and

either processed immediately or stored frozen at -80°C in 30 μL of Ringer's solution (Supporting Information, Table S2; Figs S1–S3). Genomic DNA was isolated with the MasterPure™ Complete DNA & RNA Purification Kit (Lucigen, Middleton, WI, USA).

The 18S rRNA gene was amplified using primers ArmF1 (Bourland *et al.* 2017a) and EukB (Medlin *et al.* 1988). PCR conditions were as follows: denaturation at 94°C for 4 min, 30 cycles of denaturation at 94°C for 1 min, annealing at 55°C for 1 min, and extension at 72°C for 4 min, and final extension at 72°C for 15 min. The ITS1-5.8S-ITS2 region, along with the first two domains of the 28S rRNA gene, were amplified using primers ITS-F (Miao *et al.* 2008) and LO-R (Pawlowski 2000). PCR conditions were as follows: denaturation at 95°C for 15 min, 30 cycles of denaturation at 95°C for 45 s, annealing at 55°C for 1 min, and extension at 72°C for 150 s, and final extension at 72°C for 10 min. EconoTaq® PLUS GREEN 2X Master Mix (Lucigen, Middleton, WI, USA) was used for both protocols. Amplified DNA was checked by agarose gel electrophoresis and purified with ExoSAP-IT (Thermo Fisher Scientific, Waltham, MA, USA). The purified PCR products were sequenced either on ABI 3730 automatic sequencer (Applied Biosystems, Thermo Fisher Scientific, Waltham, MA, USA) at Macrogen, Amsterdam, the Netherlands or on an ABI PRISM 3100 (Applied Biosystems, Thermo Fisher Scientific, Waltham, MA, USA) at Charles University, Prague, Czech Republic.

Phylogenetic methods

The 18S rRNA gene was sequenced from all 147 cells and the ITS1-5.8S-ITS2 region and the first two domains of the 28S rRNA were sequenced from 48 cells (Supporting Information, Table S2). All sequences relevant to Clevelandellida and outgroup sequences were downloaded from GenBank (Supporting Information, Table S3). For outgroups, we chose sequences of the metopid group IAC (defined by: Bourland *et al.* 2018), the closest known relatives of Clevelandellida. Two datasets were created: (i) a full dataset containing all newly determined sequences and all available 18S, ITS, and 28S sequences of Clevelandellidae and outgroups (Nyctotheridae and Metopida) and (ii) a reduced dataset, derived from the full dataset, containing only the strains with all three genes available. The sequences were aligned using the G-INS-I algorithm in MAFFT (Katoh *et al.* 2002, Katoh and Standley 2013) with otherwise default settings on the GENEIOUS PRIME 2023.1.1 platform. The unedited alignment comprised 3012 sites and was manually edited using BioEdit 7.0.9.0 (Hall 1999), retaining 2962 sites (98.3%). The GTR+I+G nucleotide substitution model was chosen based on analysis by ModelTest-ng (Darriba *et al.* 2020). Phylogenetic trees were constructed using maximum likelihood (ML) and Bayesian methods. ML analysis was performed with RAxML-ng (Kozlov *et al.* 2019) under the GTR+G model using 20 starting trees (10 random, 10 parsimony). Node support was assessed with 1000 bootstrap replicates. Bayesian analysis was performed using MrBayes 3.2.7a on the Cipres Portal (Miller *et al.* 2010) using the GTR+I+G model. Two parallel runs of four chains each were run for 5 000 000 generations, with a sampling frequency of 1000 generations. The first 25% of sampled trees were discarded as burn-in. The average

standard deviation of split frequencies was 0.007 after 5 million generations. Convergence was assessed by RWTY (Warren *et al.* 2017). Trees were visualized in FigTree v. 1.4.4 (<http://tree.bio.ed.ac.uk/software/figtree/>).

RESULTS

Phylogenetic analyses

The phylogenetic tree of the Metopida/Clevelandellida lineage based on the full dataset inferred from the 18S rRNA, ITS, and 28S rRNA gene sequences is shown in the Supporting Information, Figure S4. The phylogenetic tree of the Clevelandellida lineage based on the reduced dataset is shown in the Supporting Information, Figure S5. Photomicrographs of the individual cells included in the tree, as well as genes sequenced from them, are summarized in the Supporting Information, Table S2 and Figures S1–S3. Topology and support values of both trees are highly consistent, with the only notable difference being higher support value for the monophyly of the genus *Rhyncholevelandella* in the tree based on the reduced dataset (bootstrap support, BS, 99 vs. 78, Bayesian posterior probability, BPP, 1 vs. 0.99). The part of the full dataset tree showing only the Clevelandellidae lineage is shown in Figure 1. The overall topology of the tree is consistent with previous analyses (Lynn and Wright 2013, Bourland *et al.* 2017a, b, Li *et al.* 2018, Rotterová *et al.* 2018, Pecina and Vďačný 2020a, b, 2022). The order Clevelandellida is robustly monophyletic (BS 98, BPP 1). The family Clevelandellidae is monophyletic (BS 91, BPP 1) and forms an internal lineage of the family Nyctotheridae. *Antelevelandella constricta* (Kidder, 1937) forms a branch sister to the remaining Clevelandellidae, which form a robust clade (BS 89, BPP 1). Genera *Rhyncholevelandella* and *Paralevelandia* form a well-supported clade (BS 89, BPP1) sister to the genus *Clevelandella*. Genus *Rhyncholevelandella* is moderately supported (BS 78, BPP1). The isolates with *R. nipponesis* (Kidder, 1937) morphology are paraphyletic with respect to *R. hastula* (Kidder, 1937). This may be a case of cryptic diversity. The supports in the genus are, however, too weak for any meaningful assumptions. Genus *Paralevelandia* is fully supported (BS 100, BPP1). All lineages in the genus include isolates of both *Paralevelandia brevis* Kidder, 1937 and *Paralevelandia simplex* Kidder, 1937 morphology, with a majority of them including genetically identical isolates of both morphologies. Genus *Clevelandella* is moderately supported (BS 71, BPP1) and splits into 12 strongly supported lineages considered here as separate species on the basis of morphology (see below). The relationships among individual species are largely unresolved.

Morphology

Terminology: We use 'anterior' and 'posterior' in the sense of Kidder (1937) and Albaret (1975). Following Kidder (1937) we designate the margin on which the lateral part of the peristomial opening and cytoproct lie as 'left' and the margin bearing the long suture between dorsal and ventral kineties suture as 'right'. We define the portion of the cell anterior to the peristomial projection as the 'body proper' (Kidder 1937, Mandal and Nair 1974). In agreement with Kidder's original terminology (1937) followed by Mandal and Nair (1974) and Pecina, Vďačný (2020a, b), we consider cell flattening to be dorsoventral. It should be

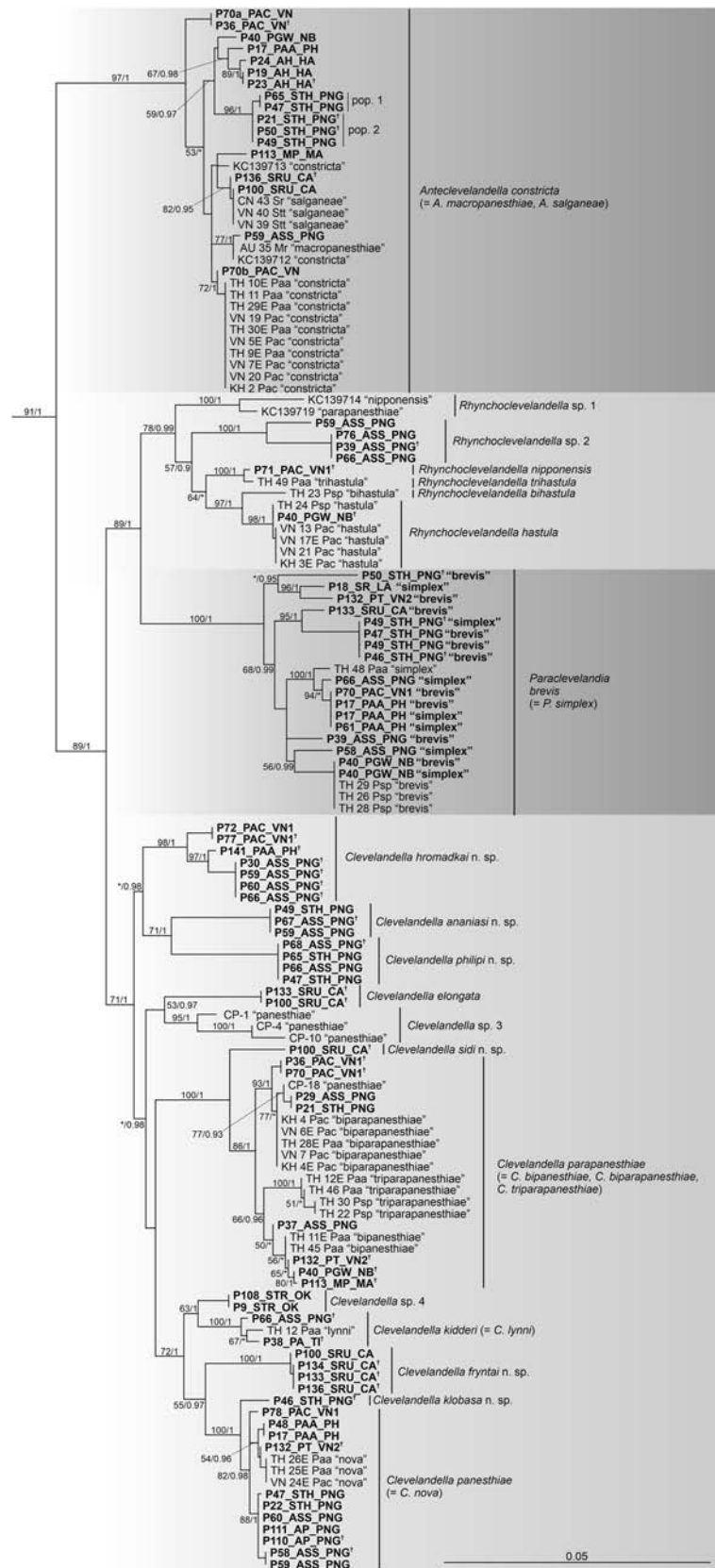


Figure 1. Part of the maximum likelihood phylogenetic tree based on the full dataset using 18S rRNA gene, ITS1-5.8S-ITS2 region, and 28S rRNA gene sequences showing the relationships among Clevelandellidae. Sequences of Nyctotheridae, Siculothoridae, and Metopida were removed (for the complete tree figure see [Supporting Information, Fig. S4](#)). Metopida was used as an outgroup. The values at the branches represent statistical support in maximum likelihood bootstrap values/Bayesian posterior probabilities. Support values below 50/0.90 are not shown or are depicted by an asterisk. Newly determined sequences are in bold. Scale bar: 5 substitutions/100 nucleotide positions. *indicates

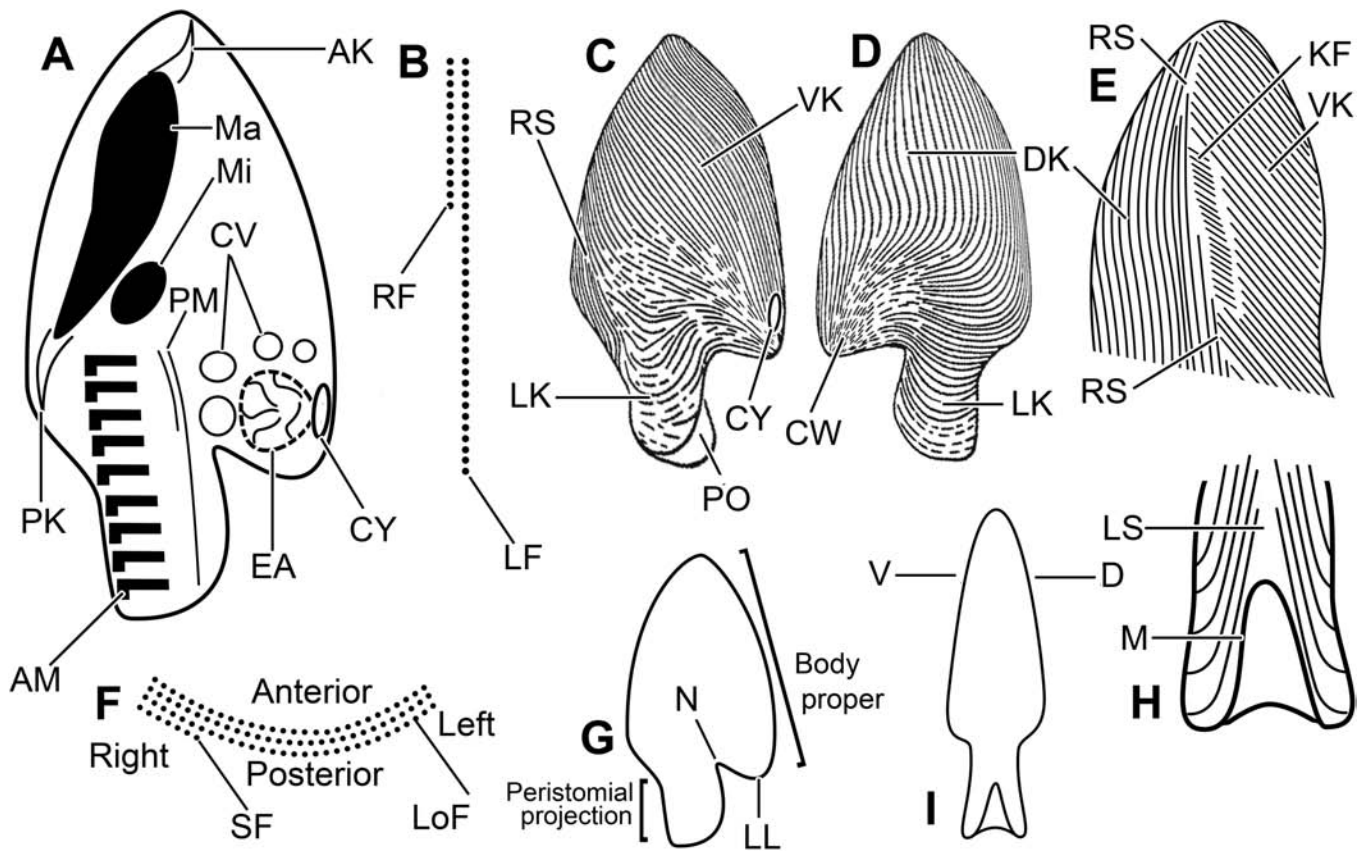


Figure 2. Schematic illustrations of various morphologic features of Clevelandellidae. A, ventral view (optical section) of a spade-shaped species. B, ventral view. C, dorsal view. D, right lateral view of *Anteclevelandella constricta*. E, composition and orientation of adoral membranelle. F, composition of diplostichomonad paroral membrane. G, left lateral view of peristomial projection. H, outline showing body parts of spade-shaped species. I, left lateral view showing dorsoventral flattening. AK, anterior karyophore; AM, adoral membranelle; CY, cytoproct; CV, collecting vesicles of contractile vacuole; CW, ciliary whorl; D, dorsal; DK, dorsal kineties; EA, ciliated excretory antrum; KF, kinetofragments; LF, left file of paroral membrane basal bodies; LL, left lobe; LoF, long file of adoral membranelle basal bodies; LS, short left suture; M, margin of the lateral extension of the peristomial opening; Ma, macronucleus; Mi, micronucleus; N, notch between left lobe and peristomial projection; PK, posterior karyophore; PM, diplostichomonad paroral membrane; PO, peristomial opening; RS, right suture; SF, short file of adoral membranelle basal bodies; V, ventral; VK, ventral kineties. See text for discussion of terminology regarding morphologic features and orientation.

noted, however, that Yamasaki (1939) and Albaret (1975) considered the same species as being laterally flattened. We refer to the distinctive incomplete somatic ciliation as ‘hemiciliation’, recognizing that the extent of partial ciliation varies somewhat between species. We define the cytoproct as the opening in the pellicle through which faecal material is discharged (Lynn 2008). We define the unique ‘cloaca-like’ ciliated intracellular antrum, through which faecal material and contractile vacuole contents pass, as the ‘excretory antrum’ (see Discussion). We use the terms ‘peristomial overture’, ‘peristomial opening’, and ‘buccal overture’ interchangeably. The peristomial overture has two continuous portions, lateral (left) and terminal (posterior), except for *Paraclevelandia brevis* in which the posterior peristomial projection is absent and the buccal overture is terminal, extending anteriorly only slightly. We consider the terms ‘spade-shaped’

and ‘spear-shaped’ as synonymous. Otherwise the terminology used mainly follows Lynn (2008) and Foissner and Xu (2007). A schematic illustration of an idealized Clevelandellidae cell showing morphologic features and orientation can be found in Figure 2.

Features common to all Clevelandellidae

Morphologic organization: Clevelandellidae show a wide diversity of body shapes and sizes but share the same general morphologic organization, i.e. ‘posteriorization’ of the oral structures in comparison with representatives of nyctotherid families of order Clevelandellida. In all Clevelandellidae, the anterior end of the cell is tapered to a rounded point oriented in the direction of swimming, while the posterior end of the cell bears the buccal

that at least two cells with identical sequences from the same host individual were characterized. The names in quotation marks indicate the species name originally assigned by previous authors and/or morphotype in case of *Paraclevelandia brevis*. For GenBank accession numbers of newly determined sequences, as well as images of individual cells, see Supporting Information, Table S2 and Figs S1–S3. For accession numbers of sequences downloaded from GenBank see Supporting Information Table S3.

or peristomial overture. All Clevelandellidae show some degree of dorsoventral flattening, most conspicuous in spade-shaped taxa and least conspicuous in *Antelevelandella constricta* and *Paraclevelandia brevis*.

The peristome leads internally to a tubular infundibulum bearing the adoral zone and paroral membrane that both end anteriorly at the cytostome, typically to the right of the midline in the posterior half of the body proper. The peristomial opening occupies the posterior end of the cell and has an inverted U- or V-shaped lateral part extending anteriorly toward the junction of the peristomial projection and the body proper. We consider the lateral part of the overture an important landmark designating the left side of the cell. All species except *Antelevelandella constricta*, *C. elongata* (Kidder 1937), *C. klobasa* sp. nov., and *Paraclevelandia brevis* have a distinct, more or less cylindrical posterior peristomial projection. In the other four species mentioned, the projection is less developed (the former three) or absent (*Paraclevelandia brevis*).

Cytoplasm and food vacuoles: All members of Clevelandellidae are colourless to slightly brownish depending on cytoplasmic contents. Food vacuoles are quite indistinct in all species, giving the cytoplasm a rather featureless, coarsely granular appearance. The cytoplasm occasionally contains colourless platelets, consistent with polysaccharide granules (Fig. 17C) possibly composed of amylopectin, also known as paraglycogen, the carbohydrate storage product found also in nyctotherids and many other free-living and parasitic protists. Although Albaret (1975) showed them to consist of polysaccharide by the Bauer reaction, no more specific identification of their composition is available (Kidder 1937, Hoyte 1961, Pecina and Vďačný 2020b, 2022, Ralton et al. 2021).

Cortex: The cortex is flexible without distinct cortical granules. However, all species studied *in vivo* by DIC have a distinct 1.5–2.5 µm-thick, hyaline subcortical layer as noted in brightfield illumination by Kidder (1937). As in nyctotherids, this probably comprises a layer of closely-packed mucocyst-type extrusomes (Albaret 1975).

Nuclear apparatus and karyophore: The nuclear apparatus of all species is located in the body proper, usually on the right in its midportion or anterior part. A notable exception is *Antelevelandella constricta*, which has a transversely oriented macronucleus attached to the right and left cell margins by the karyophore. Although features of the karyophore, a system of macronuclear suspensory fibres attached to the somatic cortex in Clevelandellida, have been considered taxonomically valuable (Kidder 1937, Albaret 1975, Pecina and Vďačný 2020a, b), in our hands, demonstration of this feature is highly inconsistent in the majority of species, except *Antelevelandella constricta* and *C. elongata* (Figs 19A, E, 25B, C, 26A, B). It is often undetectable in both live cells observed with DIC and in protargol preparations. Thus, presence or absence of the karyophore is a highly inconsistent morphologic character.

Contractile vacuole, ciliated excretory antrum, and cytoproct: The contractile vacuole is closely associated with the ciliated

excretory antrum on the left posterior margin of the body proper (Fig. 2A). The morphology is consistent with Patterson's (1980) type I contractile vacuole. The excretory antrum itself consists of a permanent, intracellular cavity, to the left of the cytostome and lined by motile cilia. The faecal material and contractile vacuole contents are propelled through this excretory antrum to empty via a slit-like cytoproct on the left margin of the body [*C. panesthiae* (Kidder, 1937): [Supplementary Information, Video S1](#)].

Somatic ciliature: In all Clevelandellidae, only the anterior portion of the cell bears cilia (i.e. 'hemiciliation'), a fact recognized by Albaret (1975), Mandal and Nair (1974), and Yamasaki (1939) but, curiously, overlooked by others (Pecina and Vďačný 2020a, b, 2022), including Kidder himself (1937). The remainder of the cell cortex bears barren dikinetids, except for the ciliated circumperistomial kineties. The somatic ciliation of the body proper extends furthest posteriorly along the right cell margin, most notably in *P. brevis* in which the somatic ciliation on the right cell margin can extend to the posterior end (Fig. 24A, B, E, F). The somatic ciliature follows a similar 'Clevelandellidae pattern' in all species, i.e. leftward-spiralling, narrowly (about 1.5–2.0 µm apart; e.g. *C. panesthiae*) to very narrowly spaced (≤ 1 µm apart; e.g. *C. elongata*) kineties consisting of densely spaced dikinetids radiating outward from the region of the cytoproct on to the ventral and dorsal surfaces of the body proper and with more widely spaced kineties looping posteriorly on to the peristomial projection. The dorsal kineties tend to be less spiralled. The ventral and dorsal kineties of the body proper meet at a long suture on the right lateral margin of the body proper and a short, inconspicuous left posterior suture near the junction of the peristomial projection with the body proper (with the exception of *Paraclevelandia brevis*, which lacks a distinct peristomial projection). The density of the ciliary pattern and the occurrence of shortened or incomplete kineties hinder precise determination of numbers of somatic kineties. Within the right suture, several species [*Antelevelandella constricta*, *C. hromadkai* sp. nov., *C. parapanesthiae* (Kidder, 1937), *C. philipi* sp. nov., *C. kidderi* Mandal and Nair, 1974, *Paraclevelandia brevis*, and *R. hastula*] have short transverse to oblique kinetofragments consisting of about five basal bodies bearing clavate cilia (Fig. 2E), as also noted by Albaret (1975). This feature was absent in *C. sidi* sp. nov., *C. fryntai* sp. nov., *C. panesthiae*, and *C. elongata* and could not be reliably assessed in *C. aniansi* sp. nov., *C. klobasa* sp. nov., *R. nipponensis*, and *Rhynchoclevelandella* sp. 2. All species have two or three ciliated circumperistomial kineties at the posterior margin of the buccal overture (e.g. Figs 4A, F, 5A, C). The somatic cilia of all examined species are distinctly shorter than those typical of free-living ciliates (about 4.5–5.5 µm vs. about 7–15 µm).

Oral structures: In all species, the adoral zone of membranelles (AZM), in contrast to nyctotherids, is located on the right wall of the infundibulum and terminates anteriorly at the cytostome. The adoral zone is usually straight or slightly oblique to the long axis of the cell, usually curving as it ends at the cytostome. The adoral membranelles consist of two or three long files of basal bodies and one short file. The polarity of the membranelles themselves is also reversed, i.e. in contrast to nyctotherids; the

short file of basal bodies is located on the posterior rather than anterior margin of each membranelle (Fig. 2A, F). The paroral membrane (POM) is opposite the AZM on the left wall of the infundibulum (Fig. 2SB) and about same length as the adoral zone. In all but one species (*C. sidi* sp. nov.) with adequate preparations, the paroral membrane is diplostichomonad (i.e. comprises two parallel files of basal bodies separated by a cortical ridge) and the right file of basal bodies is usually shortened posteriorly (de Puytorac and Grain 1976).

The above features are common to all species except as noted. The following species descriptions include only character states that differ between species.

Newly described species

Clevelandella ananiasi sp. nov.

(Figs 3–5; Supporting Information, Table S4)

Description based on population from ASS hosts from Papua New Guinea: Small *Clevelandella*, size *in vivo* 69–87 × 35–52 μm, usually about 77 × 41 μm; size in protargol preparations 44–67 × 25–34 μm, usually about 55 × 29 μm. Body proper dorsoventrally flattened; overall outline in ventral view asymmetrically spade-shaped, with prominent left lobe, anterior cell end bluntly pointed; peristomial projection joins body proper to right of midline. Left cell margin notched at base of peristomial projection forming a lobe that overhangs the peristomial projection for about one-fifth of its length. Macronucleus ellipsoidal (Figs 3A, 4A) to inverted teardrop-shape (Figs 3B, 4B–E, G), anterior end rounded, posterior end acutely tapered, chromatin coarsely granular. Karyophore attached to posterior margin of macronucleus (Figs 3A, 4A, B). Micronucleus ellipsoidal (4.4 × 3.4 μm), adjacent to anterior margin of macronucleus (Figs 3B, 4G). Swims slowly.

Somatic ciliature consists of about 60 kineties, only anterior two-thirds of body properly ciliated (Fig. 5A, B). Right sutural kinetofragments not confirmed, cannot be completely excluded due to suboptimal orientation of cells in protargol preparations.

Peristomial projection extends an average of 28% of total cell length. Lateral part of peristomial opening extends about three-quarters of length (Figs 4A, F, 5A) of peristomial projection. Adoral zone usually extends about 52% of cell length, composed of an average of 23 membranelles. Fine structures of POM unrecognizable due to poor staining but visibly stichomonad at the posterior (Fig. 5B–D).

Occurrence: *Clevelandella ananiasi* sp. nov. was found in the hindgut of two Panesthiinae species from Papua New Guinea: ASS and STH from the same locality (Wanang 3). It occurred in 56% of ASS individuals regardless of age and sex. In STH the ciliate was present only in one juvenile host individual among 10 dissected insects. When present, the ciliate is typically abundant. In ASS, infection with *C. ananiasi* sp. nov. frequently co-occurs (60%) with *C. sidi* sp. nov. requiring special care in species identification.

Clevelandella philipi sp. nov.

(Figs 6, 7; Supporting Information, Tables S5, S6)

Description based on populations from hosts ASS and STH from Papua New Guinea: Small- to medium-sized *Clevelandella*, size *in vivo* 74–99 × 40–54 μm, usually about 90 × 49 μm; size in

protargol preparations 59–88 × 35–47 μm, usually about 75 × 41 μm in STH population; size *in vivo* 73–95 × 43–59 μm, usually about 87 × 49 μm; size in protargol preparations 49–78 × 29–41 μm, usually about 63 × 34 μm in ASS population. Body proper dorsoventrally flattened; overall outline spade-shaped in ventral view, widest near junction of body proper with peristomial projection, cell outline asymmetric due to prominent left lobe, anterior end of cell tapers to blunt point; peristomial projection joins body proper near right margin; left cell margin conspicuously notched at base of peristomial projection, left lobe overhangs peristomial projection up to one-third of its length (Figs 6A–D, 7B–D, G, H). Macronucleus usually inverted teardrop-shape (Fig. 7B, E, F), right margin slightly convex, or ellipsoidal (Figs 6A, 7A, G, H), karyophore unobserved. Chromatin coarsely granular. Micronucleus ellipsoidal (5.5 × 2.5 μm), adjacent to right anterior margin of macronucleus (Figs 6B, 7G). Swims slowly.

Somatic ciliature arranged in about 55 kineties. Cilia present only on anterior two-thirds of cell (Fig. 7B). About nine widely-spaced, curved, free transverse ciliary rows on peristomial projection. Right sutural kinetofragments numerous, well developed (Fig. 7C, E). Peristomial projection averages about 24% of total body length in STH population, 28% in ASS population. Peristomial opening extends one-half (Fig. 7A) to three-quarters (Fig. 7B, H) of length of peristomial projection. Adoral zone extends anteriorly about 51% (STH) to 57% (ASS) of body length to end near posterior margin of macronucleus, composed of an average of 30 (ASS) to 32 (STH) membranelles, adoral zone widest in peristomial projection, narrows anteriorly, POM as described for the family.

Occurrence: *Clevelandella philipi* was found in the hindgut of two Panesthiinae species from Papua New Guinea: ASS and STH from the same locality (Wanang 3). Of STH individuals, all of which were juveniles, 30% harboured *C. philipi*. Since only two adults of the STH population (both males) were dissected, no conclusions can be reached about possible life-stage specificity. In the ASS population, *C. philipi* was present in 37% of cockroach individuals regardless of age and sex. When present, the ciliate is typically abundant. In ASS the infection with *C. philipi* sp. nov. frequently (90%) co-occurred with *C. ananiasi* sp. nov., requiring care in identification.

Clevelandella hromadkai sp. nov.

(Figs 8–11; Supporting Information, Tables S7–S10)

Description based on populations from hosts ASS from Papua New Guinea and PAC from Vietnam: Medium to very large *Clevelandella*, widely variable in both size and shape. In ASS population, size *in vivo* 103–262 × 39–81 μm, usually about 164 × 57 μm; size in protargol preparations 77–164 × 25–66 μm, usually about 117 × 40 μm; in PAC population, size *in vivo* 127–339 × 44–85 μm, usually about 190 × 58 μm; size in protargol preparations 110–276 × 31–83 μm, usually about 155 × 45 μm. Body shape usually broadly cultriform, ventral surface of the body proper convex, dorsal surface concave, anterior end of cell bluntly pointed and curved more (Figs 9E, 10C, E) or less (Figs 9C, H, 10B, 11A, D, E) in dorsal direction. Peristomial projection flares to merge gradually with body proper, prominence of

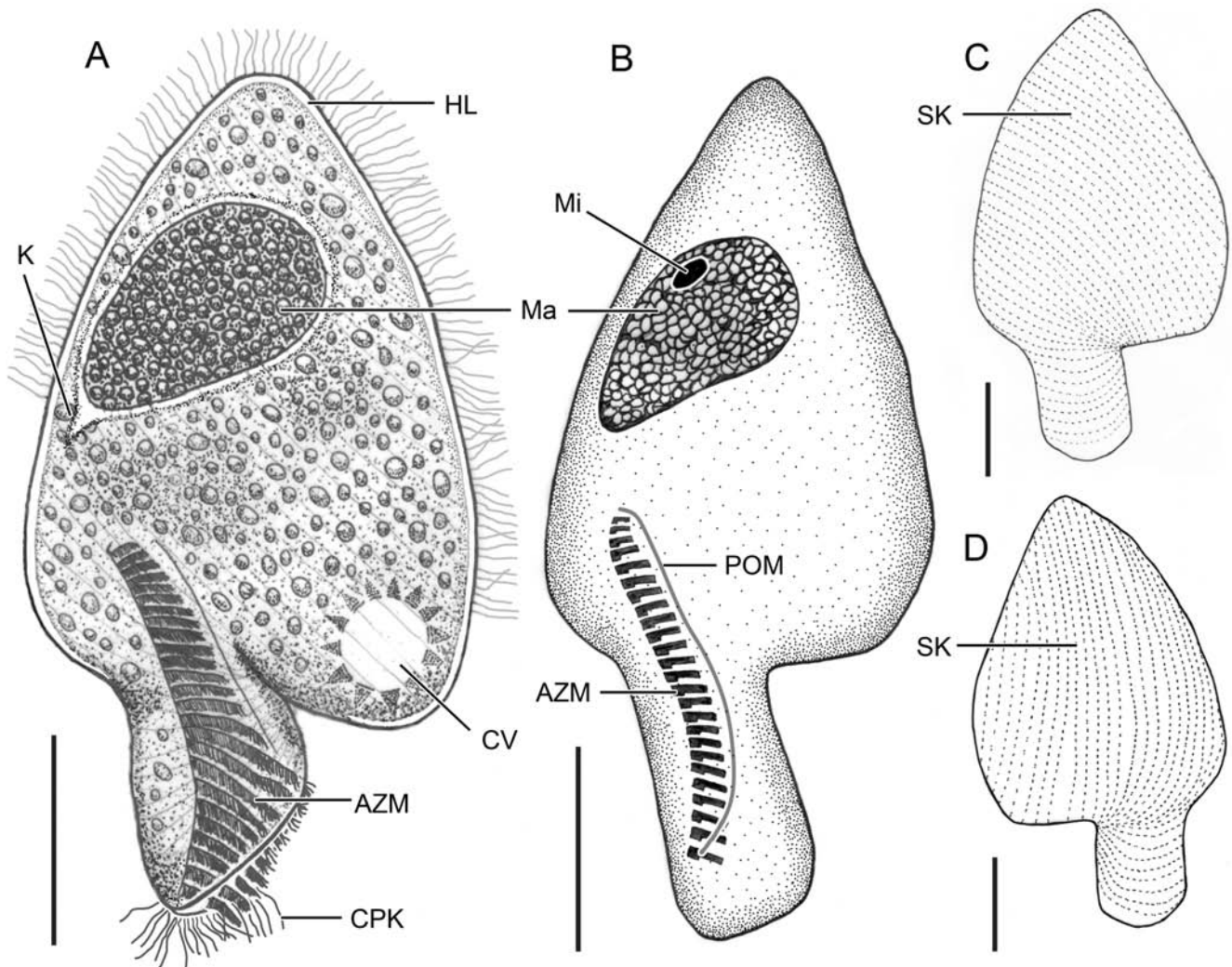


Figure 3. Schematic drawings of *Clevelandella ananiasi* from life (A) and protargol impregnation (B–D). A, ventral view of a typical individual. B, ventral view showing the oral apparatus and nuclear structures. C, ventral infraciliature. D, dorsal infraciliature. AZM, adoral zone of membranelles; CPK, circumperistomial cilia; CV, contractile vacuole; HL, hyaline subcortical layer; K, karyophore; Ma, macronucleus; Mi, micronucleus; POM, paroral membrane; SK, somatic kineties. Scale bars: 20 μm .

left lobe varies from less conspicuous (Figs 9A, B, 10A) to more prominent (Figs 8A, D, F, 9D, F–H, 10F, 11B, C, E) with a notch formed between the lobe and peristomial projection (Figs 8F, 9F), in contrast to spade-shaped species, the notch degree between peristomial projection and left lobe seems never to be under 90° ; posterior margin of peristomial projection truncate. L/W ratio highly variable in individuals from both hosts, from shorter stouter forms (Figs 8D–G, 9A–I, 11A–E) to longer more slender cells (Figs 8A, B, 10A–F). Macronucleus broadly ellipsoidal in short forms (Figs 8D, E, 9A–F), to narrowly ellipsoidal in long forms (Fig. 10A–C, E, F). Karyophore inconspicuous; when detectable, attached to posterior end of macronucleus and right body margin (Figs 8A, B, D, 10A, D). Micronucleus ellipsoidal, usually adjacent to right anterior margin of macronucleus, enclosed in separate membrane (Figs 8A, B, D, 9A, C, E, F, 10A, C–E). Swims moderately fast while rotating around long axis.

Somatic ciliature composed of about 60–85 somatic ciliary rows in Clevelandellidae pattern; cilia present only on approximately anterior half of cell; about 20–25 ciliary rows on the

peristomial projection in ASS population. Ciliary rows in PAC population not counted. Right suture has only two or three small free kinetofragments (not shown).

Peristomial projection occupies an average of 35% of total body length. Lateral part of peristomial opening extends about one-half (Figs 9B, 11B, D, E) length of peristomial projection in short cells, about one-third (Fig. 10A, B) length of peristomial projection in long cells. Adoral zone usually extends about 50% of body length, composed of an average of 54 (ASS) to 62 (PAC) membranelles, base of membranelles longest in midportion of peristomial projection. POM as described for the family (Fig. 9I).

Remarks on short and long morphotypes: *Clevelandella hromadkai* shows considerable intraspecific phenotypic variability. The ASS population, while genetically uniform, can be divided in two distinct phenotypes: short (Figs 8D–G, 9A–I, 11A–F) and long (Figs 8A, B, 10A–F). In a single host, only one phenotype seems to occur at a given time; from nine thoroughly inspected

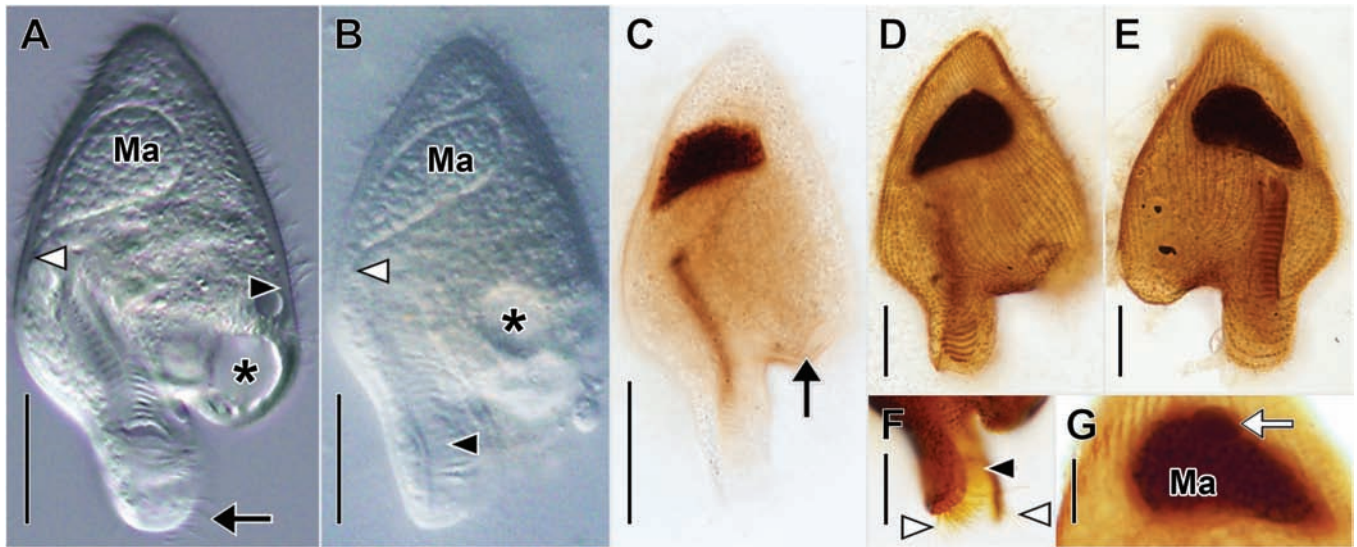


Figure 4. *Clevelandella ananiasi* sp. nov. from ASS. *In vivo* (A, B) and after protargol impregnation (C–G). A, ventral view showing karyophore (white arrowhead), contractile vacuole (asterisk), posterior extent of somatic cilia (black arrowhead), and cilia of circumperistomial kineties (black arrow). B, ventral view showing a more slender macronucleus, karyophore (white arrowhead), contractile vacuole (asterisk), and adoral membranelles (black arrowhead). C, ventral view showing excretory (black arrow). D, ventral infraciliature. E, dorsal infraciliature of same cell as (D). F, detail view of peristomial projection showing the peristomial overture (black arrowhead) and cilia of the circumperistomial kineties (white arrowheads). G, detail view showing position of micronucleus (white arrow). Ma, macronucleus. Scale bars: 20 μm (A–C), 10 μm (D–F), 5 μm (G).

hosts the short morph occurred in two females and two larvae, the long morph occurred in four males and one larva. Apart from the obvious length difference (mean *in vivo* 127 μm vs. 215 μm) and other morphological characteristics (e.g. number of adoral membranelles—see [Supporting Information, Tables S8, S9](#)), both morphs can be distinguished by their shapes: the short one is stouter (body L/W ratio 2.5) with a more rounded anterior end and the long one is more slender (body L/W ratio 3.7).

Occurrence: Three distinct populations of *C. hromadkai* were found in the hindguts of three Panesthiinae populations: ASS from Papua New Guinea, PAA from Philippines, and PAC from Vietnam. The ASS population occurred in 63% of host individuals regardless of age and sex. When present, *C. hromadkai* was less abundant (a few tens of individuals) compared to other ciliate species present in a host. The PAC population occurred in 28% of host individuals. Out of nine infected hosts, one was a large larva and eight were visibly old adult males. Most of the PAC hosts exhibited low occurrence of *C. hromadkai* (around 10 cells) with other ciliate species being more abundant. The exception was one male that harboured around 50 cells of *C. hromadkai*. When *C. hromadkai* was present in PAC hosts, the populations of other ciliates were visibly low compared to PAC host, in which *C. hromadkai* was absent. The PAA population occurred in only 17% of host individuals. Out of two infected hosts (both adult males), one exhibited a low occurrence of the *C. hromadkai* with the other ciliate species being more abundant. The other host exhibited high occurrence of *C. hromadkai* with other ciliates being scarce.

Clevelandella klobasa sp. nov.

([Figs 12, 13](#); [Supporting Information, Table S11](#))

Description based on population from STH hosts from Papua New Guinea: Large *Clevelandella*, size *in vivo* 146–206 \times 61–98

μm , usually about 170 \times 80 μm ; size in protargol preparations 123–163 \times 61–80 μm , usually about 135 \times 71 μm . Overall cell outline in ventral view more or less symmetrical, broadly lanceolate, widest at middle of cell, anterior cell end bluntly pointed, dorsoventrally flattened; peristomial projection inconspicuous, merges gradually with cell body proper at midline, thus predominant left lobe absent. Peristomial opening broad. Macronucleus long, slender sausage-shaped (mean 63 \times 12 μm) ([Figs 12A, B, 13A, C, D](#)), anterior end rounded, posterior end rounded ([Fig. 13A, B](#)) or abruptly tapered to short point ([Fig. 13C](#)); extends along nearly entire right margin of body proper, convex toward right body margin ([Fig. 13A, C](#)). Chromatin coarsely granular. Karyophore not identified. Micronucleus (4.7 \times 4.3 μm) globular, adjacent to anterior right margin of macronucleus ([Figs 12A, B, 13B, D](#)). Swims slowly.

Somatic cilia present on only anterior two-thirds of cell. Somatic ciliature composed of about 102 narrowly-spaced kineties, arranged in typical *Clevelandella* pattern. Right sutural kinetofragments not observed.

Peristomial projection indistinct, i.e. flares as it gradually merges with body proper. Lateral part of peristomial opening wide (23 μm) ([Fig. 13A–C](#)). Adoral zone extends about 56% of body length, composed of 59 membranelles ($N = 3$), markedly curved right at about three-quarters of length. Fine morphology of POM ([Fig. 13D](#)) not determined with certainty.

Occurrence: *Clevelandella klobasa* is extremely rare as it was found only in two out of 10 dissected individuals of STH: a male and a small juvenile, each of them from a different family group. The population density was very low in both cases, with no more than 15 cells of *C. klobasa* sp. nov. present in the entire hindgut. In both cases, *C. klobasa* co-occurred with cells of *Paraclevelandia brevis* (once also in 'simplex' form) and *Nyctotherus* sp..

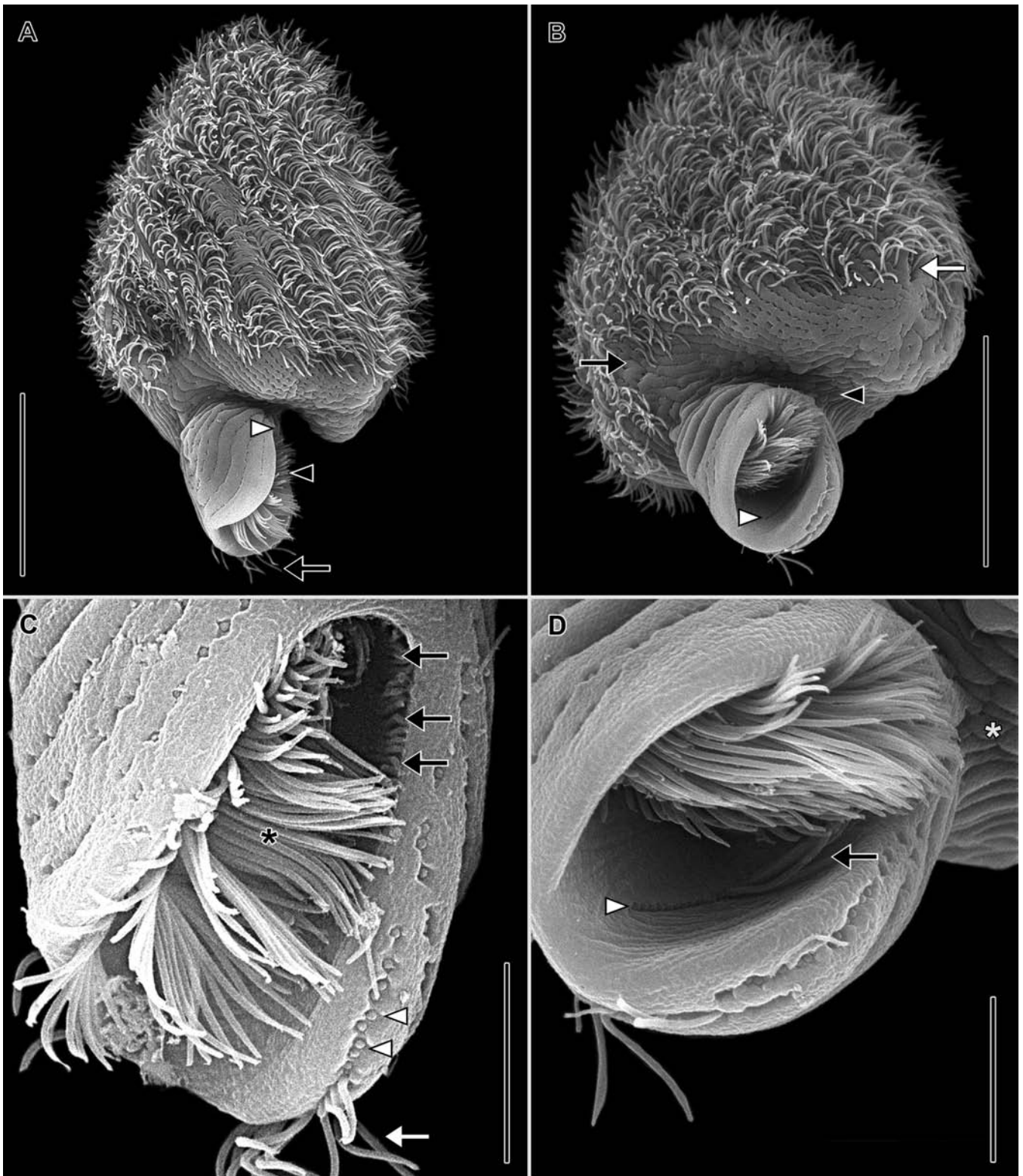


Figure 5. *Clevelandella aniansi* sp. nov. (from ASS) in the scanning electron microscope. A, ventral view showing anterior margin of peristomial overture (white arrowhead), cilia of adoral membranelles (black arrowhead), and cilia of circumperistomial kineties (black arrow). B, posteroventral view showing posterior end of the right suture (black arrow), the cytoproct with protruding cilia (white arrow), the inconspicuous left suture (black arrowhead), and the posterior end of the paroral membrane (white arrowhead). C, detail view of the peristomial overture showing adoral membranelles (black asterisk), cilia of the posterior end of the paroral membrane (black arrows), dikinotids of the posteriormost circumperistomial kinety (white arrowheads), and cilia of the circumperistomial kineties (white arrow). D, detail [same cell as (B)] showing the single file of basal bodies comprising the posterior part of the paroral membrane (white arrowhead), cilia of the paroral (black arrow), and the left suture (asterisk). Scale bars: 20 μm (A, B), 10 μm (C, D).

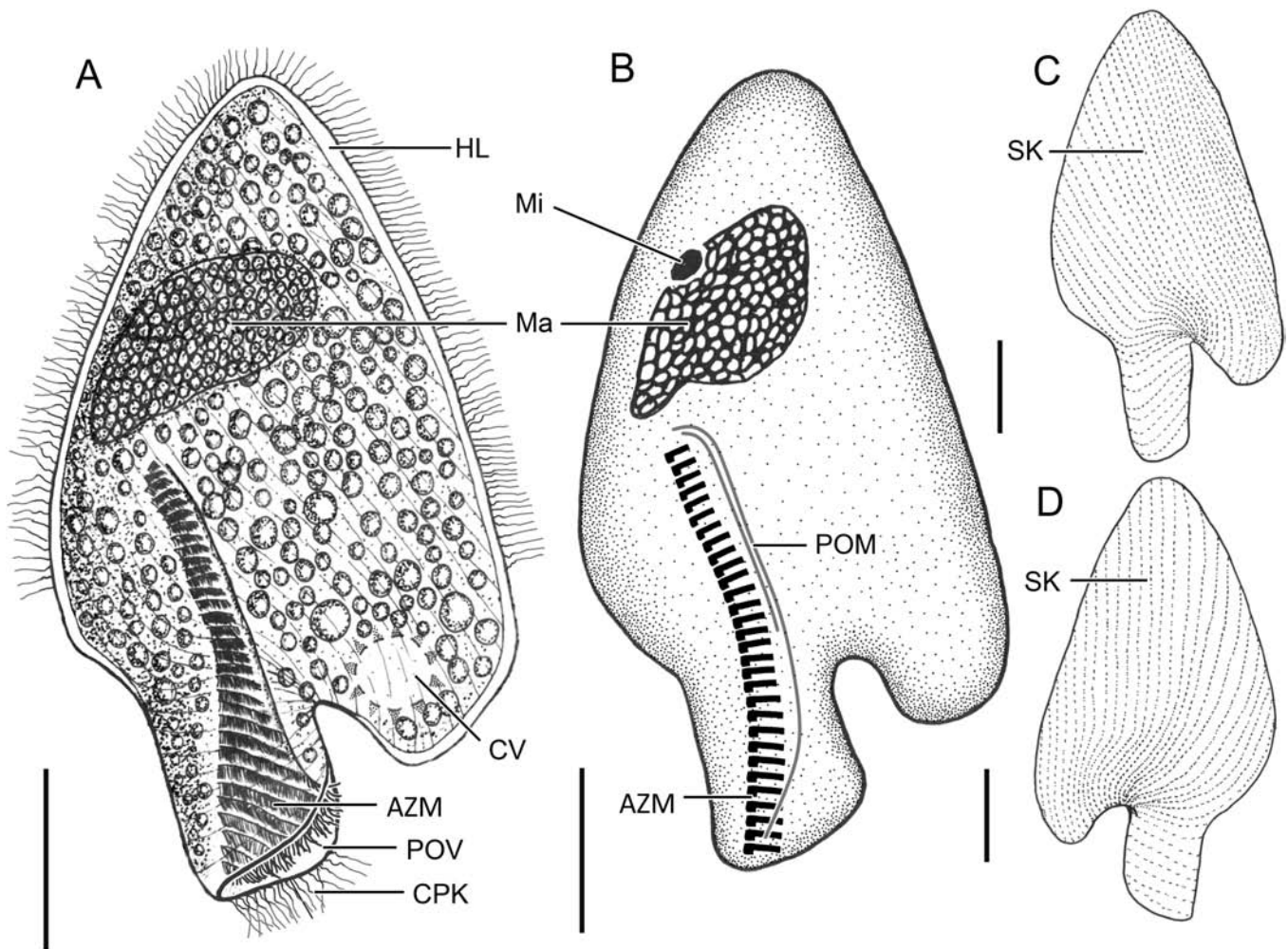


Figure 6. Schematic drawings of *Clevelandella philipi* sp. nov. from life (A) and after protargol impregnation (B–D). A, ventral view of a typical individual. B, ventral view showing the oral apparatus and nuclear structures. C, ventral infraciliature. D, dorsal infraciliature. AZM, adoral zone of membranelles; CPK, cilia of circumperistomial kineties; CV, contractile vacuole; HL, hyaline subcortical layer; Ma, macronucleus; Mi, micronucleus; POM, paroral membrane; POV, peristomial overtire; SK, somatic kineties. Scale bars: 20 μm .

Clevelandella sidi sp. nov.

(Figs 14, 15; Supporting Information, Table S12)

Description based on population from a single SRU host individual from Cambodia: Medium-sized, spade-shaped *Clevelandella*, size *in vivo* 126–154 \times 50–64 μm , usually about 142 \times 59 μm , in protargol preparations 95–142 \times 37–59 μm , usually about 117 \times 46; cell dorsoventrally flattened, prominent notch between left lobe and peristomial projection; peristomial projection about 28% of cell length, peristomial overtire extends to about three-quarters of peristomial projection (Fig. 15A, C). Macronucleus broad inverted teardrop-shaped (Figs 14A, B, 15A–C), in anterior half of cell, narrow end at right cell margin, micronucleus ellipsoidal (usually about 4.5 \times 2.7 μm), adjacent to macronucleus (Fig. 15G); karyophore usually undetectable or inconspicuous in both live, protargol-impregnated cells, located at posterior end of macronucleus (visible in 3 of 15 protargol-impregnated cells) (Fig. 15F). Swims lazily. Somatic ciliature composed of about 80–90 somatic ciliary rows in Clevelandellidae pattern, about 20–25 ciliary rows extend on to peristomial projection; cilia restricted to approximately anterior

half of cell. Sutural kinetofragments absent. Adoral zone usually extends about one-half of body length, composed of an average of 52 membranelles, base of membranelles longest in posterior one-third of adoral zone. POM entirely diplostichomonad (Fig. 15H).

Occurrence: *Clevelandella sidi* was obtained only from one wild-born SRU subadult female. Later, another wild-born female from the same family group and four of her offspring were dissected, but none of them contained *C. sidi*.

Clevelandella fryntai sp. nov.

(Figs 16–18; Supporting Information, Tables S13, S14)

Description based on populations from SRU hosts from Cambodia: Spade-shaped *Clevelandella*, size *in vivo* quite variable 113–189 \times 55–79 μm , usually about 143 \times 63 μm ; size in protargol preparations 110–167 \times 51–82 μm , usually about 130 \times 65 μm ; dorsoventrally flattened, widest in posterior half of cell, anterior end broadly tapered, cell shape varies depending on host and possibly nutritional status, i.e. morphology less variable within

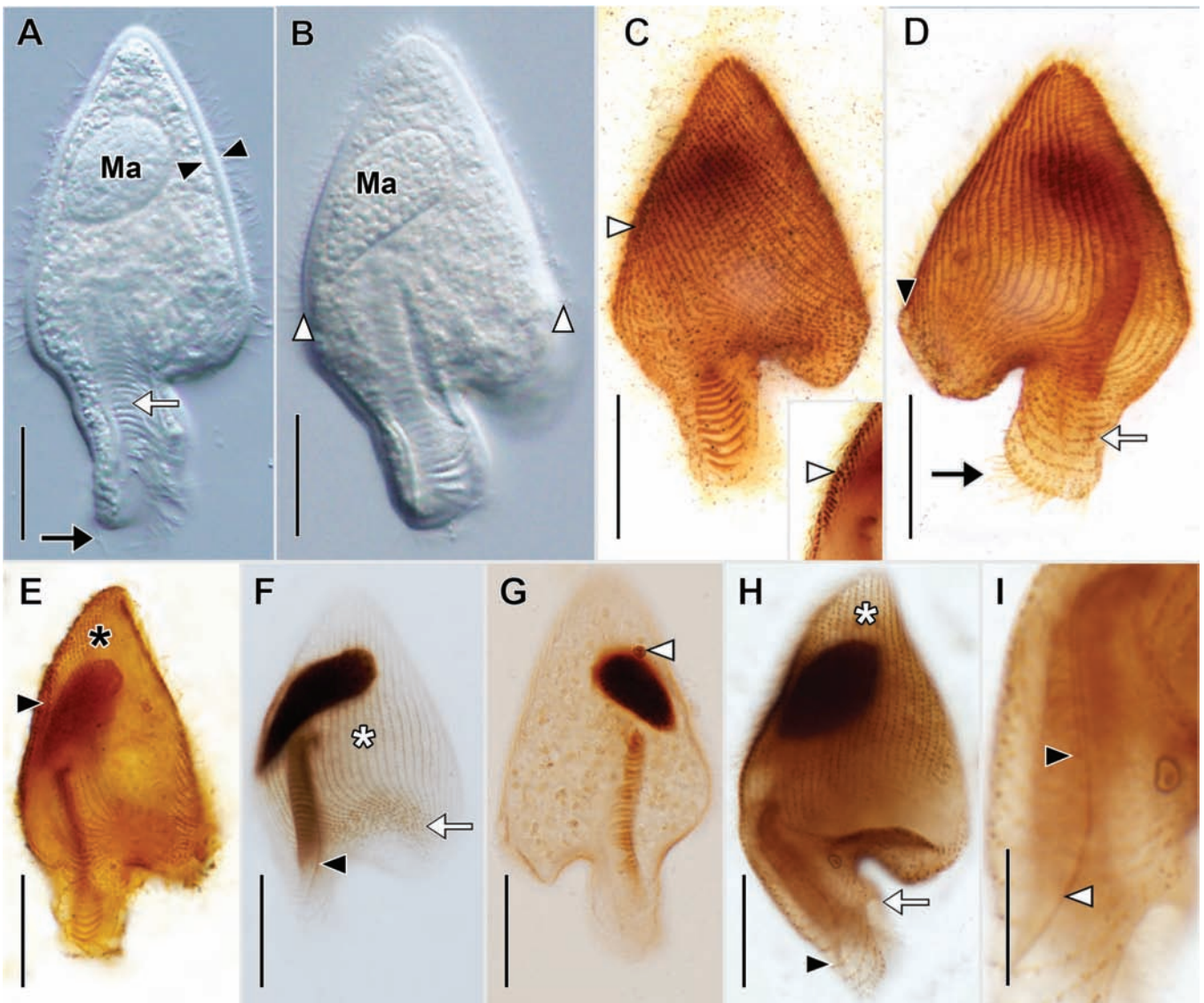


Figure 7. *Clevelandella philipi* sp. nov., *in vivo* (A, B) and after protargol impregnation (C–I). From STH (A–G) and ASS (H, I). A, ventral view showing thick, hyaline cortical layer (between black arrowheads), cilia of the circumperistomial kineties (black arrow) and adoral membranelles (white arrow). B, ventral view showing posterior extent of somatic ciliation (white arrowheads). Note variability of macronuclear shape (A, B). C, ventral infraciliature with detail (inset) showing right sutural kinetofragments (white arrowheads). D, dorsal view showing infraciliature, ciliated circumperistomial kineties (black arrow), looping kineties of peristomial projection (white arrow), and cytoproct (black arrowhead). E, ventral view showing left-hand spiralling ventral somatic kineties (black asterisk) and right sutural kinetofragments (black arrowhead). F, dorsal view showing straight somatic kineties (white asterisk), disordered basal bodies on left protuberance (white arrow), and paroral membrane (black arrowhead). G, dorsal view showing micronucleus (white arrowhead). H, dorsal view showing straight dorsal somatic kineties (asterisk), proximal margin of the peristomial overture (white arrow), and looping kineties of peristomial projection (black arrowhead). I, detail view showing diplostichomonad paroral membrane composed of shorter right file (black arrowhead) and longer left file (white arrowhead) of basal bodies. Ma, macronucleus. Scale bars: 20 μm (A–H) 10 μm (I).

than between hosts, well-fed cells plump (L/W ratio about 2.6), less well-fed cells narrower (L/W ratio about 2.1), cells of intermediate length–width ratio common (range 1.6–2.8). Peristomial projection length relative to cell length quite variable depending on nutritional status (average in all cells about 19%; about 25% in more slender, less well-fed cells; about 17% in plumper, well-fed cells), peristomial overture extends nearly entire length of peristomial projection regardless of nutritional state (Fig. 18A–D). Macronucleus in anterior half of cell, inverted teardrop-shaped (Fig. 17G) to lenticular (Fig. 17B, H),

chromatin granular; micronucleus distinctly ellipsoidal (Fig. 17H), adjacent to macronucleus, about $7 \times 4 \mu\text{m}$. Presence of karyophore highly variable, not seen or quite inconspicuous *in vivo*, when present, appearance in protargol preparations (Fig. 17G) highly variable (seen at anterior and posterior ends of macronucleus in 11 of 39 cells, anterior end only in 7 of 39 cells, at posterior end only 4 of 39 cells, undetectable in 17 of 39 cells). Swims lazily. Somatic ciliature composed of about 80–100 somatic ciliary rows in Clevelandellidae pattern, about 20–25 ciliary rows extend on to peristomial projection, somatic

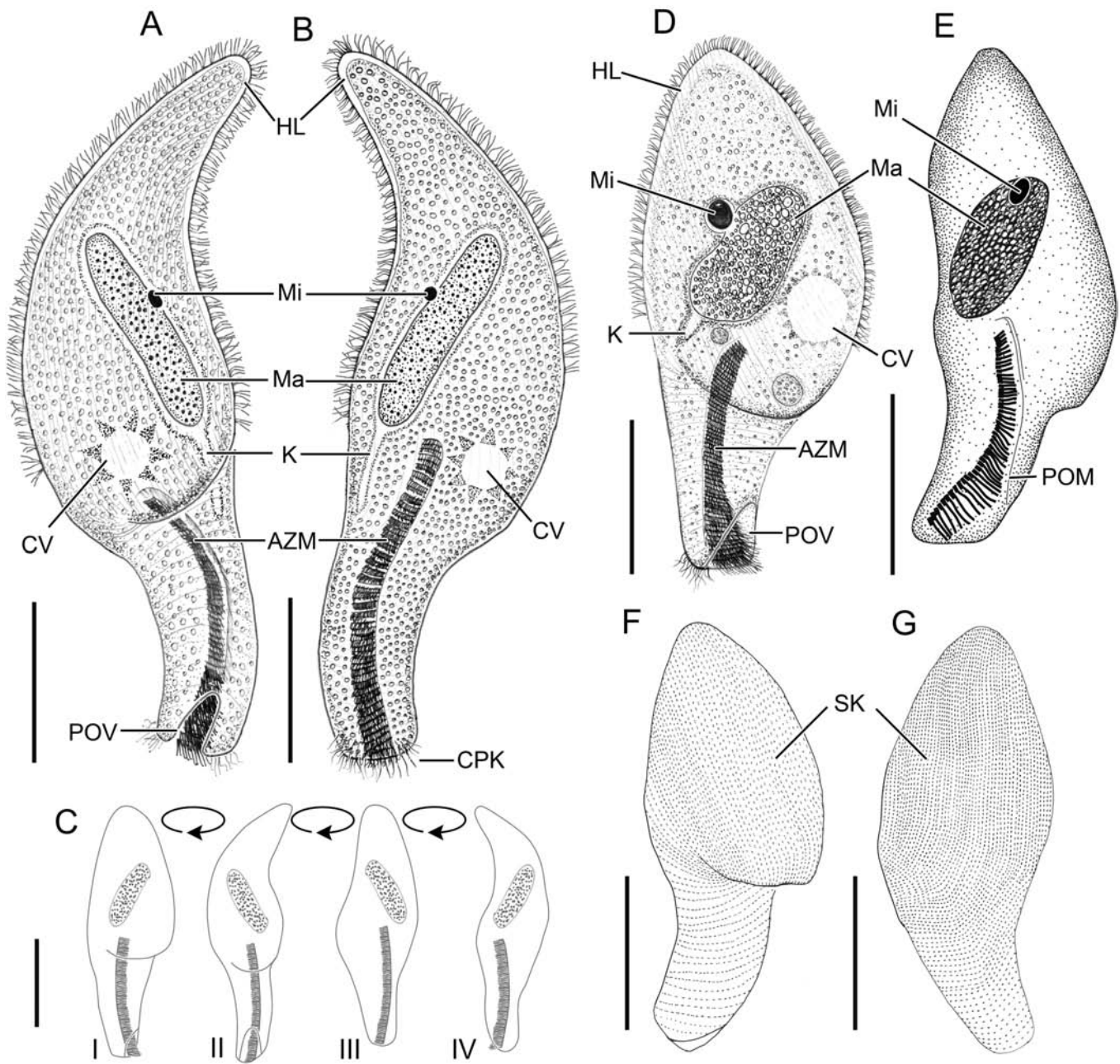


Figure 8. Schematic drawings of *Clevelandella hromadkai* sp. nov. from life (A–D) and after protargol impregnation (E–G); long morphotype (A–C), short morphotype (D–G). A, left lateral view. B, right lateral view. C, (I–IV) cell outline in clockwise rotation around long axis. D, ventral view. E, ventral view. F, ventral infraciliature. G, dorsal infraciliature. AZM, adoral zone of membranelles; CPK, cilia of circumperistomial kineties; CV, contractile vacuole; HL, hyaline subcortical layer; K, karyophore; Ma, macronucleus; Mi, micronucleus; POM, paroral membrane; POV, peristomial overtire; SK, somatic kineties. Scale bars: 50 μm .

cilia restricted to approximately anterior two-thirds of cell except for four or five ciliated circumperistomial kineties. Sutural kinetofragments absent. Adoral zone usually extends about 45% of body length, composed of an average of 60 membranelles, base of membranelles longest in posterior one-third of adoral zone. POM as described for the family.

Remarks on phenotypic variability: Two genetically different populations were detected in SRU host: (i) (Fig. 17A) and (ii) (Figs 17B–K, 18). Cells of population (i) were markedly larger than cells of population (ii)—cell size *in vivo*

180 \times 65 μm vs. 141 \times 64 μm (Supporting Information, Tables S13, S14).

Based on overall morphology, the cells can be divided into two more or less distinct morphotypes: slender (Figs 16A, 17A, B, G, 18A, B) and broad (Figs 16B–E, 17C–E, H–K, 18C–F). In population (i) only the slender morphotype was detected.

Occurrence: *Clevelandella fryntai* occurred in all six dissected SRU individuals (all from the same family group). Population (i) was detected in only one individual (subadult female), the very same in which *C. sisi* (see above) was found. The five remaining hosts

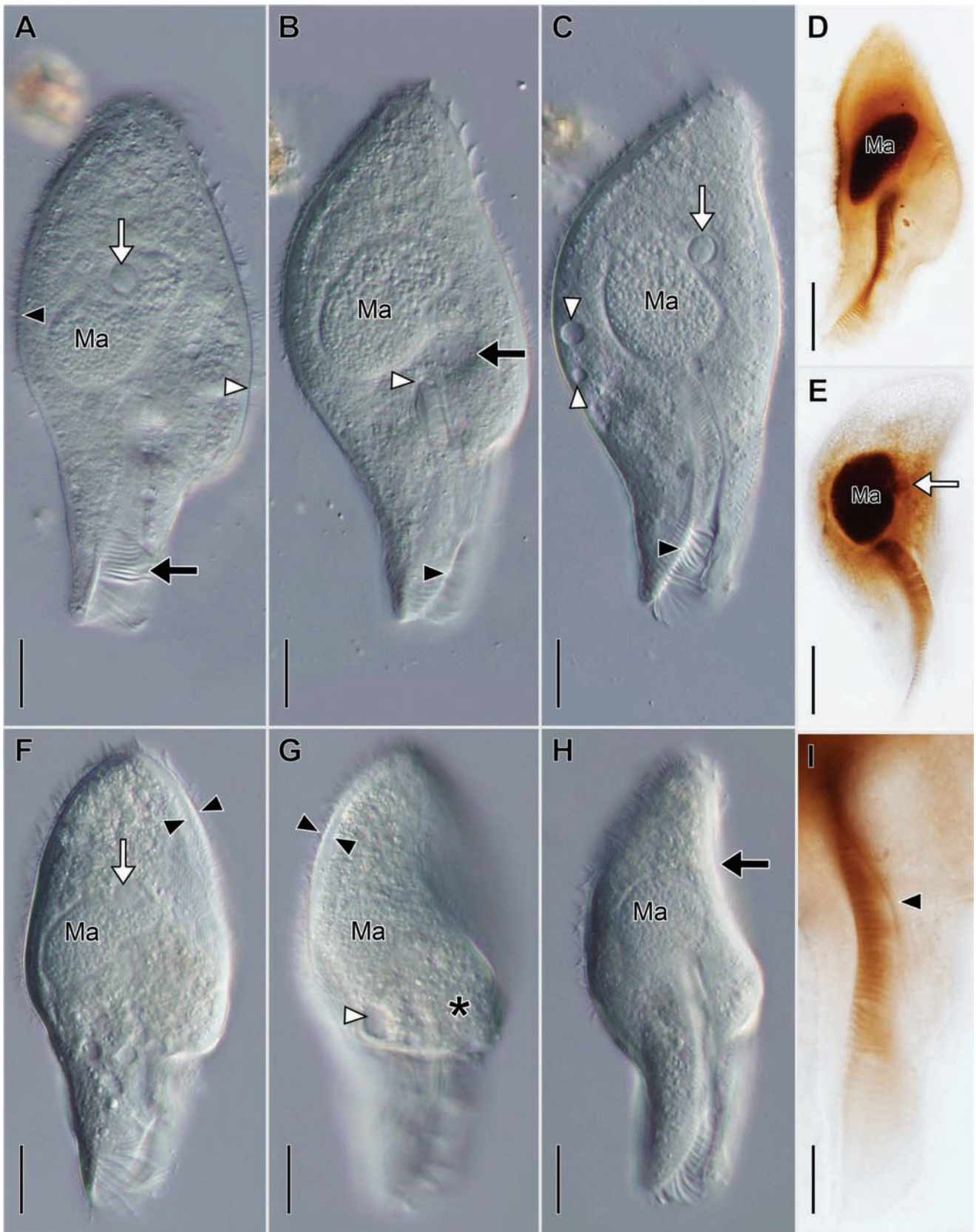


Figure 9. *Clevelandella hromadkai* sp. nov. short morph: from life (A–C, F–H) and after protargol impregnation (D, E, I). From ASS. A, left ventrolateral view showing micronucleus (white arrow), adoral membranelles (black arrow), and the posterior extent of ciliation on the right (black arrowhead) and left (white arrowhead) margins. B, ventral view, (optical section) showing the cytostome (white arrowhead), contractile vacuole (black arrow) and margin of the peristomial overture (black arrowhead). C, left lateral view showing collecting vesicles of the contractile vacuole (white arrowheads), the micronucleus (white arrow) and the margin of the peristomial overture (black arrowhead). D,

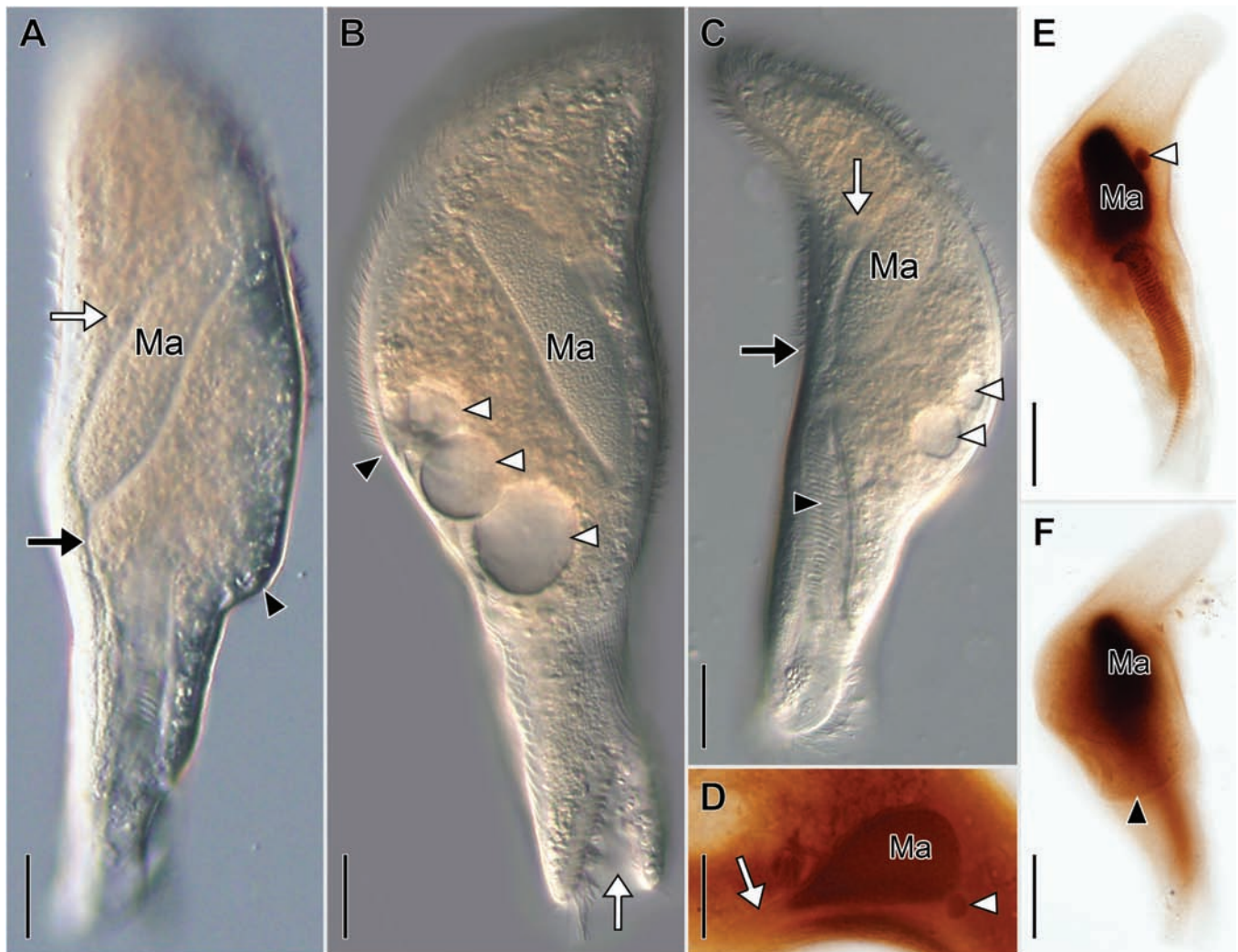


Figure 10. *Clevelandella hromadkai* sp. nov. long morph from life (A–C) and after protargol impregnation (D–F). From ASS (A, E, F), and PAC (B–D). A, ventral view showing micronucleus (white arrow), left protuberance (black arrowhead), and karyophore (black arrow). B, left ventrolateral view showing peristomial overtube (white arrow), collecting vesicles of contractile vacuole (white arrowheads), and the posterior extent of ciliation on the left ventrolateral margin (black arrowhead). C, right dorsolateral view showing contractile vacuole collecting vesicles (white arrowheads), the posterior extent of ciliation on the dorsolateral margin (black arrow), the micronucleus (white arrow), and the adoral membranelles (black arrowhead). D, detail showing micronucleus (white arrowhead) and karyophore (white arrow). E, left ventrolateral view showing micronucleus (white arrowhead). F, (same cell as E) showing posterior margin of left protuberance. Ma, macronucleus. Scale bars: 20 μm (A–C, E, F), 10 μm (D).

harboured population (ii): in four (male, two females, and a larva) of them the slender and broad morphotypes co-occurred and in one (larva) only the slender was present.

Redescriptions of known species of Clevelandellidae

In addition to the newly described species, a number of known species was observed, namely: *Anteclevelandella constricta*, *R. nipponensis*, *R. hastula*, *Paraclevelandia brevis*, *Paraclevelandia simplex*, *C. elongata*, *C. parapanesthia*, *C. kidderi* (we consider *C. lynni*

Pecina and Vdačný, 2020 as a junior synonym of *C. kidderi*, see discussion), and *C. panesthia*. Most, but not all available ciliate populations were morphologically characterized. For known species, except *C. elongata*, which has not been reported since its original discovery by *Kidder (1937)*, descriptions are limited to those characters not previously reported, previously recorded inaccurately (e.g. somatic ciliature), or deviating significantly from previous descriptions. Apart from them, two species were detected but left undescribed, namely: *Rhynchoclevelandella* sp.

left ventrolateral view. E, left lateral view showing micronucleus (white arrow). F, left ventrolateral view showing thick hyaline subcortical layer (black arrowheads) and micronucleus (white arrow). G, ventral view showing left protuberance overlying left cell margin (asterisk), contractile vacuole (white arrowhead), and thick hyaline subcortical layer (black arrowheads). H, left lateral view showing concavity of dorsal surface (black arrow). I, detail of diplostichomonad paroral membrane showing the end of the shorter right file (black arrowhead). Ma, macronucleus. Scale bars: 20 μm (A–H), 10 μm (I).

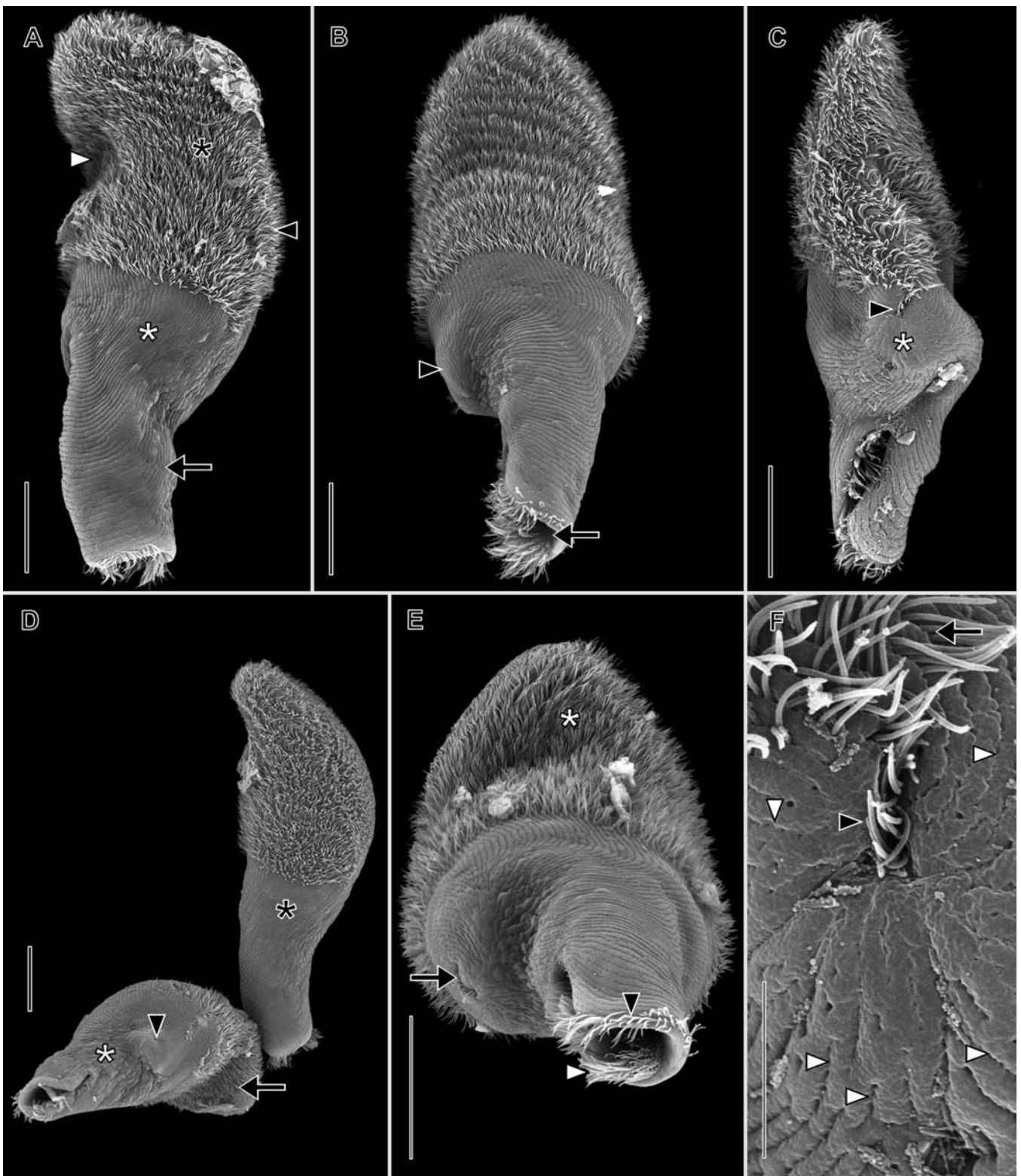


Figure 11. *Clevelandella hromadkai* sp. nov. (from ASS) in the scanning electron microscope. A, right lateral view showing overall cell shape with concave dorsal margin (white arrowhead) and convex ventral margin (black arrowhead), ciliated anterior parts (black asterisk) and unciliated posterior parts (white asterisk) of somatic kineties, and prominent posterior peristomial projection (black arrow). B, posterodorsal view showing left posterior protuberance (black arrowhead) and peristomial overture (black arrow). C, left lateral view showing dorsoventral flattening, cilia protruding from the cytoproct (black arrowhead) on the left protuberance (white asterisk). D, posterodorsal view (down left) showing spiralling somatic kineties (white asterisk) and peristomial overture (black arrow) and right lateral view (black asterisk). E, posterodorsal view showing the cytoproct on the left protuberance (black arrow), the ciliated circumperistomial kineties (white arrowhead), and the adoral membranelles on the right wall of the infundibulum (black arrowhead). F, detail view of the left protuberance showing unciliated parts of kineties (white arrowheads) converging on the ciliated cytoproct (black arrowhead) and the fully ciliated dikinetids of the anterior body part (black arrow). Scale bars: 20 μm (A–E), 5 μm (F).

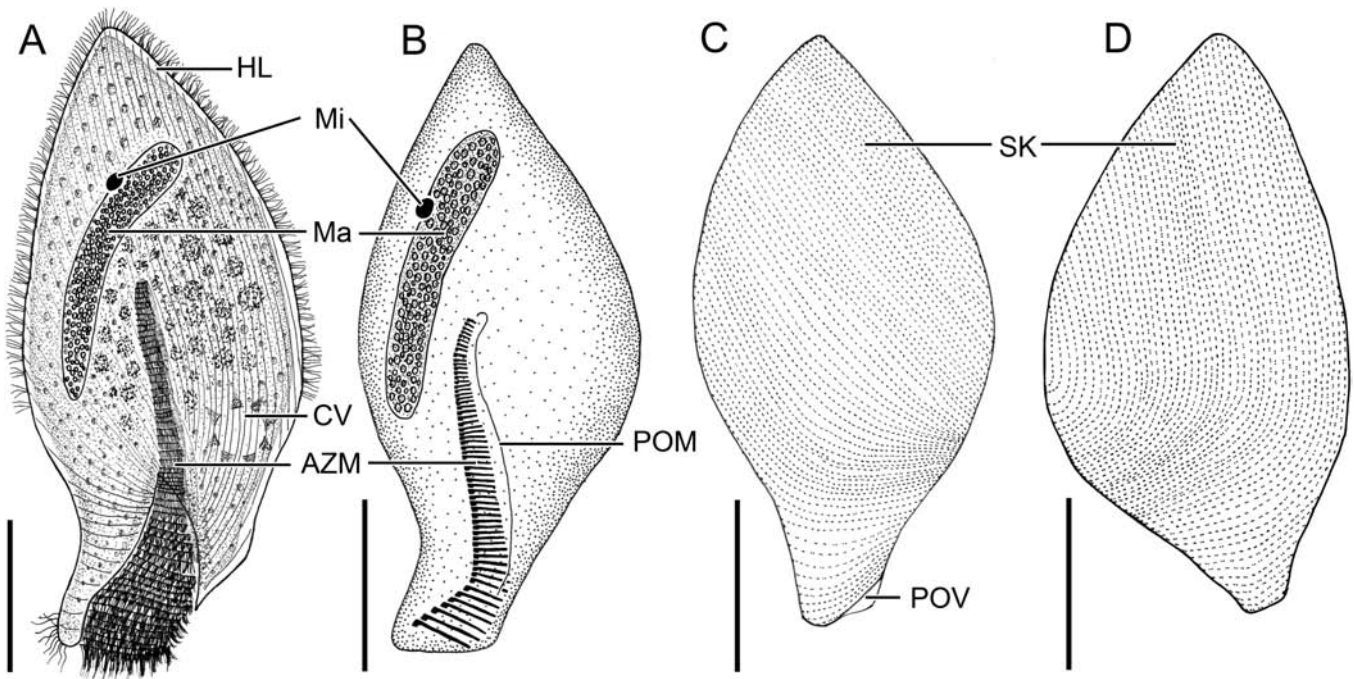


Figure 12. Schematic drawings of *Clevedella klobasa* sp. nov. from life (A) and after protargol impregnation (B–D). A, ventral view of a typical individual. B, ventral view. C, ventral infraciliature. D, dorsal infraciliature. AZM, adoral zone of membranelles; CPK, cilia of circumperistomial kineties; CV, contractile vacuole; HL, hyaline subcortical layer; Ma, macronucleus; Mi, micronucleus; POM, paroral membrane; POV, peristomial overture; SK, somatic kineties. Scale bars: 40 μ m.



Figure 13. *Clevedella klobasa* sp. nov. *in vivo* (A–C) and after protargol impregnation (D). From STH. A, left ventrolateral view showing thick hyaline subcortical layer (white arrowheads), cilia of adoral membranelles (black arrow), and margin of the peristomial overture (black arrowhead). B, left lateral view showing thick hyaline subcortical layer (white arrowheads), contractile vacuole (black arrowhead), and micronucleus (white arrow). C, optical section showing adoral membranelles (black arrow) and contractile vacuole (black arrowhead). D, left ventrolateral view (optical section) showing micronucleus (white arrow), adoral membranelles (black arrowhead), and paroral membrane (black arrow). Ma, macronucleus. Scale bars: 20 μ m.

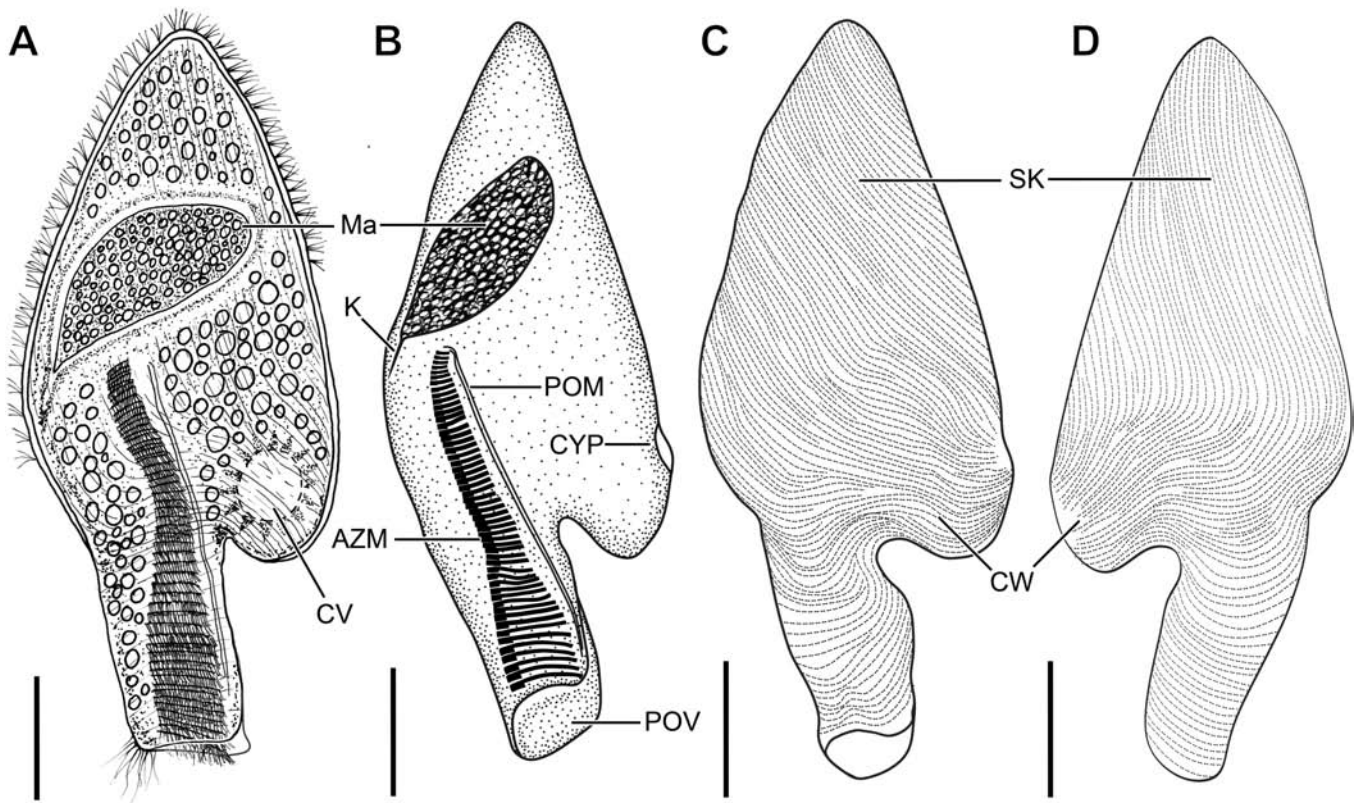


Figure 14. Schematic drawings of *Clevelandella sisi* sp. nov. from life (A) and after protargol impregnation (B–D). A, ventral view of a typical individual. B, ventral view. C, ventral infraciliature (holotype). D, dorsal infraciliature (holotype). AZM, adoral zone of membranelles; CV, contractile vacuole; CW, ciliary whorl of left protuberance; CYP, cytoproct; K, karyophore; Ma, macronucleus; POM, paroral membrane; POV, peristomial overture; SK, somatic kineties. Scale bars: 20 μ m.

2 and *Clevelandella* sp. 4. The hosts infected and the occurrence of individual species are summarized in [Supporting Information, Table S48](#).

Anteclevelandella constricta (Kidder, 1937)

(Figs 19, 20; [Supporting Information, Tables S15–S21](#))

Six populations (ASS, PAA, PRG, SRU, STH #1, and STH #2) were morphologically characterized by both *in vivo* observations and protargol preparations, and one population (PAC) was characterized *in vivo* only. When present, the ciliate was usually abundant.

Description based on the above populations: Medium- to large-sized Clevelandellidae (on average $128 \times 38 \mu\text{m}$ *in vivo*, range $78\text{--}192 \times 21\text{--}67 \mu\text{m}$; on average $117 \times 33 \mu\text{m}$ in protargol preparations, range $94\text{--}142 \times 20\text{--}47 \mu\text{m}$). Shape elongated, cylindrical, transverse constriction at level of macronucleus, anterior cell end broadly tapered, posterior end transversely truncate with short peristomial overture, peristomial projection indistinct since gradually merges with body proper. Macronucleus broadly ellipsoidal, long axis oriented transversely, karyophore at right and left ends of macronucleus. Aggregation of cytoplasmic platelets between macronucleus and anterior end of cell (possibly amylopectin).

Somatic cilia limited to approximately anterior 44% of cell length. About 15 ciliated free transverse kinetofragments,

comprising five basal bodies each, occupy right suture in anterior half of cell (Fig. 18D). Circumperistomial kineties only sparsely ciliated.

Oral ciliature as for the family. Adoral zone extends about 48% of cell length, composed of about 47 membranelles on average (range 36–56).

Remarks: Regarding measured characteristics ([Supporting Information, Tables S15–S21](#)), our populations are slightly larger than Kidder's (1937) isolates, very closely match those of Albaret (1975), and are similar to measurements published by Yamasaki (1939) and Pecina and Vďačný (2020b). Individual populations are very similar except for the number of adoral membranelles, which ranges from mean 39 (PAA) to mean 52 (STH population 1). Pecina and Vďačný (2020b) found similar variability in adoral membranelle number in their Thai population. The only visible shape variation can be seen in STH population 2, which lacks the typical constriction and has a slender, more acutely pointed anterior end, differing somewhat from the typical phenotype (Fig. 19C).

Rhynchoclevelandella nipponensis (Kidder, 1937)

(Fig. 21D–F, J, K; [Supporting Information, Table S22](#))

Rhynchoclevelandella nipponensis was detected and morphologically characterized in a single host population (PAC), never in high abundance.

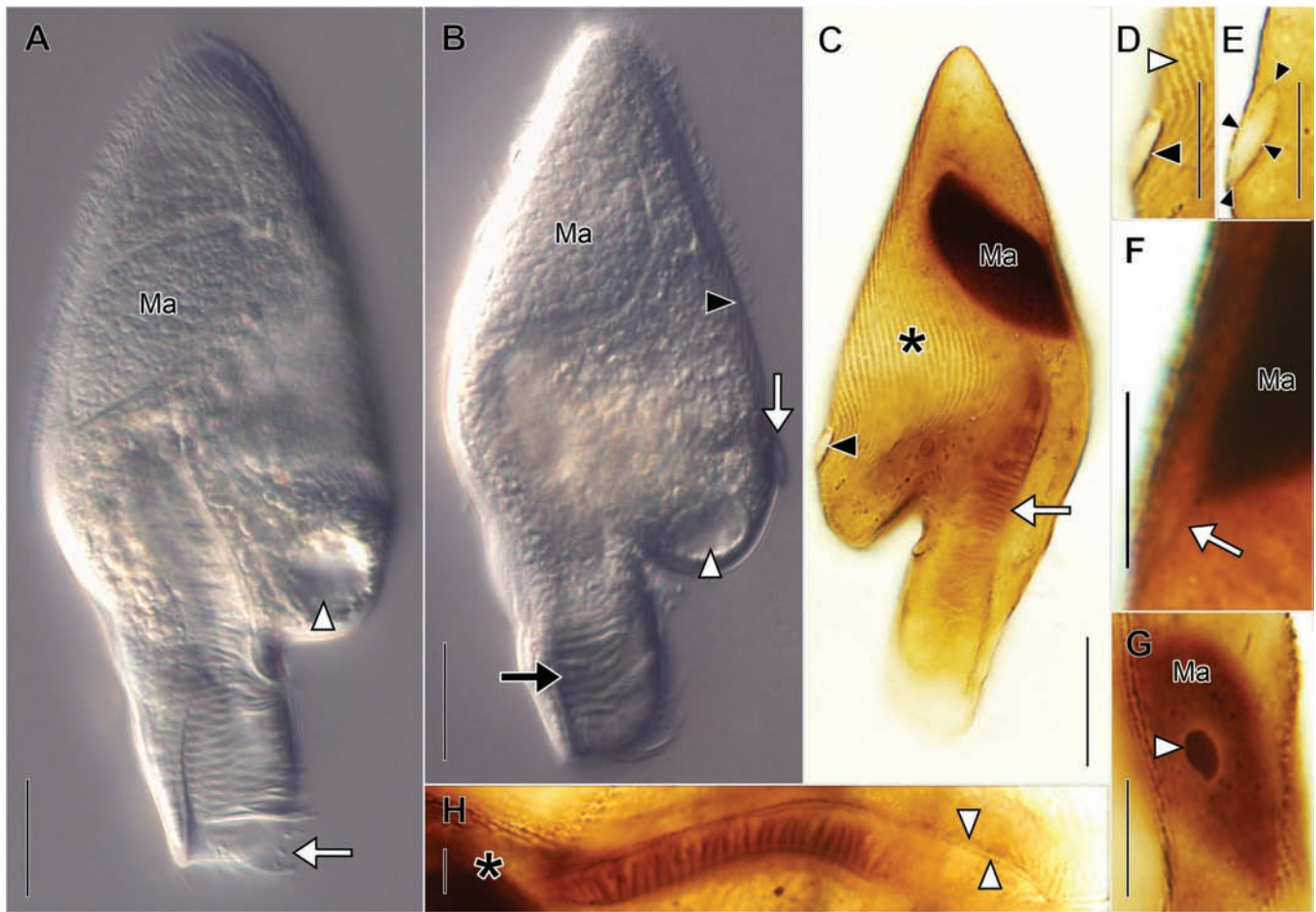


Figure 15. *Clevelandella sidi* sp. nov. *in vivo* (A, B) and after protargol impregnation (C–H). From SRU (A–H). A, ventral view showing contractile vacuole (white arrowhead) and cilia of adoral membranelles (white arrow). B, ventral view showing contractile vacuole (white arrowhead), adoral membranelles (black arrow), and elevated margin of the cytoproct (white arrow). C–E, the same cell in dorsal view: C, showing somatic infraciliature (asterisk), cytoproct (black arrowhead), and adoral membranelles (white arrow); D, showing cytoproct (black arrowhead) and dorsal kineties (white arrowhead); E, optical section showing excretory antrum within the left protuberance (black arrowheads). F, detail of the macronucleus showing the karyophore (white arrow). G, detail showing the micronucleus (white arrowhead). H, detail of the paroral membrane showing both files of equal length and extending nearly to the posterior end of the peristomial projection (white arrowheads), a feature unique to this species. Asterisk marks the anterior end. Ma, macronucleus. Scale bars: 20 μm (A–D) 10 μm (E–G), 5 μm (H, I).

Description based on PAC population: Medium-sized Clevelandellidae (on average $82 \times 33 \mu\text{m}$ *in vivo*, range $67\text{--}100 \times 27\text{--}42 \mu\text{m}$; on average $65 \times 25 \mu\text{m}$ in protargol preparations, range $47\text{--}83 \times 20\text{--}31 \mu\text{m}$). Slender spade-shaped (L/W about 2.6) with long posterior peristomial projection (about 31% of cell length). Anterior right and left margins of body proper straight or concave. Macronucleus broadly ellipsoidal (Fig. 21J, K) to broadly teardrop-shaped (Fig. 21D, F), obliquely oriented to right of midline, prominent numerous globular nucleoli *in vivo*. Karyophore extremely inconspicuous, attached to posterior of macronucleus (Fig. 21K). Micronucleus ellipsoidal (Fig. 21F, K), relatively large, about $5.5 \mu\text{m}$ across. Somatic cilia limited to approximately anterior 64% of cell length. Circumperistomial kineties only sparsely ciliated. Free right sutural kinetofragments not identified, presence of inconspicuous kinetofragments not completely excluded due to suboptimally oriented cells in protargol preparations. Adoral zone extends about 47% of cell length on average, composed of an average of 23 membranelles (range 20–25). POM unstudied.

Remarks: Overall morphology corresponds with original description and drawing by Kidder (1937) except (i) the ciliature: while Kidder (1937) depicts the cell as fully ciliated, we show that only the anterior two-thirds of the cell are ciliated and (ii) the macronuclear shape varies from broadly ellipsoidal (Fig. 21K) to broadly teardrop-shaped (Fig. 21D, F, J).

Regarding measured characteristics (Supporting Information, Table S22), our population is slightly shorter than that of Kidder (1937) and Yamasaki (1939).

A notch sometimes forms at the base of peristomial projection (Fig. 21F, J)—rarely *in vivo* but frequently in protargol-stained cells, creating a *R. hastula*-like appearance. However, *R. nipponensis* can be mostly distinguished from *R. hastula* by: length (approx. $65 \mu\text{m}$ vs. $85 \mu\text{m}$), length/width ratio (approx. 2.6 vs. 3.4), number of adoral membranelles (approx. 23 vs. 26), and characteristic curvature of the most posterior third of peristomial opening in larger cells of *hastula* (Fig. 21L, M). Very small cells of both species (e.g. Fig. 21D, N) can be rather indistinguishable.

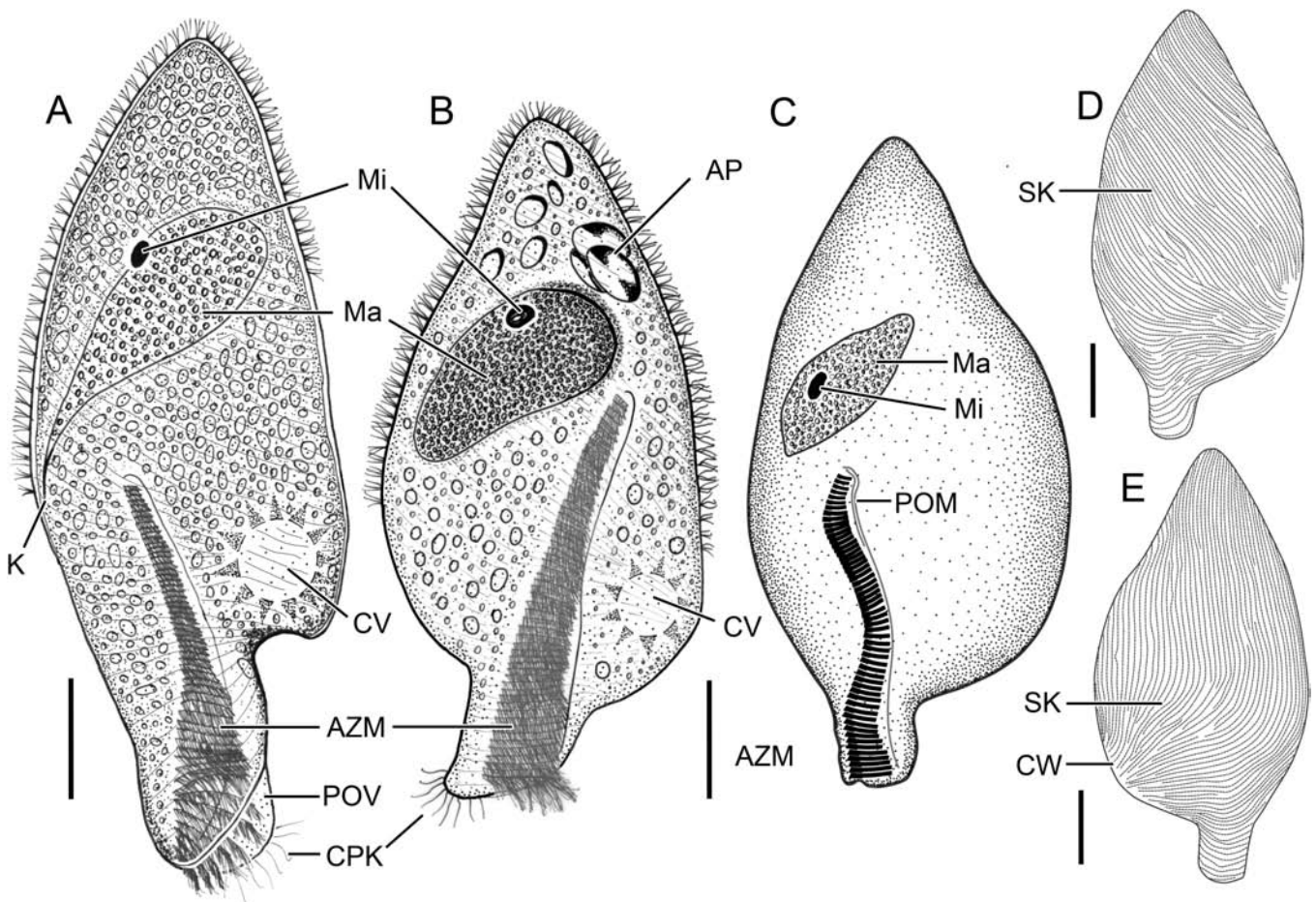


Figure 16. Schematic drawings of *Clevelandella fryntai* sp. nov. from life (A, B) and after protargol impregnation (C–E). From SRU. A, ventral view. B, ventral view. C, ventral view. D, ventral infraciliature. E, dorsal infraciliature. AP, cytoplasmic granules, possibly amylopectin; AZM, adoral zone of membranelles; CPK, cilia of circumperistomial kineties; CV, contractile vacuole; CW, ciliary whorl of left protuberance; K, karyophore; Ma, macronucleus, Mi, micronucleus; POM, paroral membrane; POV, peristomial overtire; SK, somatic kineties. Scale bars: 20 μm .

Rhynchoclevelandella sp. 2

(Fig. 21A–C, G–I; Supporting Information, Table S23)

Rhynchoclevelandella sp. 2 was detected and morphologically characterized in a single host population (ASS), with a very low abundance—no more than 10 individuals in a single host.

Rhynchoclevelandella sp. 2 is morphologically very similar to *R. nipponensis*, albeit a bit smaller: 73 (excluding one unusually large individual) vs. 82 μm *in vivo* and 56 vs. 65 μm in protargol preparations with larger micronucleus (7 \times 4.8 vs. 5.5 \times 3 μm). A single gargantuan cell (146 \times 58 μm) was seen (Fig. 21A) and molecularly characterized.

Rhynchoclevelandella hastula (Kidder, 1937)

(Figs 21L–T, 22; Supporting Information, Table S24)

Rhynchoclevelandella hastula was detected and morphologically characterized in one host population (PGW). The ciliate was present in every dissected PGW individual and moderately abundant.

Description based on PGW population: Small- to medium-sized Clevelandellidae (on average 86 \times 31 μm *in vivo*, 80 \times 28 μm excluding single unusually large (142 \times 53 μm)

individual, range 62–142 \times 23–53 μm ; on average 82 \times 24 μm in protargol preparations, range 64–94 \times 18–31 μm). Slender spear or spade shape (L/W 2.5–3.4 *in vivo*, 2.9–4.2 in protargol preparations), left-sided notch at base of peristomial projection (Fig. 21L, M, P), inconspicuous or absent in smaller cells (Fig. 21N, Q). Posterior peristomial projection conspicuously elongated (about 40% of cell length on average), typically curves rightward (Fig. 21L, M, N, P, Q), in large cells visibly curved in last third (Fig. 21L, M). Macronucleus broadly ellipsoidal, posterior end sometimes pointed (Fig. 21P, S). Karyophore rarely visible, attached to posterior end of macronucleus (Fig. 21O, S). Micronucleus ellipsoidal, about 5.1 μm across. Somatic cilia limited to approximately anterior 60% of cell length. Dorsal kineties almost straight in protargol preparations (Fig. 21R). Free right sutural kinetofragments present (Fig. 21P). Adoral zone extends about 44% of cell length on average, composed of an average of 26 membranelles (range 23–28).

Regarding measured characteristics (Supporting Information, Table S24), our population is slightly broader than that of Kidder (1937) (L/W 2.8 *in vivo*, 3.4 in protargol preparations vs. 3.8).

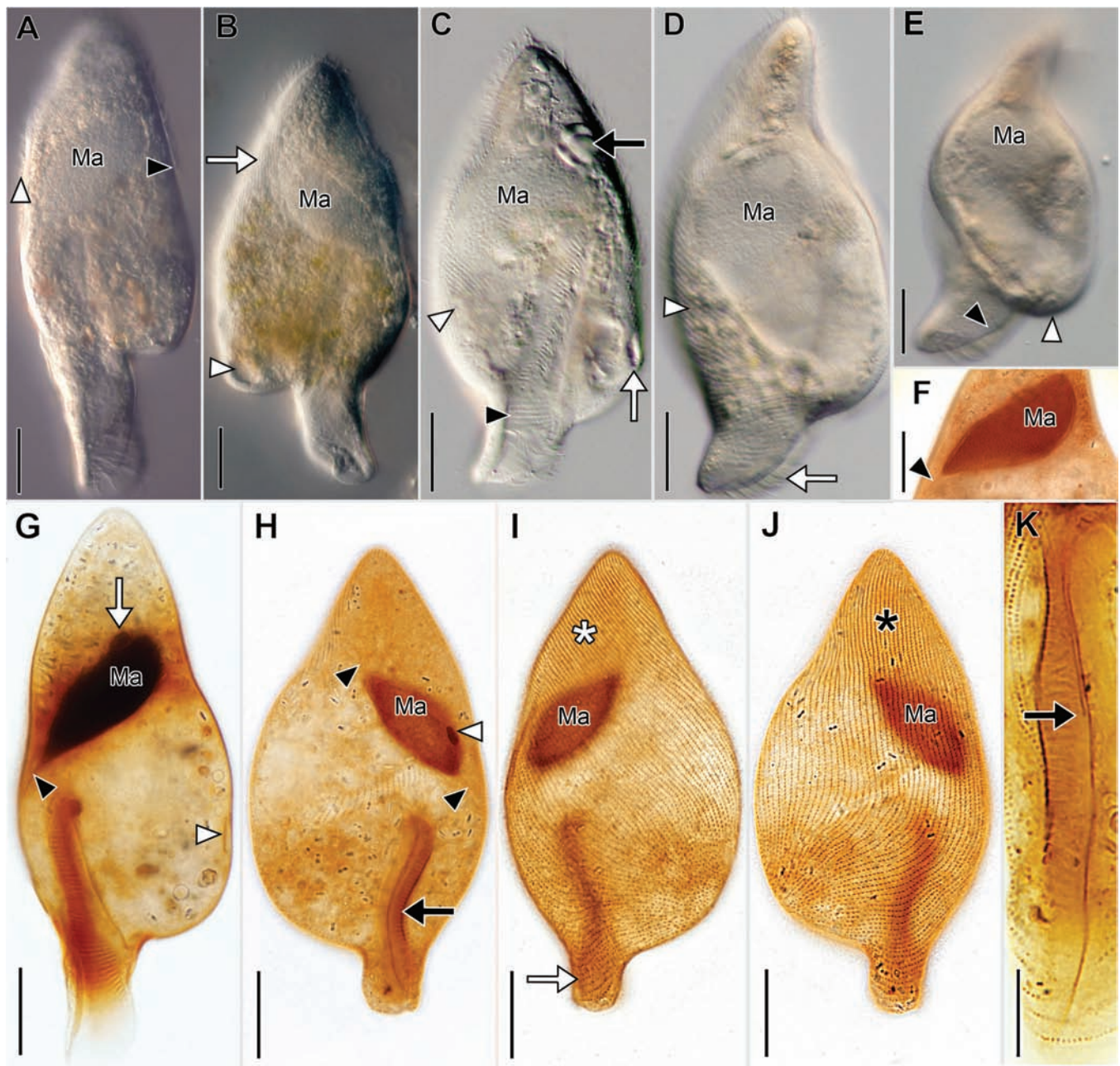


Figure 17. *Clevelandella fryntai* sp. nov. from life (A–E) and after protargol impregnation (F–K). From SRU. (A, B, F, G, K) slender morphotype, (C–E, H–J) broad morphotype. A, ventral view showing posterior extent of ciliation on the right margin (white arrowhead) and left margin (black arrowhead). B, dorsal view showing contractile vacuole (white arrowhead) and straight dorsal kineties (white arrow). C, ventral view (optical section) showing cytoplasmic granules, possibly amylopectin (black arrow), right kinetal suture (white arrowhead), adoral membranelles (black arrowhead), and cytoproct (white arrow). D, ventral view showing left-hand spiralling kineties (white arrowhead) and cilia of adoral membranelles (white arrow). E, ventral view showing the margin of the peristomial overture (black arrowhead) and bulbous left protuberance extending over left cell margin (white arrowhead). F, detail showing karyophore (black arrowhead). G, ventral view (optical section) showing the karyophore (black arrowhead), micronucleus (white arrow), and cytoproct (white arrowhead). H, dorsal view showing karyophore (black arrowheads), micronucleus (white arrowhead), and adoral membranelles (black arrow). I, ventral infraciliature showing left-hand spiralling kineties (asterisk) and looping kineties of the peristomial projection (white arrow). J, dorsal infraciliature showing straight dorsal kineties (asterisk). K, detail view showing diplostichomonad paroral (black arrow). Ma, macronucleus. Scale bars: 20 μm (A–E, G–J), 10 μm (F, K).

Paraclevelandia brevis Kidder, 1937

Synonym: *Paraclevelandia simplex* Kidder, 1937.

Paraclevelandia brevis and *Paraclevelandia simplex* as described by Kidder (1937) represent two forms of a single species (see Discussion), *Paraclevelandia brevis*. For simplicity the two morphotypes are hereafter called ‘brevis’ and ‘simplex’ forms.

Paraclevelandia brevis in ‘brevis’ form

(Figs 23A–G, 24A, B, D, E;
Supporting Information, Tables S25–S29)

When present, the ‘brevis’ form was highly abundant.

Description based on ASS, PAA, PAC, PRG, STH *in vivo*, and PRG and STH *in protargol* preparation: Small Clevelandellidae

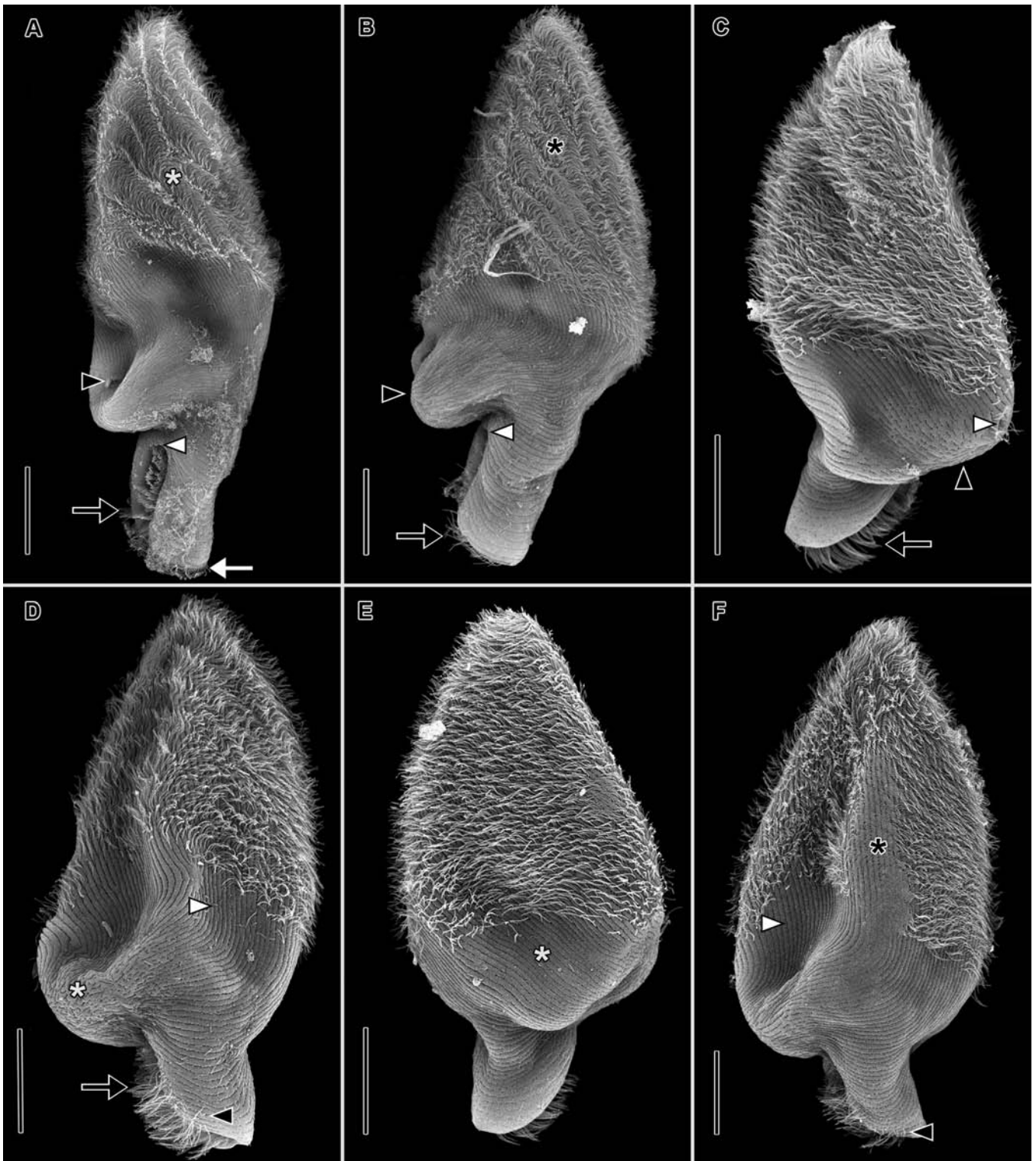


Figure 18. *Clevelandella fryntai* sp. nov. in the scanning electron microscope. From SRU. (A, B) slender morphotype, (C–F) broad morphotype. A, dorsal view showing cytoproct on left protuberance (black arrowhead), anterior margin of peristomial overture (white arrowhead), circumperistomial kineties (white arrow), cilia of adoral membranelles (black arrow), and metachronal ciliary waves (asterisk). B, dorsal view showing the left protuberance (black arrowhead), metachronal ciliary waves (asterisk), the anterior margin of the peristomial overture (white arrowhead), and cilia of the circumperistomial kineties (black arrow). C, ventral view of showing characteristic lateral twisting of left protuberance also seen *in vivo* (black arrowhead, compare Fig. 17E), the cytoproct (white arrowhead) and cilia of the adoral membranelles (black arrow). D, dorsal view showing straight course of the dorsal somatic kineties (white arrowhead), the left protuberance (white asterisk), cilia of the circumperistomial kineties (black arrowhead), and cilia of the adoral membranelles (black arrow). E, ventral view showing left-hand spiralling ventral somatic kineties (white asterisk). F, dorsal view showing straight dorsal somatic kineties (white arrowhead), cilia of circumperistomial kineties (black arrowhead), and area of somatic cilia matted during preparation (black asterisk). Scale bars: 20 μ m.

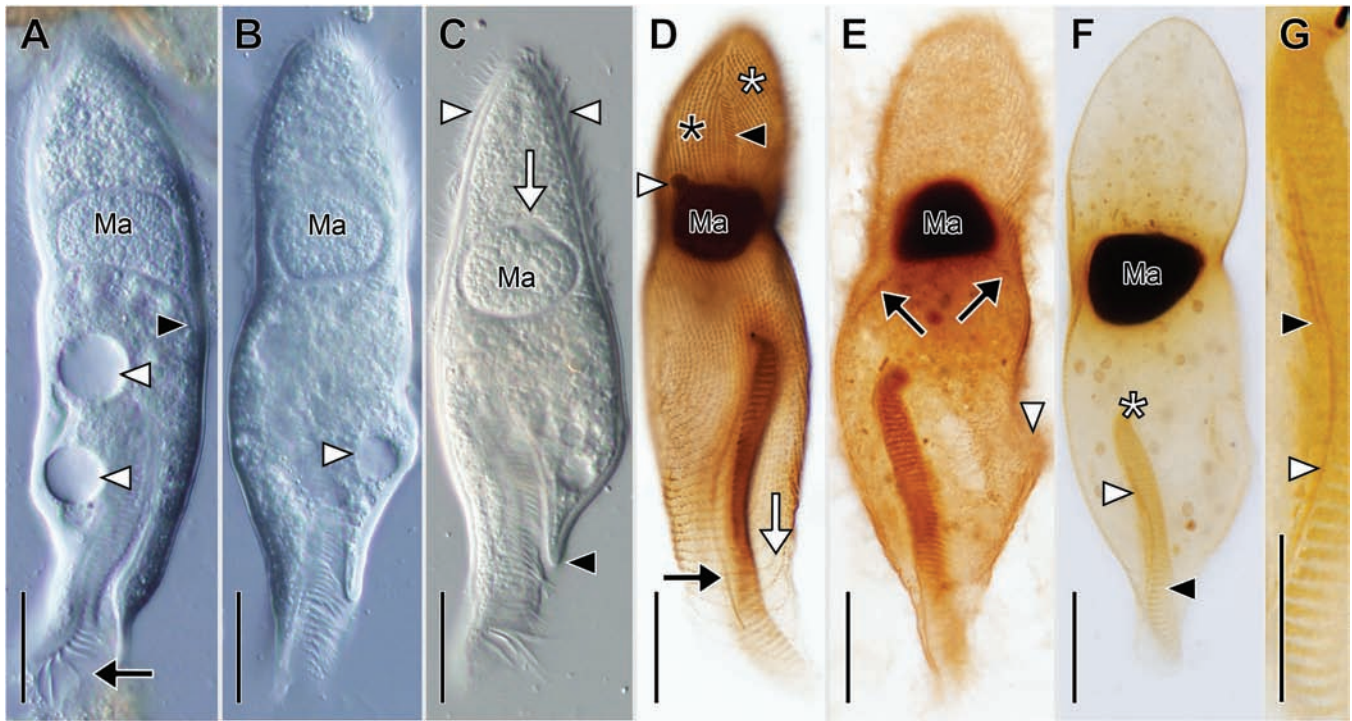


Figure 19. *Anteclelandella constricta* in vivo (A–C) and after protargol impregnation (D–G). From PAA (A), STH population 1 (B) from STH population 2 (C), from ASS (D), from STH population 1 (E), and from SRU (F, G). A, left lateral view (optical section) showing two large contractile vacuole collecting vesicles (white arrowheads), adoral membranelles (black arrow) and left part of the karyophore (black arrowhead). B, ventral; view (optical section) showing contractile vacuole on the small left protuberance (white arrowhead). C, ventral view (optical section) showing shape variation with more narrowly tapered anterior end (white arrowheads), the micronucleus (white arrow), and the margin of the peristomial overture (black arrowhead). D, right lateral view showing kinetofragments in suture between ventral (white asterisk) and dorsal (black asterisk) somatic kineties, micronucleus (white arrowhead), paroral membrane (black arrow), and looping kineties on the peristomial projection (white arrow). E, ventral view (optical section) showing the transverse orientation of the macronucleus with right and left parts of the karyophore (black arrows) and slightly pronounced left lobe (white arrow). F, ventral view showing position of the cytostome (white asterisk), paroral membrane (white arrowhead), and adoral membranelles (black arrowhead). G [same cell as (F)], detail view of the long (white arrowhead) and short (black arrowhead) files of the paroral membrane. Ma, macronucleus. Scale bars: 20 μm (A–F), 10 μm (G).

(on average $44 \times 28 \mu\text{m}$ in vivo, range $34\text{--}58 \times 21\text{--}48 \mu\text{m}$; on average 34×21 in protargol preparations, range $26\text{--}47 \times 15\text{--}28 \mu\text{m}$). Broadly ovate, slightly dorsoventrally flattened, anterior end tapers to rounded point, posterior end transversely truncate. Posterior peristomial projection absent. Peristomial overture on left posterior margin of cell. Macronucleus elongated ellipsoidal, chromatin coarsely granular. Micronucleus ellipsoidal, relatively large ($4\text{--}6 \mu\text{m}$ across), dorsal to macronucleus (Fig. 23D). Karyophore not detected. A sack-like structure formed between anterior margin of macronucleus and anterior end of cell as reported by Kidder (1937, 1938), not evident in protargol preparations (Fig. 23A). Cortex with refractile interkinetal granules, probably mucocysts (Fig. 23B). Somatic kineties strongly spiralled leftward (Fig. 24B). Somatic cilia absent on right, ventral, left parts of posterior cortex (Fig. 24A, B, E), extend to posterior cell margin dorsally. Kinetal furrows prominent. Two ciliated circumperistomial kineties. About 10 ciliated kinetofragments in midportion of right suture, increase in length from posterior to anterior (Figs 23E, F, 24B, D). Organization of oral ciliature as for the family except, in absence of peristomial projection, oral structures are situated in body proper (Fig. 23A, B, D, H, J). Adoral zone narrows from posterior to anterior, extends about

50% of cell length on average, composed of an average of 15 membranelles (range 14–17).

Paraclelandia brevis in 'simplex' form

(Figs 23H–P, 24C, F; Supporting Information, Tables S30–S33)

When present, the simplex form was present in low to moderate abundance.

Description based on ASS, PAA and STH in vivo, and PAA, STH, and SRU in protargol preparations: Medium-sized Clelandellidae (on average $84 \times 47 \mu\text{m}$ in vivo, range $70\text{--}101 \times 38\text{--}58 \mu\text{m}$; on average 76×45 in protargol preparations, range $61\text{--}98 \times 37\text{--}53 \mu\text{m}$). Ovate to almost broadly fusiform, anterior end tapers to rounded point, posterior end broadly rounded, peristomial projection absent as in 'brevis' form; distinct left lobe absent. Macronucleus elongated, cylindrical, situated longitudinally in anterior half of cell near right cell margin. Micronucleus oval, near midportion of macronucleus, smaller compared to brevis form (3.4 vs. $5.3 \mu\text{m}$). A sack-like structure formed between anterior margin of macronucleus and anterior end of cell

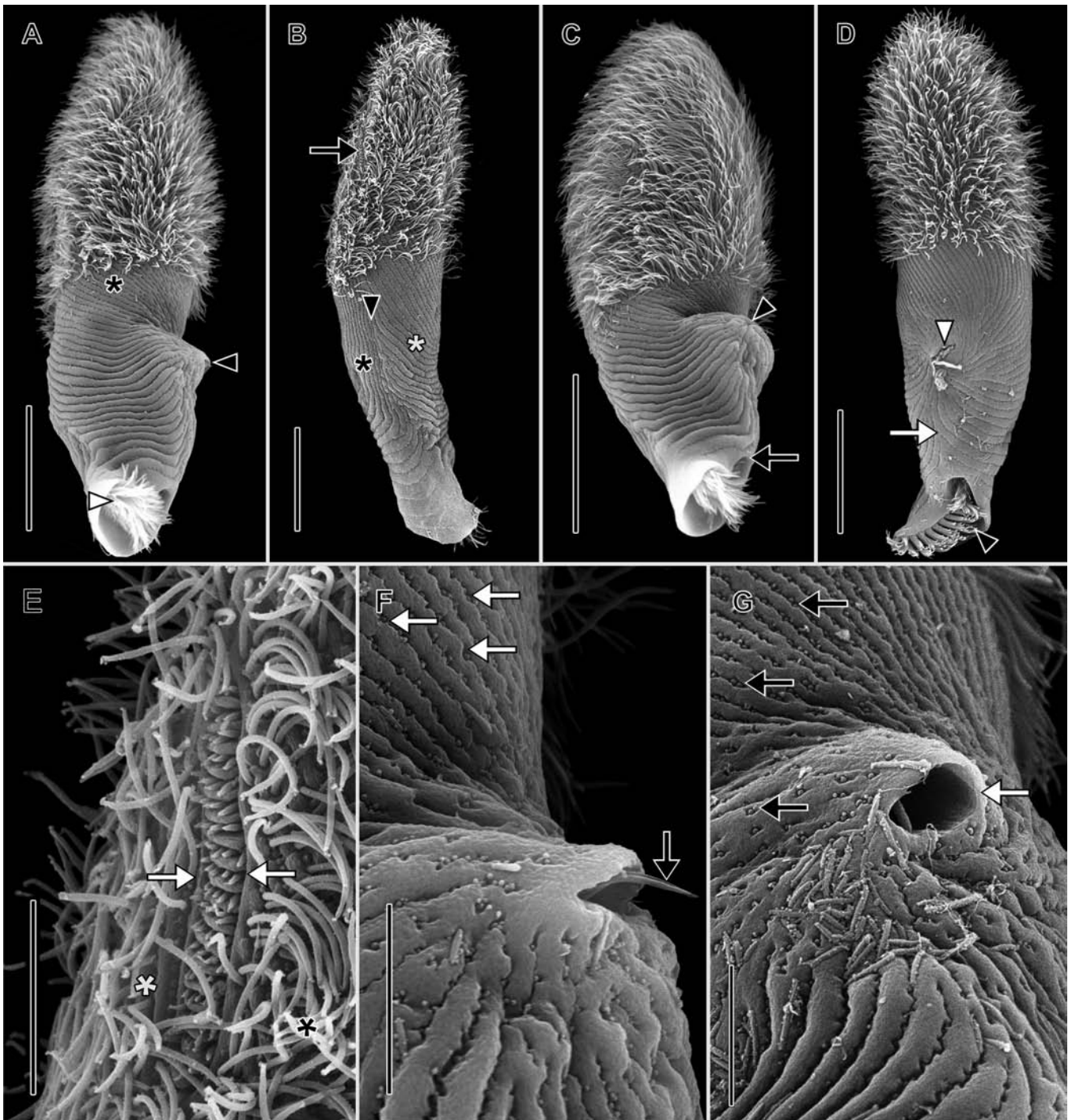


Figure 20. *Anteclevelandella constricta* in the scanning electron microscope. From PAA. A, ventral view showing cilia of the adoral membranelles protruding from the peristomial overture (white arrowhead), the unciliated posterior body part (black asterisk), and cilia protruding from cytoproct on the left lateral protuberance (black arrowhead). B, dorsal view showing the right kinetal suture (black arrowhead) between the dorsal kineties (black asterisk) and ventral kineties (white asterisk) right suture, and sutural kinetofragments (black arrow). C, left ventrolateral view showing position of cytoproct on left posterior protuberance (black arrowhead) and the anterior margin of the peristomial overture (black arrow). D, left lateral view showing the location of the cytoproct (white arrowhead), short left kinetal suture (white arrow), and adoral membranelles (black arrowhead). E, detail of same cell as (B) showing short transverse kinetofragments in anterior part of right suture (white arrows) between dorsal (black asterisk) and ventral (white asterisk) kineties. F, showing the leftward-spiralling ventral kineties which lack normal cilia (white arrows) and a cilium protruding from the cytoproct (black arrow). Scale bars: 20 μm (A–D), 5 μm (E–G).

as reported by Kidder (1937, 1938), visible both *in vivo* (Fig. 23H, I) and protargol preparations (Fig. 23J). Karyophore inconspicuous, not visible *in vivo*, sometimes visible in protargol

preparations (Fig. 23J, O), attached to both anterior and posterior end of macronucleus. Cortex with refractile interkinetal granules, probably mucocysts (Fig. 23I). Somatic ciliature in

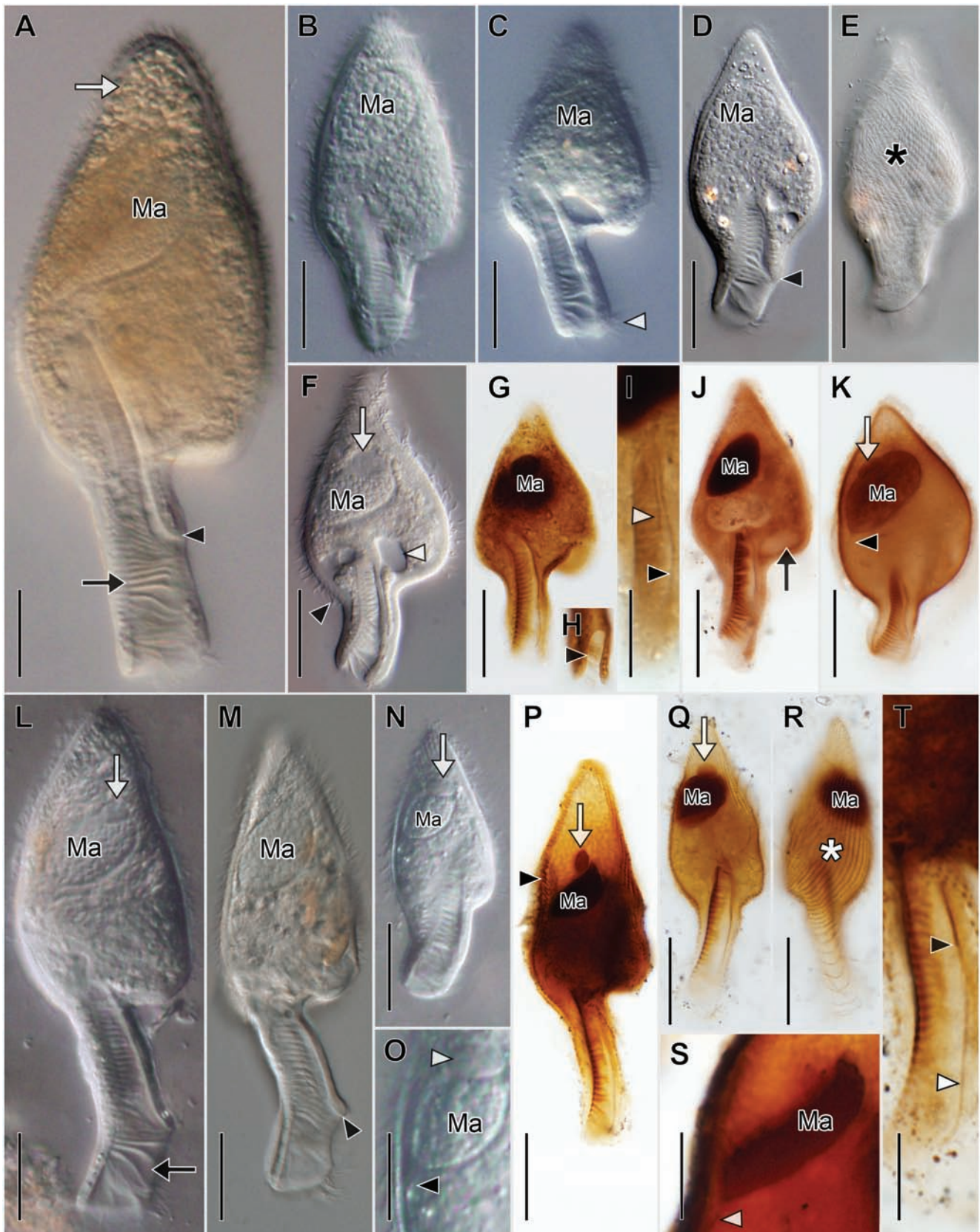


Figure 21. *Rhynchoclevelandella* sp. 2 (A–C, G–I) from ASS. *Rhynchoclevelandella nipponensis* (D–F, J, K) from PAC. *Rhynchoclevelandella hastula* (L–T) from PGW. *In vivo* (A–F, L–O) and after protargol impregnation (G–K, P–T). A, ventral view (optical section) showing margin of the peristomial overture (black arrowhead) and adoral membranelles (black arrow). B, ventral view. C, ventral view showing cilia of circumperistomial kineties (white arrowhead). D, ventral view showing anterior margin of peristomial overture (black arrowhead). E, same cell showing ventral kineties (asterisk). F, ventral view showing contractile vacuole (white arrowhead), the relatively large micronucleus

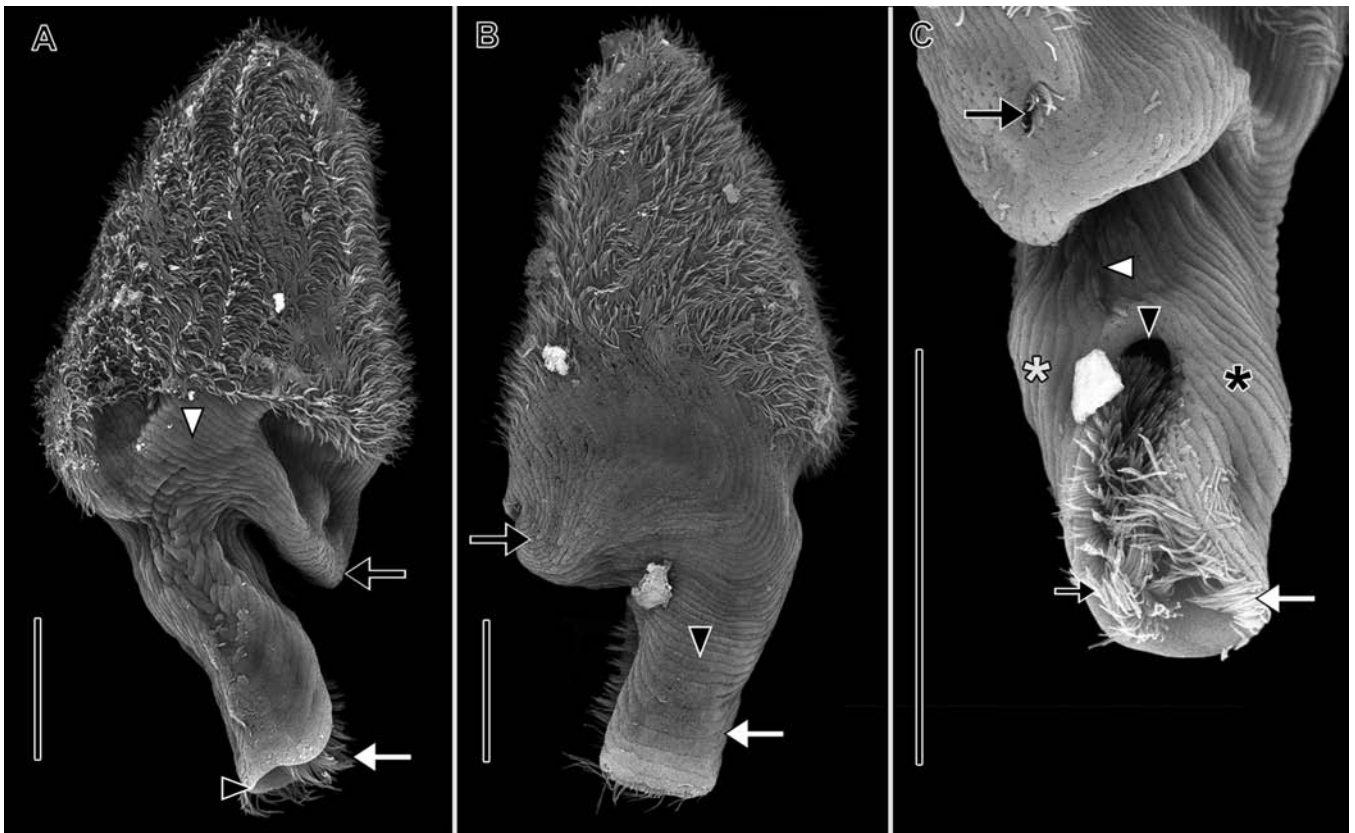


Figure 22. *Clevelandella hastula* in the scanning electron microscope. From PGW. A, ventral view showing collapsed left lobar protrusion (black arrow), right margin of the peristomial overture (black arrowhead), left-hand spiralling unciliated part of ventral kineties (white arrowhead), and cilia of adoral membranelles (white arrow). B, dorsal view showing left lobar protrusion (black arrow) and unciliated parts of dorsal somatic kineties (black arrowhead) on the characteristically elongated peristomial protrusion (white arrow). C, left lateral view of posterior part of cell showing cilia protruding from the cytoproct on the dome of the left lobar protrusion (black arrow), the anterior margin of the peristomial overture (black arrowhead), cilia of the adoral membranelles (small black arrow), cilia of the circumperistomial kineties (white arrow), and the inconspicuous left posterior suture (white arrowhead) between dorsal kineties (black asterisk) and ventral kineties (white asterisk). Scale bars: 20 μm .

same pattern and distribution as ‘brevis’ form. Kinetal furrows conspicuous. Up to 20 free kinetofragments in right suture (Fig. 23K, P). Organization of oral ciliature as for the family with same exceptions as ‘brevis’ form. Adoral zone narrows from posterior to anterior, extends about 50% of cell length on average, composed of an average of 28 membranelles (range 25–32).

Clevelandella elongata (Kidder, 1937)

(Figs 25–27; Supporting Information, Table S34)

Clevelandella elongata was detected and morphologically characterized in one population (SRU). When present, *C. elongata*

was moderately abundant (20–30 cells per host) with the other ciliate species being more abundant.

Description based on SRU population:

Largest member of Clevelandellidae (on average $285 \times 54 \mu\text{m}$ *in vivo*, range $245\text{--}321 \times 43\text{--}71 \mu\text{m}$; on average $220 \times 61 \mu\text{m}$ in protargol preparations, range $184\text{--}259 \times 43\text{--}75 \mu\text{m}$). Elongated, almost vermiform *in vivo*, slightly dorsoventrally flattened, anterior end bluntly pointed, posterior end truncate and slightly flared, ventral margin convex, dorsal margin concave (Figs 25C, 27C). Cells shrink asymmetrically in protargol preparations (see Supporting Information, Table S50) and long axis straightens

(white arrow), and the posterior extent of ciliation on the right margin (black arrowhead). G, H, the same cell in ventral view, with detail of peristomial overture (black arrowhead). I, detail view of the long file (black arrowhead) and short file (white arrowhead) of the paroral membrane. J, ventral view (optical section) showing excretory antrum within left protuberance (black arrow). K, ventral view showing micronucleus (white arrow) and karyophore (black arrowhead). L, ventral view (optical section) showing micronucleus and adoral membranelles (black arrow). M, ventral view (optical section) showing anterior margin of the peristomial overture (black arrowhead). N, ventral view showing relatively large micronucleus (white arrow). O, detail of same cell as (N) showing micronucleus (white arrowhead) and karyophore (black arrowhead). P, ventral view showing micronucleus (white arrow). Q, ventral view showing micronucleus (white arrow). R, dorsal view of same cell as (Q) showing straight dorsal kineties (asterisk). S, detail of karyophore (white arrowhead). T, detail view of the long file (white arrowhead) and short file (black arrowhead) of the paroral membrane. Ma, macronucleus. Scale bars: 20 μm (A–H, J–N, P–R), 10 μm (I, O, S, T).

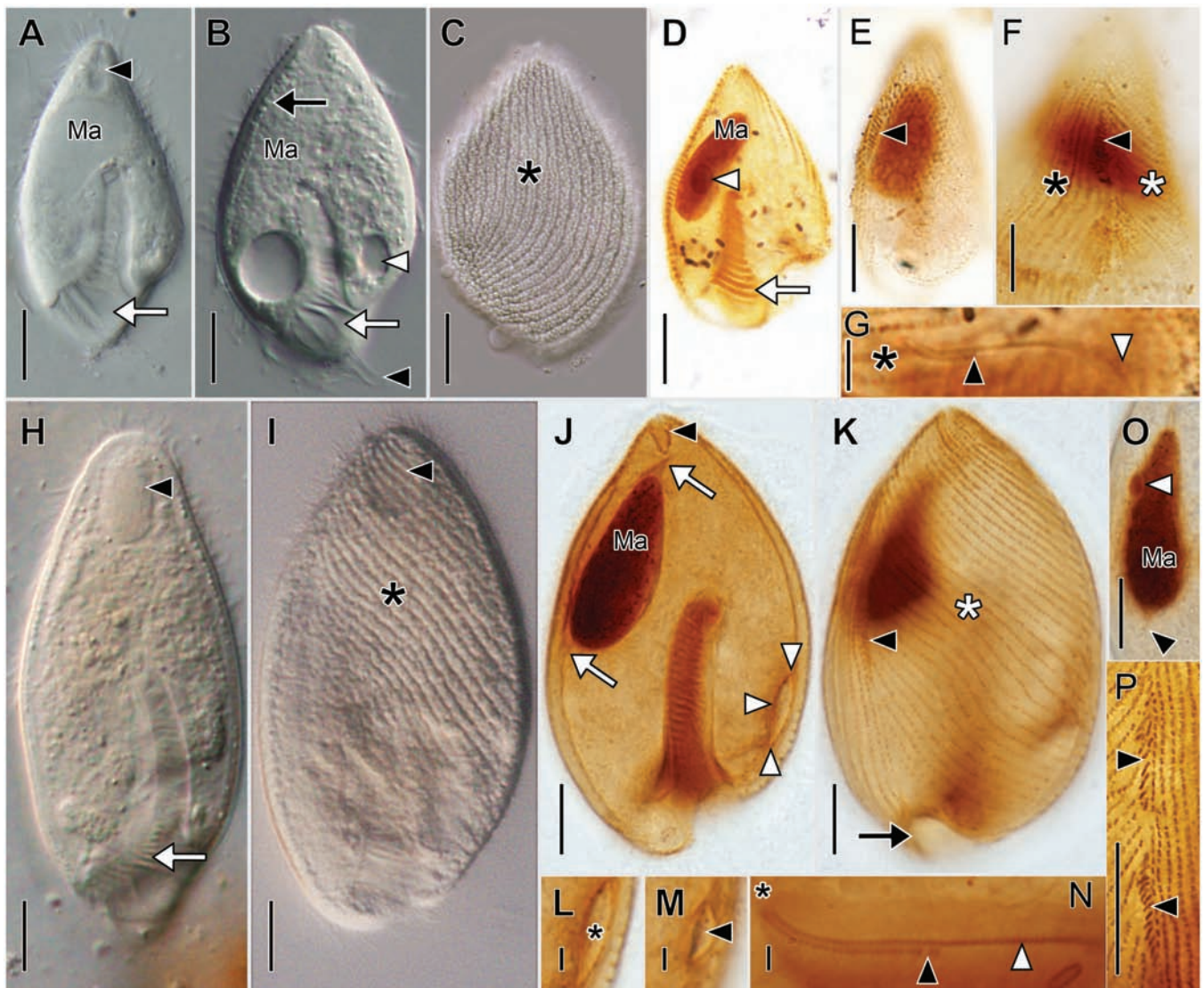


Figure 23. *Paraclevelandia brevis*, from life (A–C, H, I) and after protargol impregnation (D–G, J–P). Small ‘brevis’ morphotype (A–G), large ‘simplex’ morphotype (H–P); from ASS (A, H, I), SRU (J–M, K, O, P), STH (B, N), PAA (C), PGW (D–G). A, ventral view (optical section) showing the apical sac-like structure (black arrowhead) and adoral membranelles (white arrow). B, ventral view showing the subcortical layer of globules (probable mucocysts, black arrow), contractile vacuole (white arrowhead), adoral membranelles (white arrow), and circumperistomial cilia (black arrowhead). C, dorsal view showing relatively straight course of somatic kineties (asterisk). D, Ventral view (optical section) showing the micronucleus (white arrowhead) and adoral membranelles (white arrow). E, right ventrolateral view showing sutural kinetofragments (black arrowhead). F, right lateral view showing sutural kinetofragments (black arrowhead), ventral (white asterisk) and dorsal (black asterisk) kineties. G, detail view showing long (white arrowhead) and short (black arrowhead) files of the paroral membrane, asterisk indicates direction to anterior end of cell. H, ventral view (optical section) showing adoral membranelles (white arrow) and apical sac-like structure (black arrowhead). I, ventral view showing left-hand spiralling somatic kineties (asterisk) and apical sac-like structure (black arrowhead). J–M, the same cell in ventral view: J, optical section showing inconspicuous anterior and posterior karyophore (white arrows), the separate apical sac-like structure (black arrowhead), and elliptical excretory antrum (white arrowheads); K, surface view showing sutural kinetofragments (black arrowhead), left-hand spiralling ventral somatic kineties (asterisk), and peristomial overture (black arrow); L, excretory antrum (asterisk); M, elliptical cytoproct on left protuberance (black arrowhead). N, detail view showing long (white arrowhead) and short (black arrowhead) files of the diplostichomonad paroral membrane. Asterisk indicates anterior end. O, detail of macronucleus and micronucleus (white arrowhead) and karyophore (black arrowhead). P, kinetofragments in right suture (black arrowheads). Ma, macronucleus. Scale bars: 5 μm (A–F), 1.25 μm (G), 10 μm (H–K, O, P), 2 μm (L–N).

compared with more sinuous living specimens. Peristomial projection merges gradually with body proper hampering precise length measurement but, on average 20% of cell length (range 14–23%). Macronucleus broadly lenticular, situated slightly obliquely in anterior half of cell, large relative to cell

(on average $51 \times 24 \mu\text{m}$), karyophore at anterior and posterior ends of macronucleus, usually distinct *in vivo* and in protargol preparations but sometimes indiscernible. Micronucleus large, globular (on average 7 μm diameter), adjacent to anterior end of macronucleus. Somatic cilia arranged in very closely spaced

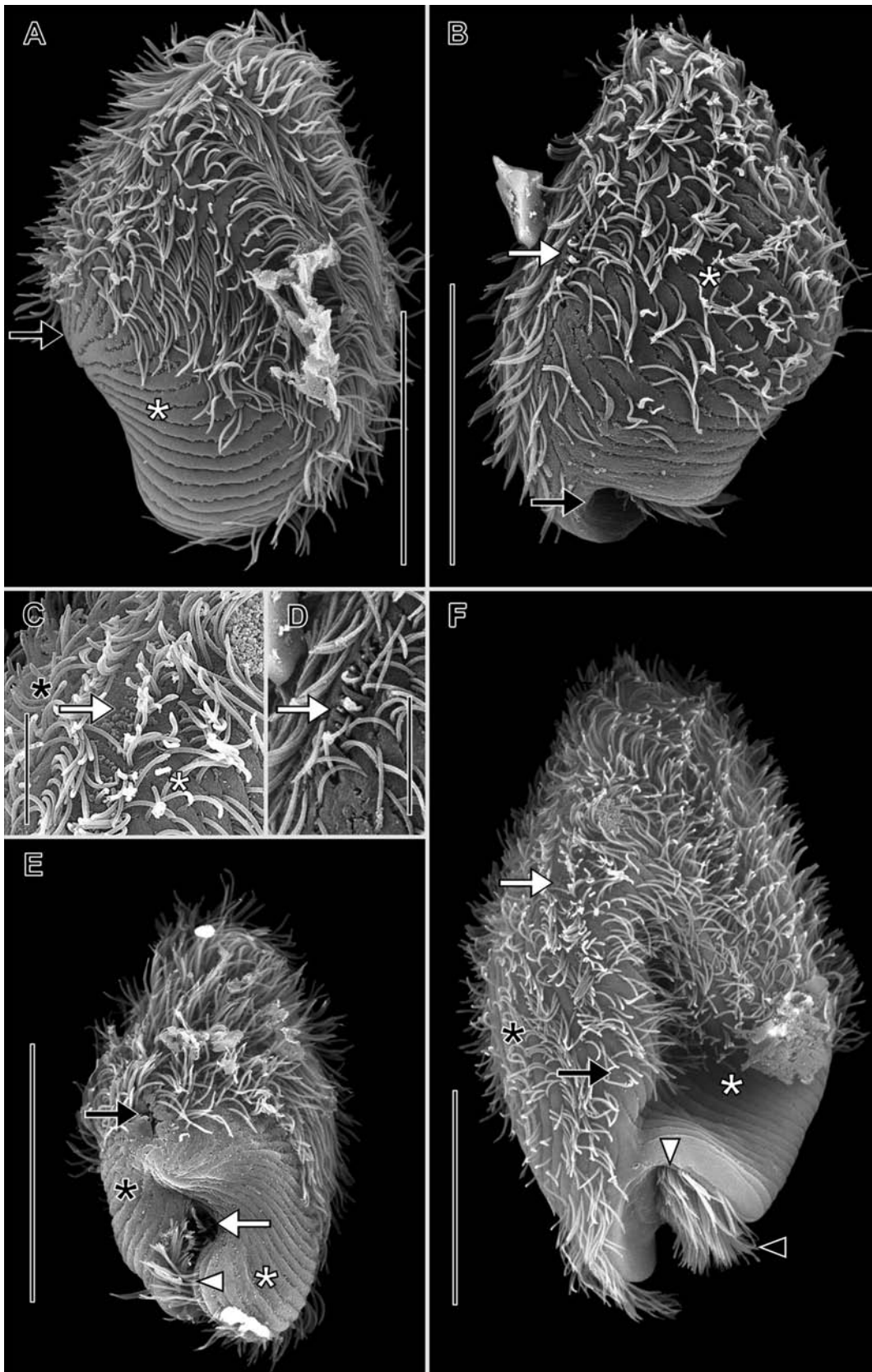


Figure 24. *Paraclevelandia brevis* in the scanning electron microscope. From PAC. Small 'brevis' morphotype (A, B, D, E), large 'simplex' morphotype (C, F). A, dorsal view of showing unciliated posterior parts of dorsal somatic kineties (white asterisk) and convergence of somatic kineties (whorl) on inconspicuous left posterior protuberance (black arrow). B, right ventrolateral view showing right sutural kinetofragments (white arrow) and margin of the peristomial overture (black arrow). C, detail view of right sutural kinetofragments (white arrow) between dorsal (black asterisk) and left-spiralling ventral (white asterisk) somatic kineties, from same cell as (F). D, detail view of same cell as (B)

kineties, somatic cilia limited to approximately anterior 50% of cell, usually a short 'tail' of ciliated cortex extends posteriorly (Fig. 27A, B, D). Right sutural kinetofragments absent. Circumperistomial kineties very densely ciliated (Fig. 27A, B, D, E). Adoral zone extends about 45% of cell length on average, composed of an average of 94 membranelles (range 75–120). POM diplostichomonad only in anterior quarter (Fig. 26A, E).

Remarks: Individuals of our population were longer and distinctly more slender *in vivo* than indicated by Kidder's diagnosis for the species. Kidder (1937) did not specify whether his diagnosis for *C. elongata* was based on measurements from *in vivo* observations or fixed material, although the latter possibility seems most plausible given the technology available at that time.

Clevelandella parapanesthiae (Kidder, 1937)

(Figs 28, 29; Supporting Information, Tables S35–S40)

Four populations (ASS, PGW, PAC, and MP) were morphologically characterized by both *in vivo* observations and in protargol preparations and two (PT and STH) only *in vivo*. The ciliate was moderately to highly abundant.

Description based on ASS, PGW, PAC, and MP populations: Medium-sized *Clevelandella* (on average $99 \times 55 \mu\text{m}$ *in vivo*, range $66\text{--}119 \times 31\text{--}71 \mu\text{m}$; on average $86 \times 46 \mu\text{m}$ in protargol preparations, range $70\text{--}114 \times 33\text{--}56 \mu\text{m}$). Spade-shaped with distinct left notch and protrusive left lobe; peristomial projection short, broad, about 24% of body length. Macronucleus from slender inverted teardrop-shape (Fig. 28A, G, H) to scimitar-like (Fig. 28C, E, F), obliquely oriented, situated right of midline, posterior end extends into posterior part of body proper, karyophore at posterior end of macronucleus, visible only inconsistently *in vivo* and in protargol preparations. In MP population cells with S-like (Fig. 28B) macronucleus (as well as normal teardrop-shaped) were observed. Micronucleus ellipsoidal, inconspicuous. Somatic cilia limited to approximately anterior 67% of cell. About 10 obliquely oriented, free right sutural kinetofragments in the right suture (Fig. 28D). Adoral zone extends about 56% of cell length on average, composed of an average of 38 membranelles (range 35–42). POM diplostichomonad only in anterior quarter (Fig. 28F).

Clevelandella kidderi Mandal and Nair, 1974

(Figs 30, 31; Supporting Information, Tables S41, S42)

One population (ASS) was morphologically characterized by both *in vivo* observations and in protargol preparations and one (PA) only *in vivo*. The ciliate was moderately to highly abundant.

Description based on ASS and PA populations: Medium-sized *Clevelandella* (on average $128 \times 58 \mu\text{m}$ *in vivo*, range $101\text{--}168 \times 44\text{--}72 \mu\text{m}$; on average $94 \times 50 \mu\text{m}$ in protargol

preparations, range $84\text{--}107 \times 42\text{--}59 \mu\text{m}$). Spade-shaped, peristomial projection about 32% of body length, conspicuous left-sided notch at junction of peristomial projection and body proper, left lobe well developed. Macronucleus inverted teardrop-shape with finely granular chromatin, obliquely oriented, situated right of midline in anterior half of body proper. Karyophore at posterior end of macronucleus, visible inconsistently (Fig. 30E). Micronucleus globular near anterior margin of macronucleus. Somatic cilia limited to approximately anterior 60% of cell. Right sutural kinetofragments probably developed (Fig. 30C), but better oriented and stained cells would be needed to know for sure. Adoral zone extends about 58% of cell length on average, composed of an average of 47 membranelles (range 45–49). POM as described for the family (Fig. 30D).

Clevelandella panesthiae (Kidder, 1937)

(Figs 32–34; Supporting Information, Tables S43–S47; Video S1)

Three populations (ASS, PAA, and STH) were morphologically characterized by both *in vivo* observations and in protargol preparations and two (PAC and PT) only *in vivo*. When present, the ciliate was highly abundant.

Description based on ASS, PAA, STH, PAC, and PT populations: Large-sized *Clevelandella* (on average $133 \times 62 \mu\text{m}$ *in vivo*, range $109\text{--}168 \times 43\text{--}84 \mu\text{m}$; on average $114 \times 56 \mu\text{m}$ in protargol preparations, range $93\text{--}157 \times 39\text{--}89 \mu\text{m}$). Broadly spade-shaped, distinct left-sided notch inconspicuous (Figs 32A, 34D, E) or absent (Figs 32B–E, 34A, B). Macronucleus relatively large, slender, inverted teardrop-shape, obliquely oriented in right half of body proper, chromatin finely granular, karyophore not clearly identified *in vivo* or in protargol preparations. Micronucleus ellipsoidal (about $4.5 \times 2 \mu\text{m}$). Somatic cilia limited to approximately anterior 60% of cell. Right sutural kinetofragments absent. Circumperistomial kineties only sparsely ciliated (Figs 32A, 34B). Adoral zone extends about 60% of cell length on average, composed of an average of 47 membranelles (range 42–52). Paroral membrane not studied.

Clevelandella sp. 4

Clevelandella sp. 4 was detected in both dissected STR hosts in which it was highly abundant.

Description based on STR population: Large-sized *Clevelandella* (*in vivo* on average $152 \pm 20 \times 63 \pm 10 \mu\text{m}$, range $127\text{--}185 \mu\text{m}$, $N = 9$), spade-shaped, and dorsoventrally flattened. Left cell margin conspicuously notched at the base of peristomial projection, the lobe does not overhang the peristomial projection. The peristomial projection constituted approx. one-third to one-quarter of cell length.

showing sutural kinetofragments (white arrow). E, left lateral view showing ciliated cytoproct (black arrow), unciliated parts of the dorsal (black asterisk) and ventral (white asterisk) somatic kineties, the peristomial overture (white arrow) and cilia of the circumperistomial kineties (white arrowhead). F, right lateral view showing the right suture (black arrow) between dorsal (black asterisk) and ventral (white asterisk) somatic kineties and sutural kinetofragments (white arrow, compare Fig. 23P), the margin of the peristomial overture (white arrowhead), and the cilia of the adoral membranelles (black arrowhead). Scale bars: 20 μm (A, B, E, F), 5 μm (C, D).



Figure 25. *Clevelandella elongata* in vivo. From SRU. A, ventral view showing adoral membranelles (black arrow), cytostome (white arrow), contractile vacuole (white arrowhead), and hyaline subcortical layer (black arrowheads). B, left ventrolateral view (optical section) showing micronucleus (white arrow), karyophore (black arrows), contractile vacuole (white arrowhead), and posterior extent of ciliation (black arrowheads). C, left ventrolateral view showing micronucleus (white arrow), karyophore (black arrow), and cilia of the circumperistomial kineties (white arrowheads). D, detail of same cell as (C) showing peristomial overture (black arrowhead) and cilia of adoral membranelles (white arrow). Ma, macronucleus. Scale 20 μm .

Morphological analyses of cells

A NMDS (non-parametric multi-dimensional scaling) analysis of 455 morphologically characterized protargol-stained cells showed a significant grouping of cells based on their affiliation

to particular species (Fig. 35). Two clusters were clearly separated along the first NMDS axis, based on the presence/absence of the peristomial projection. The first cluster consisted of *Antelevelandella constricta*, *C. klobasa*, *P. brevis* in 'brevis'

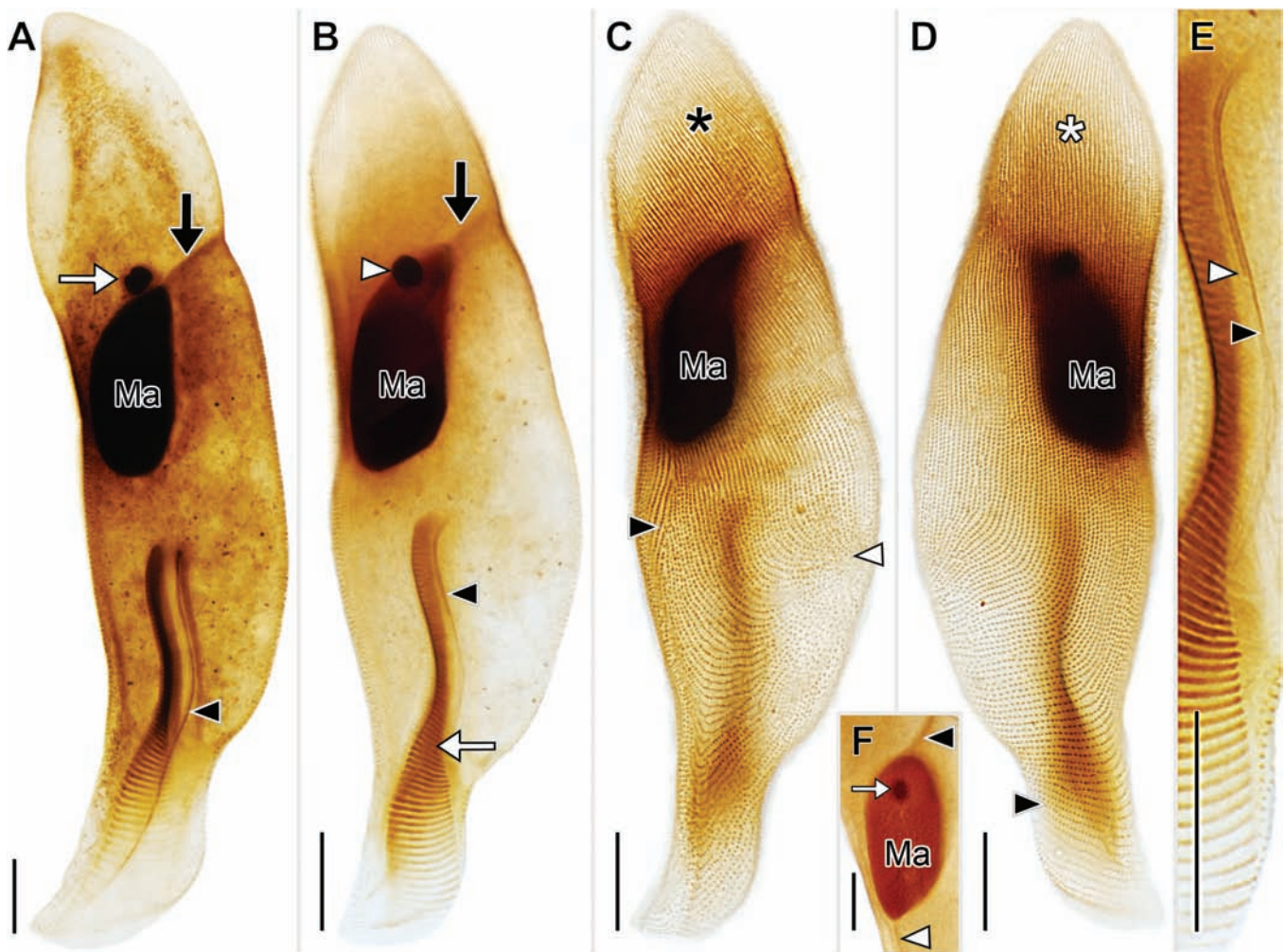


Figure 26. *Clevelandella elongata* after protargol impregnation. From SRU. A, ventral view (optical section) showing micronucleus (white arrow), anterior part of the karyophore (black arrow), and paroral membrane (black arrowhead). B–E, the same cell in ventral view: B, (optical section) showing anterior part of karyophore (black arrow), micronucleus (white arrowhead), adoral membranelles (white arrow), and paroral membrane (black arrowhead); C, ventral infraciliature showing right kintal suture (black arrowhead), left-hand spiralling ventral kineties (asterisk), and kineties converging to form ciliary whorl on inconspicuous left protuberance (white arrowhead); D, dorsal infraciliature showing straight course of dorsal kineties (asterisk) and looping kineties of peristomial projection (black arrowhead); E, detail view of the long file (black arrowhead) and short file (white arrowhead) of the paroral membrane. F, detail showing anterior (black arrowhead) and posterior (white arrowhead) parts of the karyophore and the micronucleus (white arrow). Ma, macronucleus. Scale bars: 20 μm.

form and *P. brevis* in ‘simplex’ form; the second cluster contained remaining species. The second NMDS axis was related to peristomial projection length, macronucleus length, and body width (variable scores -0.054, 0.047, and 0.040, respectively). The linear discriminant analysis (LDA) resulted in the model accuracy of 0.892, meaning that 89.2% of the cells were correctly assigned to the appropriate species based on the morphological traits only. The mean accuracy for all the species was 85%. According to the classification matrix (Supporting Information, Table S49), the lowest correct discrimination levels were recovered in *Rhynchoclevelandella* sp. 2 (14.3%) and *C. kidderi* (55.6%).

The mean shrinking during protargol preparations for all Clevelandellidae species combined is $18.6 \pm 7.4\%$ for length and $16.6 \pm 10.9\%$ for width. However, close observation on shrinking of individual species (Supporting Information, Table S50) uncovered the striking difference among species, with length

shrinking ranging from 4.2% in *R. hastula* to 29.2% in the long morph of *C. hromadkai* and width shrinking ranging from 1.1% in *C. fryntai* to 31.9% in the long morph of *C. hromadkai*. In addition, there is an apparent disparity between shrinkage of the cell length and cell width in some species. The most notable example is *C. elongata*, whose length decreases in protargol preparations by 22.9%, but its width increases by 12.5%. The GLM model revealed the significant effect of species ($F_{16,840} = 361.26$, $P < 0.001$), cell condition ($F_{1,840} = 343.92$, $P < 0.001$), and their interaction ($F_{16,840} = 4.5$, $P < 0.001$) on the cell length. The effect of species ($F_{16,827} = 143.98$, $P < 0.001$), cell condition ($F_{1,827} = 232.94$, $P < 0.001$), and their interaction ($F_{16,827} = 4.85$, $P < 0.001$) on the cell width were also significant. As shrinkage is calculated directly from the cell measurements (i.e. cell length and width), the GLM model clearly indicates that the rate of shrinkage differs among species considerably. RMA regression did not reveal significant relationship

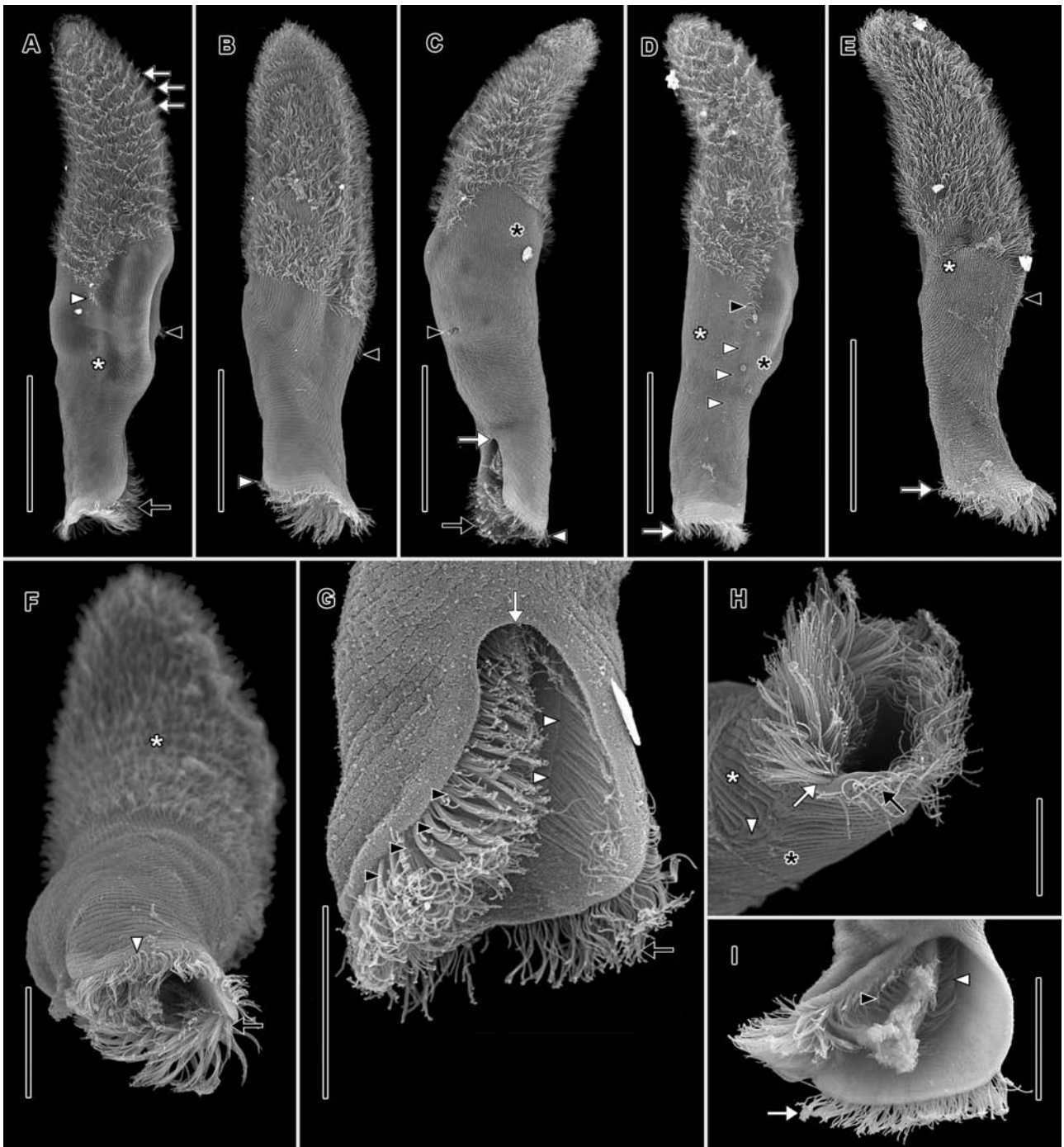


Figure 27. *Clevelandella elongata* in the scanning electron microscope. From SRU. A, right ventrolateral view showing metachronal ciliary waves (white arrows), and 'tail' of ciliated basal bodies extending posteriorly on right ventrolateral surface (white arrowhead) near the right suture (white asterisk). Cilia of the adoral membranelles protrude from the buccal overture (black arrow). Cilia of the collecting chamber protrude from the cytoproct (black arrowhead). B, dorsal view showing 'tail' of ciliated basal bodies extending posteriorly on right ventrolateral surface (black arrowhead) and cilia of circumperistomial kineties (white arrowhead). C, left dorsolateral view showing the cytoproct (black arrowhead), dorsal kineties (black asterisk), proximal margin of buccal overture (white arrow), cilia of the adoral membranelles (black arrow), and circumperistomial kineties (white arrowhead). D, right dorsolateral view showing posteriorly extending 'tail' of cilia (black arrowhead), right suture between dorsal kineties (white asterisk) and ventral kineties (black asterisk), and densely ciliated circumperistomial kineties (white arrow). E, dorsal view showing straight dorsal kineties (white asterisk), the ciliary 'tail' (black arrowhead), and cilia of circumperistomial kineties (white arrow). F, posterodorsal view showing convexity of the right dorsolateral cell surface (white asterisk), cilia of circumperistomial kineties (white arrowhead), and cilia of adoral membranelles (black arrow). G, left lateral detail view showing proximal margin of buccal overture (white arrow), circumperistomial cilia (black arrow), adoral membranelles (black arrowheads), and paroral membrane (white arrowheads). H, posterolateral detail view of the buccal overture showing posteriormost adoral membranelle (white arrow), circumperistomial cilia (black arrow), right suture (white arrowhead) between ventral kineties (black asterisk) and dorsal kineties (white asterisk). I, posterior view of buccal overture showing adoral membranelles (black arrowhead), paroral membrane (white arrowhead), and circumperistomial cilia (white arrow). Scale bars: 50 μm (A–E), 20 μm (F–I).

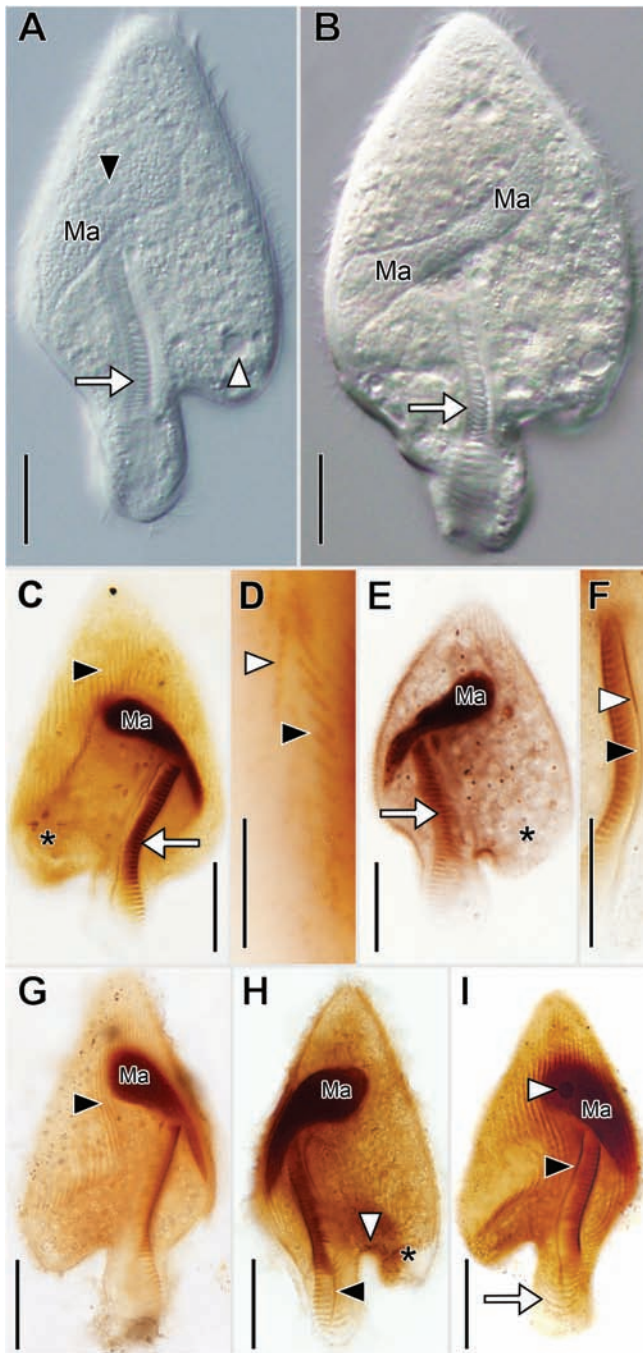


Figure 28. *Clevelandella parapanesthia*. In vivo (A, B) and after protargol impregnation (C–H). From PGW (A), MP (B, F), ASS (C, D), PT (E), and PGW (G, H). A, ventral view showing adoral membranelles (white arrow), contractile vacuole (white arrowhead), and micronucleus (black arrowhead). B, ventral view showing atypical macronuclear ‘S’-shape and adoral membranelles (white arrow). C, dorsal view (optical section) showing straight dorsal kineties (black arrowhead), adoral membranelles (white arrow), and left protuberance (asterisk). D, right lateral detail view of sutural kinetofragments (black arrowhead) and dorsal kinety (white arrowhead). E, ventral view (optical section) showing adoral membranelles (white arrow) and left protuberance (asterisk). F, detail view of paroral membrane showing short (white arrowhead) and long (black arrowhead) files. G, dorsal view showing straight dorsal kineties (black arrowhead). H, ventral view showing paroral membrane (black arrow head), prominent notch (white arrowhead)

between shrinkage and cell size either in length ($R^2 = 0.036$, $P = 0.466$) or width ($R^2 = 0.143$, $P = 0.133$). Nevertheless, a weak positive relationship between shrinkage and cell length (Supporting Information, Fig. S6) and a weak negative relationship between shrinkage and cell width (Supporting Information, Fig. S7) was found.

DISCUSSION

Morphologic peculiarities of Clevelandellidae

The Clevelandellidae all share several similar morphologic peculiarities that have been previously unmentioned or inconsistently and, sometimes, incorrectly described and/or depicted. The most important of these are discussed below.

Somatic ciliature: Kidder himself (1937) and others (Lynn 2008, Pecina and Vďačný 2020a, b) have described or depicted members of the Clevelandellidae as having complete (i.e. holotrichous) somatic ciliation (Fig. 36A, C, H). However, all Clevelandellidae actually share what we term a ‘hemitrichous’ distribution of somatic cilia (the ciliature of *C. contorta* has not been assessed since its original description). Both basal bodies of somatic dikinetids are ciliated in the (approximately) anterior half of the cell, while in the posterior part of the cell the dikinetids are barren, except for several ciliated circumperistomial kineties at the terminal margin of the peristomial overture (e.g. Figs 5C, 27G, 29C, 31A). Although the circumperistomial kineties have previously been overlooked, Albaret (1975) recognized the otherwise partial somatic ciliation of the three Clevelandellidae species he redescribed, and Mandal and Nair (1974) recognized the restriction of somatic cilia to the anterior half of the cell in *C. kidderi* (Fig. 36I; here considered as a senior subjective synonym of *C. lynni*). Yamasaki (1939) recognized the restriction of somatic cilia to half of the cell in the three species he described, but he considered the half to be posterior (Fig. 36F, J). Albaret (1975) described ‘short’ cilia in the posterior part of the cell, but his transmission electron photomicrograph and scanning electron microscopy studies indicate that the posterior somatic dikinetids are actually barren. Although Pecina and Vďačný (2020a, b, 2022) describe holotrichous (complete) ciliation in Clevelandellidae and depict it in their drawings, their photomicrographs clearly show the invariable restriction of somatic cilia to the anterior part of the cell in the species they consider (Fig. 36D, G; Pecina and Vďačný 2020a: fig. 2E–G; 2020b: figs 3F, G, 5G, H, 8E–G, 11E–G, 14B, C).

The somatic cilia (including those of the circumperistomial kineties) of all Clevelandellidae are unusually short, i.e. about 5 μm long in both living and fixed states (e.g. Figs 4A, 7A, 10B, 23A). Somatic ciliary length in ciliates is highly variable, ranging from 6 to 100 μm (Grain 1984). The somatic cilia of Clevelandellidae may be near the lower limit of length for motile cilia since the minimum length required for organized ciliary beating of motile

between peristomial projection and left protuberance (asterisk). I, dorsal view showing micronucleus (white arrowhead), paroral membrane (black arrowhead), and looping kineties of peristomial projection (white arrow). Ma, macronucleus. Scale bars: 20 μm (A–C, E–I), 10 μm (D).

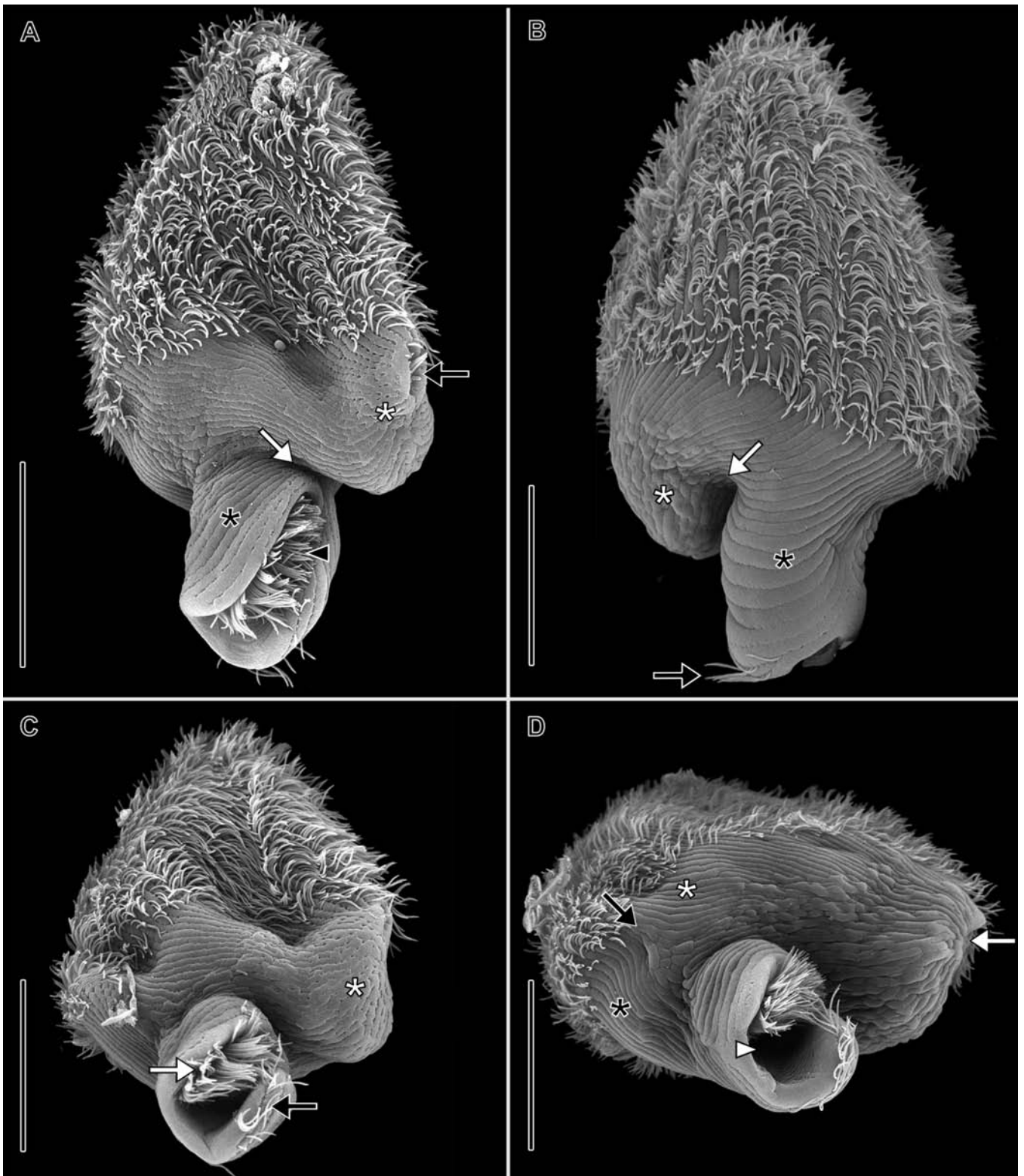


Figure 29. *Clevelandella parapanesthia* in the scanning electron microscope. From PAC. A, ventral view showing notch (white arrow) between left protuberance (white asterisk) and peristomial projection (black asterisk), cilia protruding from cytoproct (black arrow), and cilia of adoral membranelles (black arrowhead). B, dorsal view showing notch (white arrow) between left protuberance (white asterisk) and peristomial projection (black asterisk), and cilia of circumperistomial kineties (black arrow). C, posteroventral view showing posterior protuberance (white asterisk), cilia of adoral membranelles (white arrow), and cilia of circumperistomial kineties (black arrow). D, posterior view showing dorsoventral flattening, right kintal suture (black arrow) between ventral kineties (white asterisk) and dorsal kineties (black asterisk), position of cytoproct (white arrow), and peristomial overture (white arrowhead). Scale bars: 20 μm (A–D).

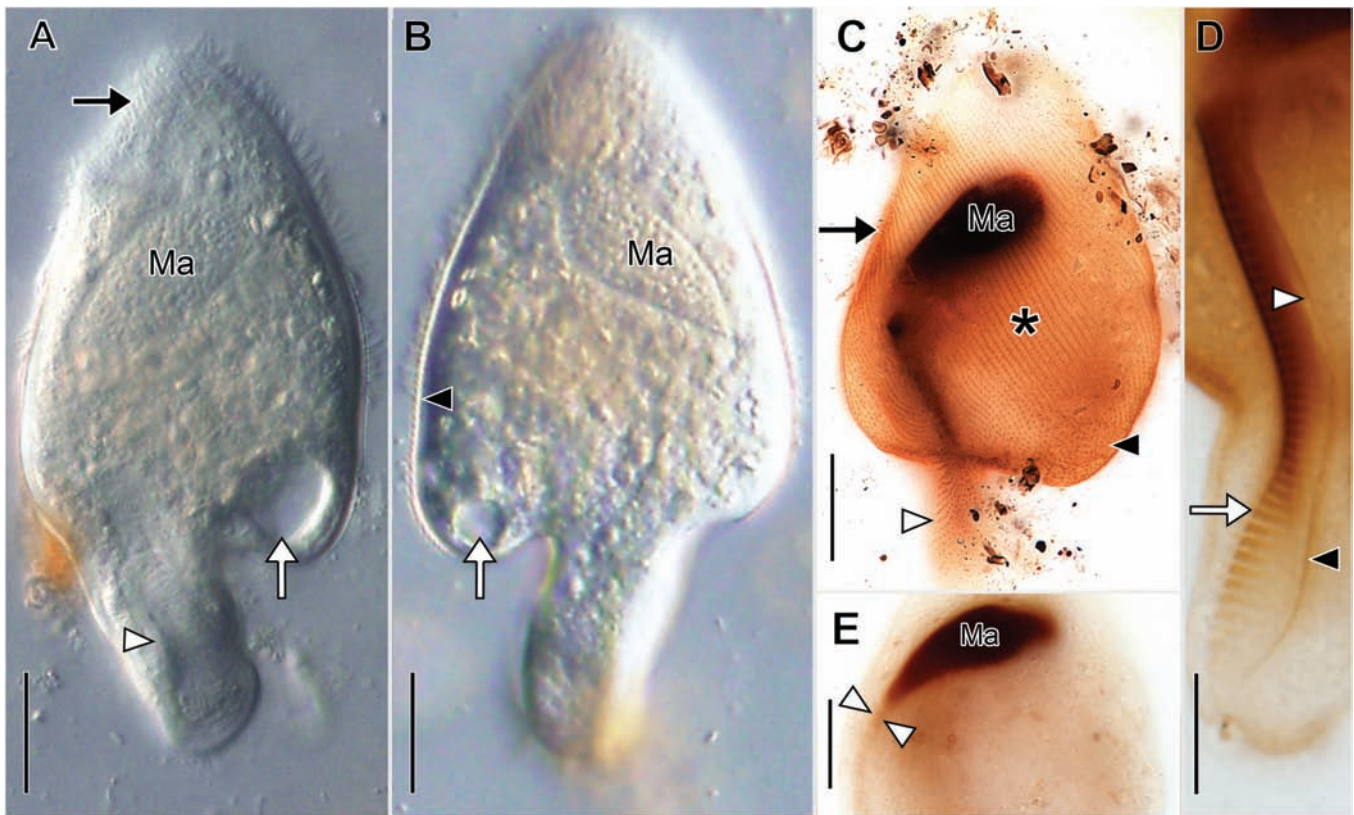


Figure 30. *Clevelandella kidderi* in vivo (A, B) and after protargol impregnation (C–E). From ASS (A–E). A, ventral view showing contractile vacuole (white arrow), ventral kineties (black arrow), and margin of peristomial overture (white arrowhead). B, dorsal view showing contractile vacuole (white arrow) and posterior extent of ciliation on the left margin (black arrowhead). C, ventral infraciliature showing right sutural kinetofragments (black arrow), left-hand spiralling ventral kineties (asterisk), and looping kineties of the peristomial projection (white arrowhead). D, detail view of paroral membrane showing short (white arrowhead) and long (black arrowhead) files, and adoral membranelles, (white arrow). E, detail of macronucleus, ventral view showing inconspicuous karyophore (black arrow). Ma, macronucleus. Scale bars: 20 μm (A–C), 10 μm (D).

cilia is about 2–4 μm (Bottier et al. 2019). A reduction of both cell surface ciliation and somatic ciliary length are possibly adaptations to the viscous content of the host gut. In mucous media, a short ciliary length (5–7 μm) is necessary for effective ciliary propulsion (Satir and Sleight 1990). At least some *Nyctotherus* species inhabiting cockroaches, although holotrichous, also bear similarly short somatic cilia (Pecina and Vďačný 2020a: figs 4A, 5E). The somatic kineties of all Clevelandellidae have a left-handed spiral arrangement, i.e. toward the right side of the cell (Kidder 1937, Mandal and Nair 1974, Albaret 1975, Jankowski 2007). The depictions of right-handed-spiralling kineties (with respect to the viewer) in *Antelevelandella constricta* (Fig. 36C, D, E; Pecina and Vďačný 2020b: figs 1A, M, N, 3F, G) are misinterpretations. All *Antelevelandella constricta* cells from the current report, Kidder (1937), and Albaret (1975), as well as all other species depicted by Pecina and Vďačný (2020b), show left-hand-spiralling of somatic kineties (Fig. 36A, B, H, I, K). The small sutural kinetofragments recognized by Albaret (1975) in *Antelevelandella constricta*, *C. parapanesthiae*, and the ‘simplex’ form of *Paraclevelandia brevis*, and confirmed in *Antelevelandella constricta* by transmission electron microscopy, were also found in six of the species we studied (*Antelevelandella constricta*, *R. hastula*, *Paraclevelandia brevis*, *C. kidderi*, *C. parapanesthiae*, and *C. philipi* sp. nov.). In seven

species (*C. ananiasi* sp. nov., *C. elongata*, *C. fryntai* sp. nov., *C. hromadkai* sp. nov., *C. klobasa* sp. nov., *C. panesthiae*, and *C. sidi* sp. nov.) this feature was clearly absent and in two (*R. nipponensis* and *Rhynchoclevelandella* sp. 2) it could not be determined.

The ciliated excretory antrum: Describing the general morphologic features of the Clevelandellidae, Kidder (1937) stated: ‘Just ventral to the contractile vacuole and near the whorl of peripheral cilia occurs a slit-like cytoproct’ (sometimes referred to as the ‘cytopyge’). ‘Through this permanent slit the contractile vacuole empties its contents. No canal can be detected, but the contractile vacuole comes in contact with the interior edge of the cytopyge just before systole.’ Lynn (2008) mentions, without a citation, that ‘...in clevelandellids [the cytoproct] may open to the outside by a cilia-lined channel’. Albaret (1975) does not describe the cytoproct of Clevelandellidae in detail, but depicts it as a short, narrow canal adjacent to the contractile vacuole. The actual morphology of the clevelandellid excretory system (contractile vacuole, cytoproct, and intervening structures) is quite unusual in addition to its location on the lateral aspect of the cell. In all species studied, we identified what we term the ‘ciliated excretory antrum’, a distinct, permanent, ciliated chamber situated between the contractile vacuole and the slit-like cortical cytoproct (e.g. Figs 2A, C, 15D, E, 17C, 23L, M;

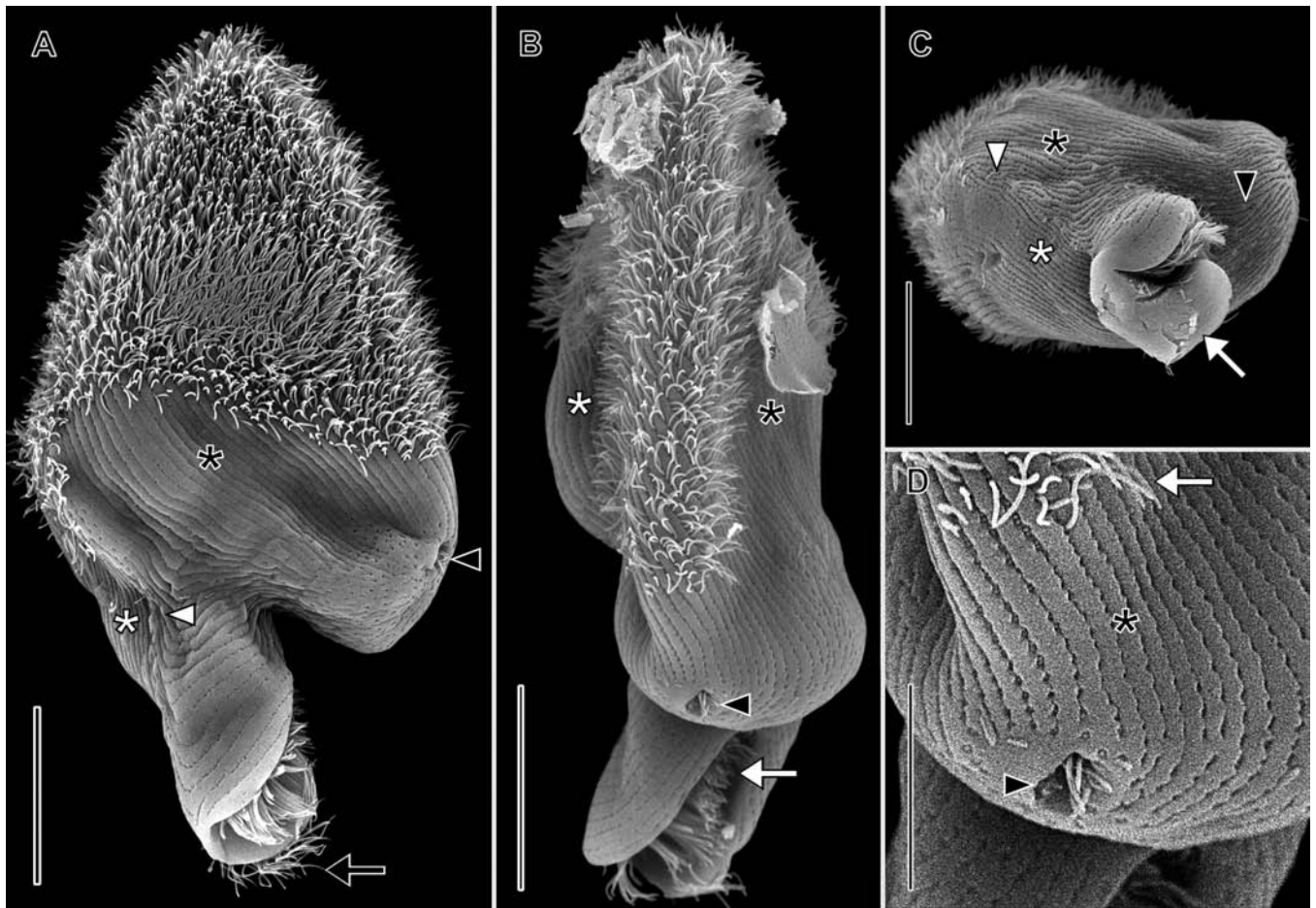


Figure 31. *Clevelandella kidderi* in the scanning electron microscope (A–D). From ASS. A, ventral view showing left-hand-spiralling ventral kineties (black asterisk) meeting dorsal kineties (white asterisk) to form right kinetal suture (white arrowhead), cilia protruding from cytoproct (black arrowhead), and ciliated circumperistomial kineties (black arrow). B, left lateral view showing unciliated parts of dorsal kineties (black asterisk) and ventral kineties (white asterisk), cilia protruding from cytoproct (black arrowhead), and cilia of adoral membranelles seen in peristomial overture (white arrow). C, posterior view showing dorsoventral flattening and right kinetal suture (white arrowhead) between ventral kineties (black asterisk) and dorsal kineties (white asterisk), and dorsal margin of the posterior peristomial projection (white arrow). D, detail of the same cell as (B) showing cilia protruding from cytoproct (black arrowhead) on the left protuberance (asterisk), and posterior extent of somatic ciliation (white arrow). Scale bars: 20 μm (A–C), 10 μm (D).

Supporting Information, Video S1). The contents of the contractile vacuole and faecal material are collected in this chamber and propelled from it, through the cytoproct by long, fine, cilia arising from the wall of the chamber. In SEM images these cilia can often be seen protruding from the cytoproct (e.g. Figs 11F, 20F, 22C, 33D). The antrum itself is rather inconspicuous and likely to be overlooked without careful *in vivo* study by DIC illumination. It is also quite difficult to discern even in optimally developed protargol preparations since the basal bodies of the chamber are very fine and irregularly distributed and obscured by overlying somatic kineties (Figs 15E, 23L). The cytoproct of the nyctotherids as described by Geiman and Wichterman (1937), McKean (1972), and Albaret (1975) differs in that it is situated in a more or less invaginated area of the posterior cell cortex. However, a very thorough ultrastructural investigation of *Nyctotherus ovalis* Leidy, 1894 showed a structure at the posterior end of the cell probably homologous to the ciliated excretory antrum of Clevelandellidae, namely a 20–25 μm long ‘expulsion vesicle canal’ lined by cilia, some of which protruded from the

cytoproct (McKean 1972: figs 3, 81). In the class Armophorea, these complex structures are unique to the order Clevelandellida suggesting that a ciliated excretory chamber was probably present in the last common ancestor.

Morphology of the paroral: The morphology of the paroral of all Clevelandellidae is invariably diplostichomonad, i.e. composed of two parallel single files of ciliated basal bodies, one usually longer than the other, separated by a cortical ridge (e.g. Fig. 7I). In all species we studied, both files extend posteriorly from the cytostome, the left file being longer and usually reaching the posterior margin of the peristome (e.g. Figs 5D, 7I, 26A, 30D). The right file is always shorter, with the exception of *C. sidi* sp. nov. in which both files are of the same length (Fig. 15H). The paroral of the nyctotherids is also diplostichomonad (de Puytorac and Grain 1976, Takahashi and Imai 1989). A diplostichomonad paroral occurs in various metopid lineages and may be more widely distributed in this group than assumed, since the shorter proximal file might be obscured within the buccal cavity and thus

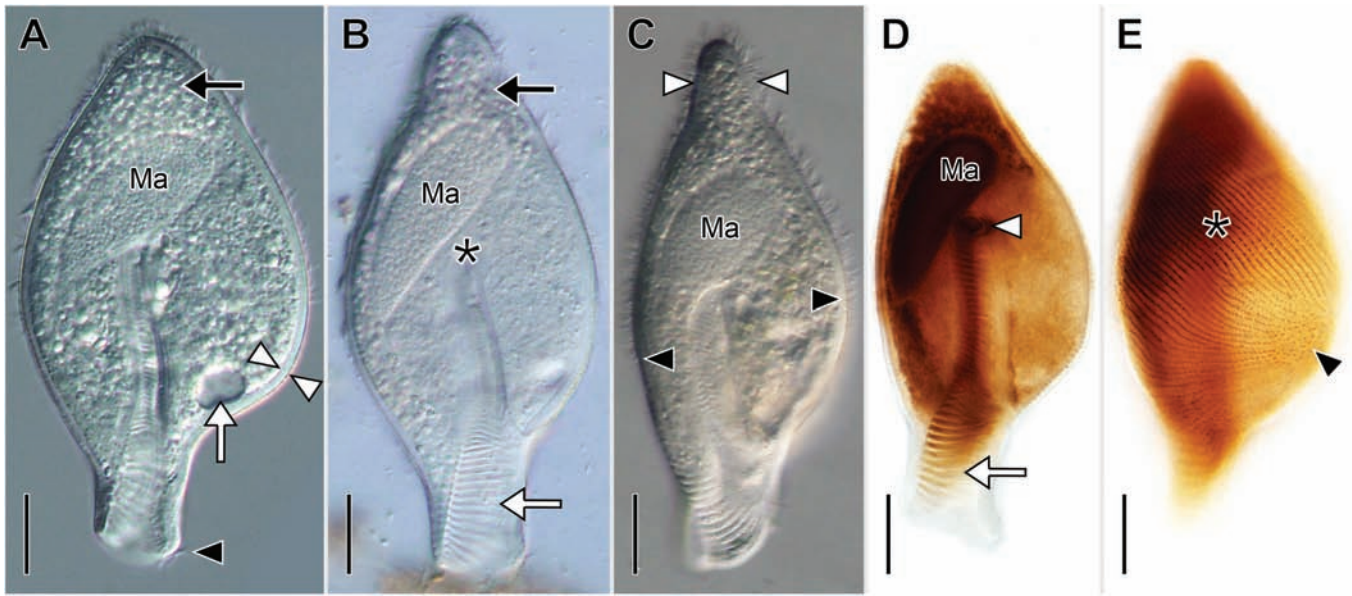


Figure 32. *Clevelandella panesthiae* in vivo (A–C) and after protargol impregnation (D, E). From ASS (A), PAA (B, D, E), and PT (C). A, ventral view (optical section) of typical form showing the contractile vacuole (white arrow), cytoplasmic granules, possibly amylopectin (black arrow), circumperistomial kineties (black arrow), and hyaline subcortical layer (white arrowheads). B, ventral view (optical section) showing location of the cytostome (asterisk), adoral membranelles, (white arrow), and cytoplasmic granules, possibly amylopectin (black arrow). C, ventral view (optical section) showing posterior extent of ciliation on the right margin and left margin (black arrowheads), and unusually tapered anterior end of cell (white arrow heads). D, E, the same cell in ventral view: D, optical section showing cytostome (white arrowhead) and adoral membranelles (white arrow); E, surface view showing ventral infraciliature showing left-hand spiralling ventral kineties (asterisk), disordered basal bodies on left protuberance (black arrowhead). Ma, macronucleus. Scale bars: 20 μ m.

easily overlooked (Bourland and Wendell 2014, da Silva-Neto *et al.* 2016, Bourland *et al.* 2018, 2020). The caenomorphids also have a diplostichomonad paroral (Lynn 2008). The possibility that the diplostichomonad character state is plesiomorphic in Armophorea should be considered. Our findings differ from a previous report by Pecina and Vdačný (2020a, b) who claim that both files of the paroral are always of the same length and that the paroral terminates more anteriorly at the proximal margin of the buccal overture.

Position and polarity of oral structures: The most striking characteristic of the Clevelandellidae is the posteriorization of oral structures. Other armophorean lineages (e.g. *Brachonella* spp.) also have posteriorized oral structures. However, in these cases the adoral membranelles are oriented in the same direction (i.e. with the shortest file of basal bodies anterior), as in taxa with anterior buccal cavities, and the membranelles have the same left-sided location with respect to the paroral. Thus, in these cases, the posteriorization can be accounted for by a simple posterior displacement of both structures without rotation. However, the orientation of the individual elements in Clevelandellidae is entirely different from the latter examples. Terms of orientation in the Clevelandellidae have been inconsistent, even with regard to the true anterior and posterior ends of the cell (Yamasaki 1939, Albaret 1975). As in all other ciliate taxa, the polarity of somatic dikinetids in Clevelandellidae obeys the rule of desmodoxy (i.e. the kinetodesmal fibre projects to the right side of the cell from the posterior kinetosome near microtubular triplets 5 and 6), thus the somatic kineties of Clevelandellidae are not reversed (Chatton and Lwoff 1935, Albaret 1975, Lynn 1975, 2008). The

peristomial opening is thus considered to be ‘posteriorized’, as are the adoral membranelles, in which the shortest file of basal bodies faces posteriorly and not anteriorly as is typical of spirotrich, heterotrich, and metopid ciliates (Tuffrau and Fleury 1994). The selective pressures and structural constraints that resulted in this remarkable reorientation are unknown.

Duality of morphotypes: Several Clevelandellidae species exhibit two very distinct morphs that differ not only in size, but also in shape and other characteristics (e.g. number of adoral membranelles). The difference in appearance can be striking enough that two morphs of *Paraclevelandia brevis* (Kidder 1937)—‘brevis’ and ‘simplex’—have been identified as separate species. Similarly, prior to obtaining molecular data, we assumed ‘slender’ and ‘broad’ morphotypes of *C. fryntai* to be separate species. In the aforementioned cases, both morphotypes frequently co-occur in a single host. Furthermore, in *Paraclevelandia brevis* the large ‘simplex’ morphotype seems to never occur in the absence of the smaller ‘brevis’ morphotype. Conversely, the ‘short’ and ‘long’ morphotypes of *C. hromadkai* seem to never co-occur in the same host. The relationships between these morphotypes, and the factors leading to their formation, are unknown. It is probable that, in the case of *Paraclevelandia brevis*, the two morphotypes, which are strikingly different in size, number of adoral membranelles, and nuclear morphology, may represent different life stages. Morphotypes of *C. fryntai* have a different shape, but their metrics overlap strongly. It is thus possible that the difference is caused by the nutritional state of the cell or other environmental factors. In *C. hromadkai* the ‘long’ morph can be found mostly in adult male hosts, while the ‘short’ morph is found in females and larvae. Since

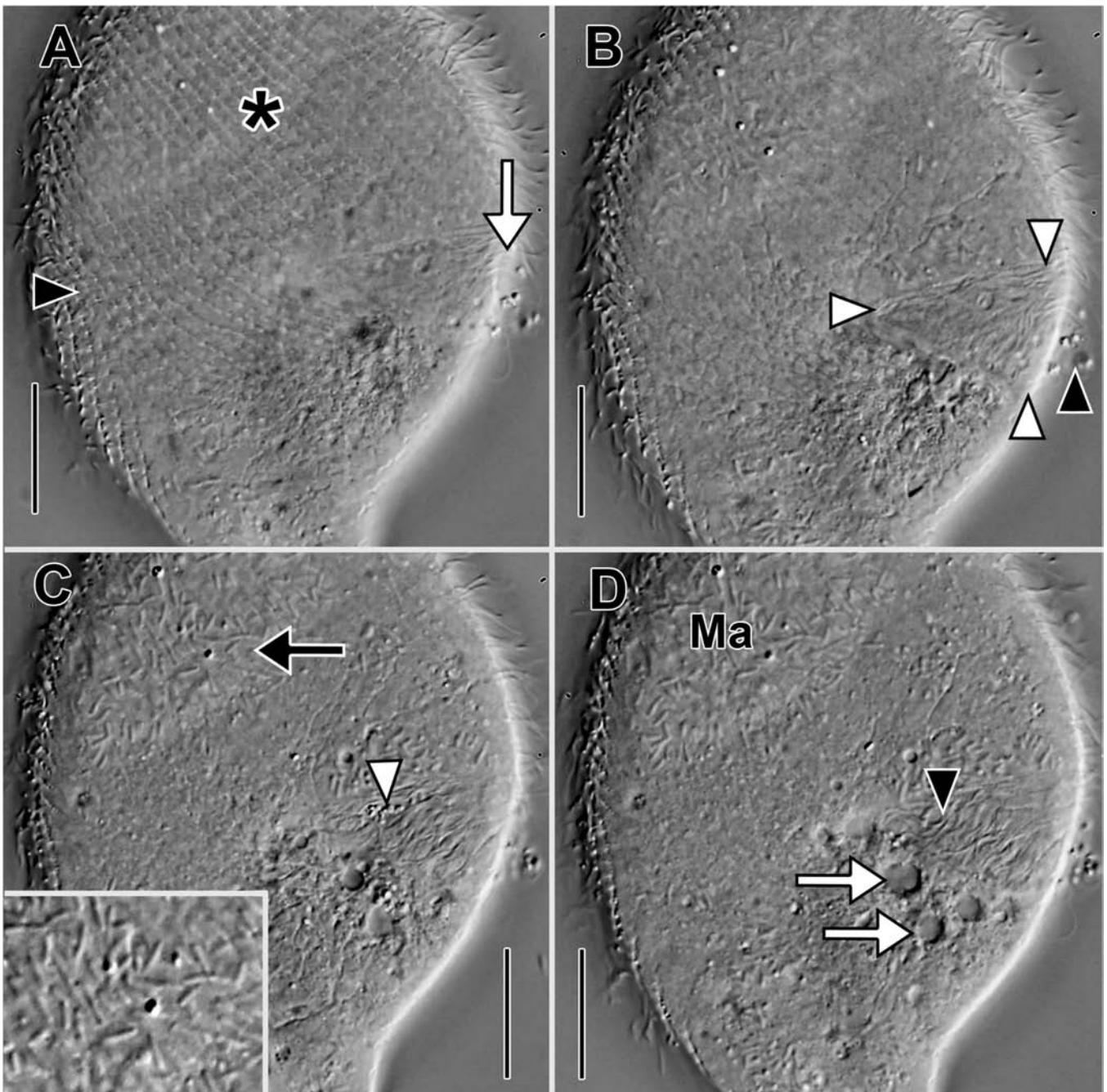


Figure 33. *Clevelandella panesthiae* in vivo (optical sections of same cell). From ASS. A, surface view showing left-hand spiralling ventral kineties (asterisk), right kinetal suture (black arrowhead), and position of the cytoproct (white arrow). B, slightly deeper focal plane showing conical ciliated excretory antrum within left protuberance (white arrowheads) and defecated material (black arrowhead). C, slightly deeper focal plane than (B) showing faecal material transiting the ciliated excretory antrum (white arrowhead) and numerous rod-shaped perinuclear symbionts (black arrow and inset). D, approximately same focal plane as (C) showing collecting vesicles of contractile vacuole (white arrowhead) which will coalesce and empty into the excretory antrum and the dense, fine cilia lining the antrum (black arrowhead). Ma, macronucleus. Scale bars: 20 μm .

the male cockroaches are of smaller or similar size as females and larger larvae, the host size is probably not the determining factor. However, the environment in the gut of the adult male is more stable than that of females and larvae. The insect larvae go through a number of ecdyses during ontogeny, first emptying their hindgut and then also shedding their hindgut cuticular lining (we have witnessed hindguts full of encysted ciliates in pre-ecdysis larvae).

Female cockroaches undergo repeated reproductive cycles accompanied by behavioural changes, including the period of drastic reduction in food intake while provisioning nutrients to egg case (Gore and Schal 2005, Varadínová *et al.* 2015). It is possible that, unlike the short-lived hindgut environment of larvae and females, the relatively stable environment of the male hindgut allows *C. hromadkai* to achieve the greater size of the 'long' morph.

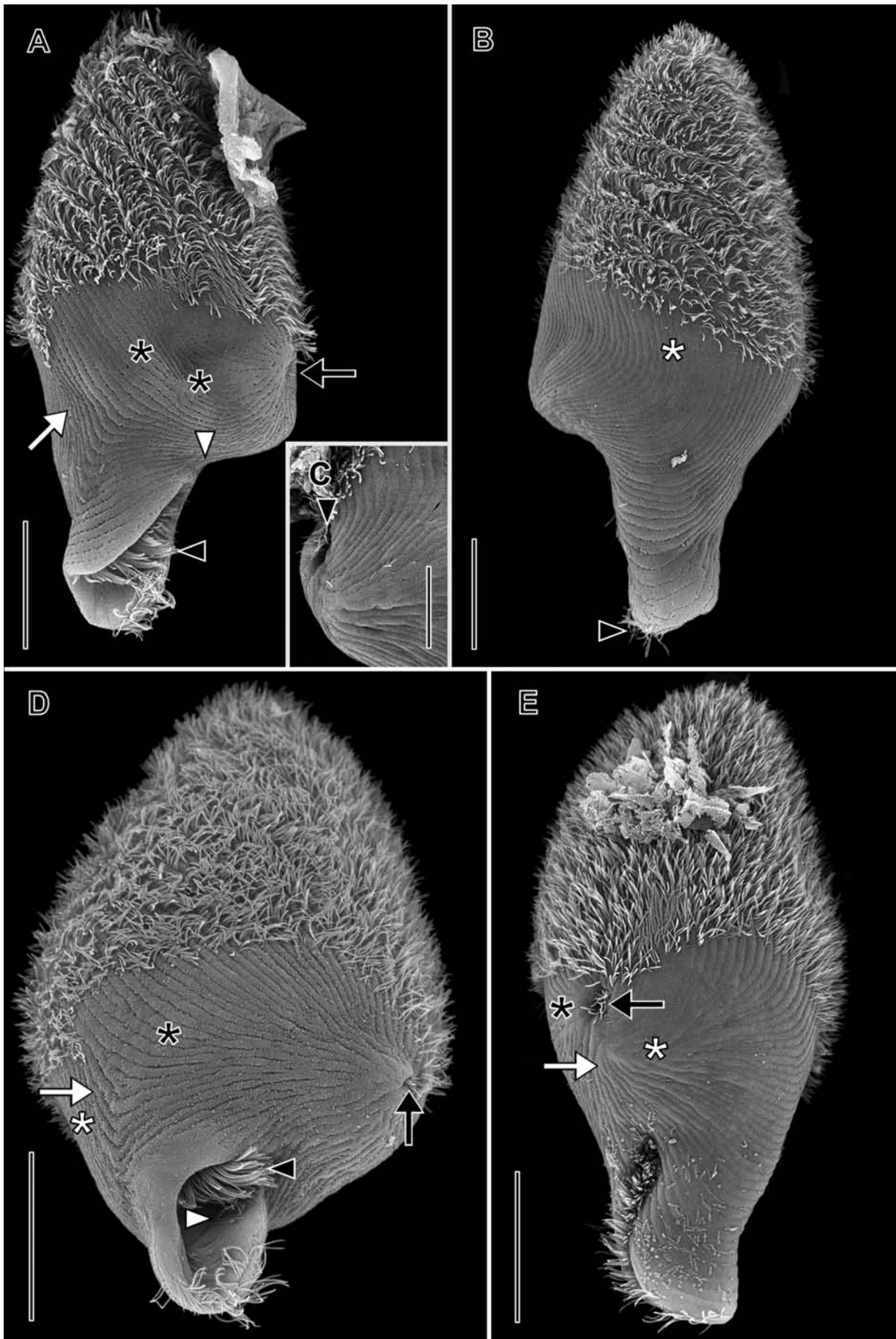


Figure 34. *Clevelandella panesthiae* in the scanning electron microscope. From ASS. A, ventral view showing right kinetal suture (white arrow) and short left suture (white arrowhead), cilia of adoral membranelles (black arrowhead), and ciliated cytoproct (black arrow).

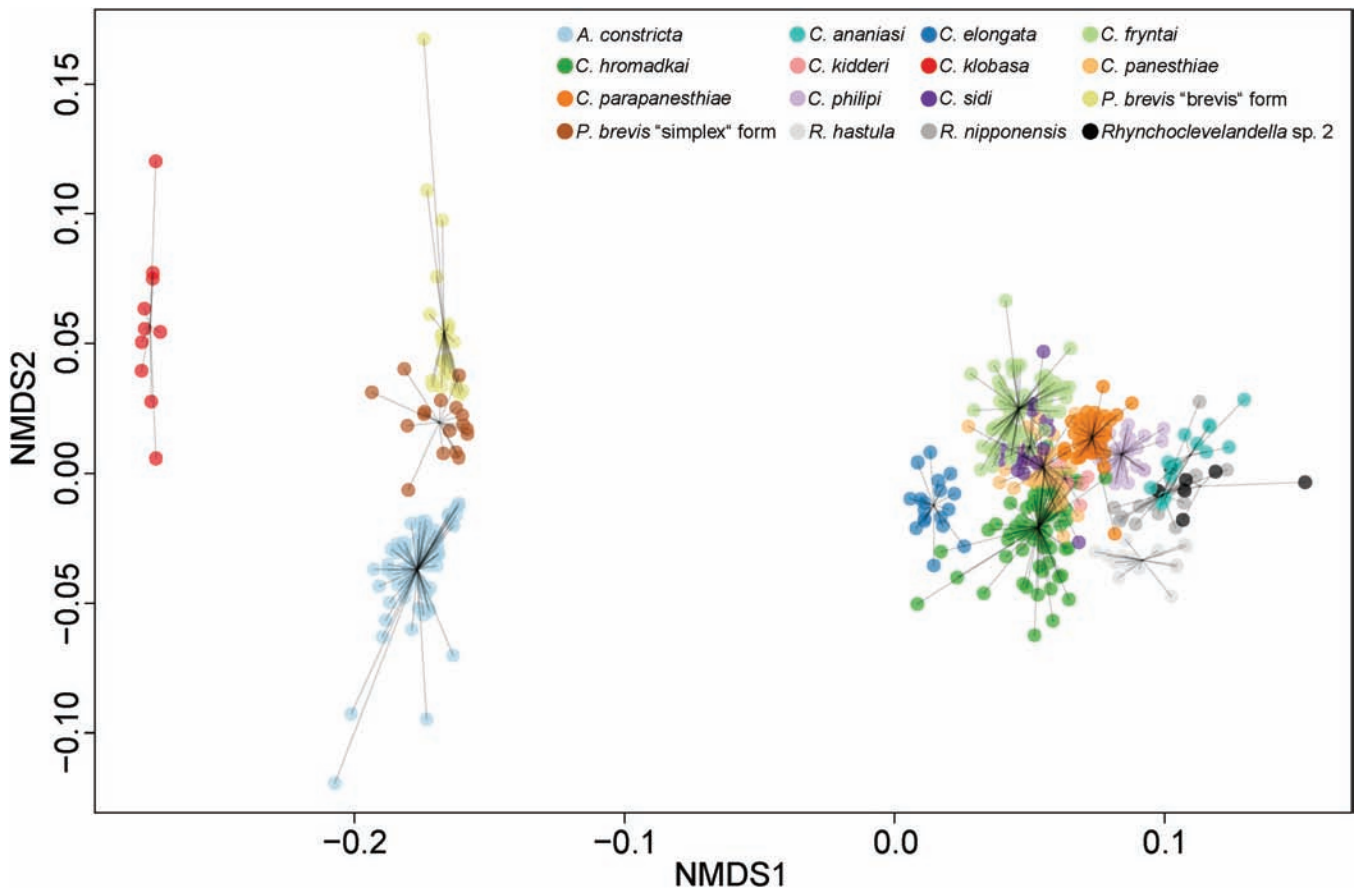


Figure 35. Non-metric multidimensional scaling (NMDS) plot based on the morphological analysis of traits measured on 455 scales. The cells are colour-coded and clustered based on their affiliation to 16 investigated strains.

Congruence of morphological and molecular data in taxonomy of Clevelandellidae

In order to test the congruence of morphological and molecular data, Pecina and Vďačný (2020b) employed a three-way integrative approach incorporating morphometric measurements, cell geometrical information (both obtained from their protargol preparations), and 18S rRNA gene sequences derived mostly from their own data (Pecina and Vďačný 2020a, b) but also from Lynn and Wright (2013). They had shown that the clevelandellid morphospecies, as defined by Kidder (1937), are fully consistent in both morphometric and geometrical analyses. However, they suggested that the morphospecies [based on their own data as well as *in vivo* data from Lynn and Wright (2013)] are not consistent with the 18S rRNA gene phylogeny, with *Anteclevelandella constricta*, *Paraclevelandia brevis*, and *R. hastula* being monophyletic, but *C. panesthiae* and *C. parapanesthiae* morphospecies comprising more or less phylogenetically disparate genotypes. This led to the conclusion that ‘morphology

and genetics are rather inconsistent’ in Clevelandellidae and that the morphospecies are complexes of cryptic taxa. Expanding on this idea, the authors decided that the majority of the studied genotypes represent separate species and tried to employ CBC concept to find species-delimiting characters for them (Pecina and Vďačný 2022). The concept is based upon supposed correlation between the presence of a double-sided base change of a nucleotide pair in a helix of the ITS2 rRNA gene region (a so-called compensatory base change—CBC), and the inability of strains to sexually cross. It was initially proposed for Volvoclean green algae (Coleman 2000) and was later used for ciliates as well (e.g. Coleman 2005), but was also shown numerous times to fail in delimiting species (Caisová *et al.* 2011, 2013, Assunção *et al.* 2012, Škaloud and Rindi 2013). However, Pecina and Vďačný did not find a compensatory base change in any of their proposed species and they concluded that ‘the ITS2 molecule per se failed to determine multiple clevelandellid species, as its primary sequence structure transcended several species boundaries’

Note absence of notch between posterior peristomial projection and left posterior protuberance. B, dorsal view showing unciliated posterior parts of somatic kineties (white asterisk) and cilia of circumperistomial kineties (black arrowhead). C, detail of cilia protruding from cytoproct (black arrowhead). D, posteroventral view showing right kinetal suture (white arrow) between ventral kineties (black asterisk) and dorsal kineties (white asterisk), cilia of adoral membranelles (black arrowhead), single file of ciliated basal bodies comprising posteriormost end of paroral membrane (white arrowhead), and cilia protruding from the cytoproct (black arrow). E, left dorsolateral view showing ventral kineties (black asterisk) and dorsal kineties (white asterisk) converging to form ciliary whorl on left protuberance, and kineties forming inconspicuous left posterior suture (white arrow). Scale bars: 20 μm (A, B, D, E), 10 μm (C).

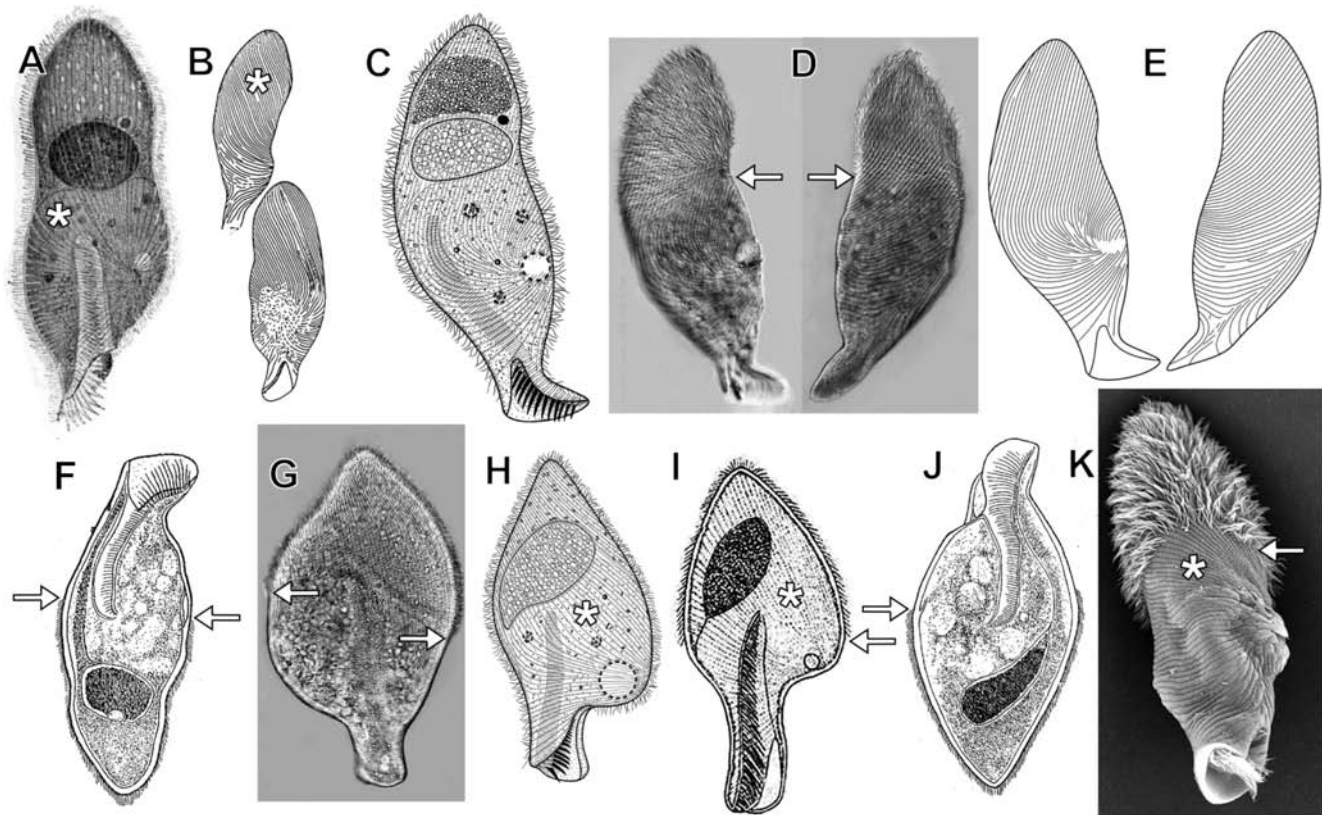


Figure 36. Various depictions of Clevelandellidae from the literature (A–J) and our picture (K). A, *Antecelelandella constricta*, ventral view [modified from Kidder (1937), with permission]. B, *Antecelelandella constricta* ventral view [modified from Alabaret (1975), with permission]. C–E, *Antecelelandella constricta*, ventral view (C, viewer's left D, E), dorsal view (viewer's right D, E; modified from Pecina and Vďačný, 2020). F, *Emmaninius plantiformis*, now *Antecelelandella constricta* [after Yamasaki (1939: fig. 8)]. G, H, *Clevelandella panesthiae*, dorsal and ventral view respectively (modified from Pecina and Vďačný, 2020). I, *C. kidderi* ventral view [modified from Mandal and Nair (1974), with permission]. J, *Emmaninius papilloris*, now *Clevelandella panesthiae* [after Yamasaki (1939: fig. 2)]. K, *Antecelelandella constricta* under the scanning electron microscope, ventral view. Asterisk indicate true orientation of ventral kineties. Arrows depict true posterior extent of somatic ciliation.

(Pecina and Vďačný 2022). Despite that, they still did opt to describe eight new species based on minor molecular differences. *Clevelandella bipanesthiae*, for example, is diagnosed by just two bases in the 18S rRNA gene, which, according to the authors, is sufficient to distinguish and describe a species.

The abandonment of morphology in favour of purely molecular taxonomy is problematic in our view. The main basis for considering morphology and molecular taxonomy as incongruous in Clevelandellidae is that isolates with *C. panesthiae* morphology represent several genotypes, which do not form a clade, but branch at four different positions in the tree: three genotypes occupy three different places within the *C. parapanesthiae* branch; the rest of the genotypes form a separate lineage, which is rather distantly related to *C. parapanesthiae* (referred to as *Clevelandella* sp. 3 in our study). Since cells of the *C. panesthiae* morphotype cluster within a group of cells with *C. parapanesthiae* morphotype, and *C. parapanesthiae* morphotype cells do not form a clade, four new species were erected, based on molecular data, without defining which of them is the original *C. parapanesthiae* or *C. panesthiae* (Pecina and Vďačný 2020b, 2022). Two problems confound the species delimitation:

- (i) A widespread problem of sample identity in the study of Lynn and Wright (2013) should be noted. While in a more recent study (Pecina and Vďačný 2020b) cells were assigned to morphotypes based mostly on observation of protargol impregnated cells, Lynn and Wright (2013) assigned morphotypes solely on the basis of *in vivo* observations, which is, in our experience, often misleading. The cells of *Clevelandella* sp. 3 supposed by Lynn and Wright (2013: figs 3, 4) to be *C. panesthiae* have a very different shape than Kidder's (1937) description, the description in our current study (Fig. 32), and that of Pecina and Vďačný (2020b), being much smaller and more symmetrical and possessing more broadly rounded anterior. Thus, they cannot be reconciled to the same morphotype. Then, the peculiar isolate CP18 from Lynn and Wright with supposedly *C. panesthiae* morphology is most probably erroneous misidentification or typo, because it nests within *C. parapanesthiae* lineage (Pecina and Vďačný 2020b; this study). Lastly, the authors state that they isolated *C. parapanesthiae* from the host. The isolate marked as *C. parapanesthiae*, however, nests in *Rhynchoclevelandella* (this study).

(ii) Two genotypes within *C. parapanesthiae* are described as exhibiting the *C. panesthiae* morphotype but the precise genotype associated with the morphology shown is not specified (Pecina and Vďačný 2020b). One of these genotypes is later described as a new species, *C. bipanesthiae* (Pecina and Vďačný 2022). Moreover, the isolates of the second genotype were coupled with cells of the *C. parapanesthiae* morphotype (TH 30 Psp + TH 22 Psp) and described as a new species, *C. triparapanesthiae*. We have studied the morphology of four genotypes (P37_ASS_PNG, P132_PT_VN2, P40_PGW_NB, P113_MP_MA; see Fig. 1), which are genetically almost identical to *C. bipanesthiae*, and all exhibit a clear *C. parapanesthiae* morphotype (Fig. 28A, B, E–H), so it seems highly improbable that *C. panesthiae* would not. While we cannot 100% rule out the possibility of dual morphology in the *C. parapanesthiae* lineage, we have never observed such a case. All our isolates in the lineage are consistently of *C. parapanesthiae* morphology. This raises the possibility that in the previous work (Pecina and Vďačný 2020b) either the cell shape might have been confused during the isolation or sequences and morphotype might have been incorrectly associated, i.e. the molecular sequences obtained might not belong to the cells with *C. panesthiae*-like morphology. This possibility is further suggested by the fact that an organism formally described as *Clevelandella nova* was later reported from the same cockroach population but without morphologic data (Pecina and Vďačný 2022). Several populations studied by us are closely related to *C. nova*, including the genetically almost identical P132_PT_VN2 (Fig. 32C), and all clearly exhibit the *C. panesthiae* morphology (Fig. 32). We conclude that it is possible that the *C. panesthiae*-like cells coupled with gene sequences from isolates TH 11E Paa and TH 45 Paa (Pecina and Vďačný 2020b), and later erected as *C. bipanesthiae* (Pecina and Vďačný 2022), probably belong to isolates TH 24–26 Paa of *C. nova*—which, in turn, we consider a junior synonym of *C. panesthiae* (see below).

In the aforementioned studies, images of cells isolated for molecular characterization were not provided. We provide these data (Supporting Information, Figs S1–S3, Table S2) to document the morphology of the sequenced cells and recommend that such data be included in future studies to exclude the possibility of misidentification when dealing with samples including multiple quite similar organisms. Despite the monophyly of the *R. hastula* group, it was split into three species (*R. hastula*, *R. bihastula* Pecina and Vďačný, 2022, and *R. trihastula* Pecina and Vďačný, 2022), for which the morphology of only one (*R. hastula*) was shown (Pecina and Vďačný 2020b, 2022). Apart from considerations of the subjective topic of splitting, conflicting morphology is also problem here: genotype P71NI_PAC_VN1 from the current study, which is genetically very similar to *R. trihastula*, clearly exhibits the *R. nipponensis* morphology, raising the possibility that *R. trihastula* might as well be *R. nipponensis*. However, the absence of morphologic data for *R. trihastula* leaves this matter unresolved. To show that

morphology is a valid tool for discrimination of clevelandellids, we performed ordination via non-metric multidimensional scaling (NMDS) based on 12 morphological traits measured from protargol-impregnated cells from a large sample of genotypes. We found that the molecularly defined monophyletic species (mostly comprising numerous genotypes) were clearly grouped into visible clusters (Fig. 35). Moreover, our linear discriminant analysis (LDA) confirmed that Clevelandellidae cells can be correctly attributed to genetically defined species based solely on morphometrical data with 88% success (Supporting Information, Table S49). While some of the species are weaker in this regard (*C. ananiasi*, *C. kidderi*, and *Rhynchoclevelandella* sp. 2), they can be easily distinguished by qualitative characteristics, such as the cell or nucleus shape.

The basis for proposed synonymizations in Clevelandellidae

Antelevelandella salganeae Pecina and Vďačný, 2022 and *Antelevelandella macropanesthiae* Pecina and Vďačný, 2022 branch within a well-supported clade of isolates with *Antelevelandella constricta* morphology (Fig. 1). We have inspected morphology of isolates with identical 18S rRNA gene sequences and almost identical ITS/28S rRNA gene sequences to *Antelevelandella salganeae* (P100_SRU_CA, P136_SRU_CA) and isolate with almost identical 18S sequence as *Antelevelandella macropanesthiae* (P59_ASS_PNG) and they all exhibit clear *Antelevelandella constricta* morphology (Fig. 19D, F) and are indistinguishable from other *Antelevelandella constricta* isolates. We thus consider *Antelevelandella salganeae* and *Antelevelandella macropanesthiae* junior subjective synonyms of *Antelevelandella constricta*.

Isolates of *Paraclevelandia brevis* and *Paraclevelandia simplex* form a well-supported clade composed of a mix of both morphotypes. Moreover, we can see instances of both morphotypes belonging to the same genotype and coming from the same host individual (P49_STH_PNG, P17_PAA_PH, P40_PGW_NB). We thus regard *Paraclevelandia simplex* as a junior synonym of *Paraclevelandia brevis* and assume that both morphotypes probably represent two life stages of the same species.

Clevelandella biparapanesthiae Pecina and Vďačný, 2022, *C. triparapanesthiae* Pecina and Vďačný, 2022, and *C. bipanesthiae* branch within a well-supported clade of isolates having *C. parapanesthiae* morphology. The morphology of *C. biparapanesthiae* and *C. triparapanesthiae* isolates (Pecina and Vďačný 2020b) is highly similar to our various *C. parapanesthiae* isolates and consistent with the original description of this species by Kidder (1937). As mentioned above, the morphology published by Pecina and Vďačný (2020b) possibly does not represent the *C. bipanesthiae* isolates, and all four genotypes from the current study, which are genetically nearly identical to *C. bipanesthiae*, exhibit canonical *C. parapanesthiae* morphology. We thus consider *C. biparapanesthiae*, *C. triparapanesthiae*, and *C. bipanesthiae* junior synonyms of *C. parapanesthiae*.

Clevelandella kidderi matches *C. lynni* very closely in size, shape, and macronuclear morphology. Despite that, the authors of the latter description did not compare the species. Both organisms have the same spade-shaped silhouette and conspicuous left posterior lobe with a distinct notch, a feature not well illustrated but mentioned in the description of *C. kidderi*: ‘... left side

more arched and forms a notch where it joins the peristomial projection' (Mandal and Nair 1974). They also share the same broadly ovoidal macronucleus with a posterior karyophore and a peristomial overture occupying about two-thirds of the length of the peristomial projection. Fixed individuals of *C. kidderi* and *C. lynni* have a similar length (105 vs. 94 μm) and width (52 vs. 46 μm), and the peristomial projection occupies a similar portion of the cell body (33% vs. 34%). Considering these facts, and after examination of the type material deposited by Pecina and Vdačný (2020a), we consider *C. lynni* a junior synonym of *C. kidderi*. The hemicyclia so characteristic of Clevelandellidae, and mentioned by Mandal and Nair (1974), is also present in *C. lynni* but was previously overlooked (Pecina and Vdačný 2020a: figs 2A, E–G, 3A).

Clevelandella nova Pecina and Vdačný, 2022 branches within a well-supported clade of isolates with *C. panesthiae* morphology. The isolates correspond with Kidder's (1937) original description and the clade includes isolates from the type host (PAA) from Philippines as was studied by Kidder (1937). Therefore, the isolates appear to be conspecific with the *C. panesthiae* population of Kidder (1937) and not with the Australian isolates of Lynn and Wright (2013) or the isolates of Pecina and Vdačný (2020b), the latter two having possibly been misidentified as discussed above. In addition, we have studied the morphology of isolate P132PA_PT_VN2 (Fig. 32C) genetically almost identical to *C. nova*, which exhibits typical *C. panesthiae* morphology. Moreover, if the morphology earlier described by Pecina and Vdačný (2020b) for isolates, which were later described as *C. bipanesthiae* (Pecina and Vdačný 2022), truly belongs to *C. nova* (as discussed above), *C. nova* is morphologically indiscernible from our *C. panesthiae* isolates. We thus consider *C. nova* a junior synonym of *C. panesthiae*.

Rhynchoclevelandella trihastula is genetically very similar to *R. nipponensis*. Similarly, *R. bihastula* is genetically very similar to *R. hastula*. But until their morphology is studied, we prefer to retain their current species status.

Comments on recently erected genera in Clevelandellidae

Genus *Anteclevelandella* was described as follows: 'AZM on the left wall and PM on the right wall of vestibulum' (Pecina and Vdačný 2022). This is probably a misinterpretation since, if one accepts the morphologic chirality of Clevelandellidae as depicted by Kidder (1937), Albaret (1975), and Mandal and Nair (1974), all Clevelandellidae have a right-sided adoral zone and a left-sided paroral (with respect to the organism). Neither *Clevelandella constricta* nor any other species deviate from this arrangement (Fig. 19A–D). It also has to be noted that the depiction of the infraciliature of *C. constricta* (Pecina and Vdačný 2020b) showing right-hand spiralling somatic kineties is inconsistent with all previous descriptions (Kidder 1937, Mandal and Nair 1974, Albaret 1975) and the data from the current study (Figs 19D, 20A–D). One possible explanation is inadvertent reversal of images (Fig. 36D; Pecina and Vdačný 2020b: fig. 3F, G) from which drawings appear to have been made (Fig. 36C, E; Pecina and Vdačný 2020b: fig. 1A, M, N); no deposition of voucher material is mentioned in the study, which could help resolve the problem. All Clevelandellidae have left-hand spiralling ventral somatic kineties and straighter (i.e. more or less longitudinal)

dorsal kineties (Albaret 1975, Kidder 1937, Mandal and Nair 1974; this study). We propose a new diagnostic character for the genus: constriction of the cell at the level of the macronucleus.

Genus *Rhynchoclevelandella* was morphologically defined by the absence of a karyophore (Pecina and Vdačný 2022). We, however, show, that its representatives do have a karyophore (Fig. 21K, O, S). We note that, in our experience, the presence or absence of the karyophore (anterior, posterior, or both) is a highly unreliable taxonomic character in Clevelandellidae. This leaves the genus without morphological characterization. Despite this we prefer to consider the genus as valid. This may seem like an inconsistency in light of the numerous species-level synonymizations we made above. However, the species we synonymize are not only morphologically indistinguishable, but also genetically almost identical with already existing species. *Rhynchoclevelandella*, on the other hand, is a distinct phylogenetic lineage. Furthermore, if we did not synonymize these species, many of the current species would become paraphyletic. Conversely, if we synonymize *Rhynchoclevelandella* with *Clevelandella*, then *Clevelandella* would become paraphyletic with respect to *Paraclevelandia*. Although *Rhynchoclevelandella* lacks a recognized morphological apomorphy, at the current state of knowledge, we prefer to retain it.

Purely molecular taxonomy as applied to Clevelandellidae

The abandonment of morphology and its replacement by purely molecular species diagnoses, as done by Pecina and Vdačný (2022), is hampered, at least in the case of clevelandellids, by possible incorrect assignment of genotypes to various morphotypes as discussed in detail above. In the current study, we found that morphological data are highly consistent with the molecular phylogenetic data. The employment of geometrical methods (Pecina and Vdačný 2020b) can be potentially useful if applied to error-less datasets, and also with the addition of more characters than just body shape alone (e.g. macronuclear shape). On the other hand, using purely molecular methods to describe new species in a group for which we know very little about the possible diversity or what the genetic boundaries among species might be or how to apply a barcode-based delimitation approach, seems fraught with difficulties as described above. Perils of such an approach can be best seen on the example of *C. nova*, which we consider a junior synonym of *C. panesthiae*, the type species of the genus.

A number of species have been described by just splitting the existing ones (*Anteclevelandella constricta*, *R. hastula*, and *C. parapanesthiae*), generally making every population a separate species regardless of similar morphology (Pecina and Vdačný 2022). If we adopt this approach, we would have to add approximately 30 species just from the data in the current study, resulting in the disruption of clevelandellid systematics by artefactual species inflation. However, as we were able to find and describe six new morphologically and molecularly distinct species of genus *Clevelandella* by inspecting just a small fraction of host diversity, there is probably a great diversity of clevelandellids yet to be explored and there is no need to erect new species inside already existing ones, especially if such species are diagnosed by just a few nucleotide bases. Ironically, providing DNA barcodes as species diagnoses, or what has been termed the 'minimalist

approach' (Zamani *et al.* 2022), was editorially roundly criticized (Engel *et al.* 2021) in the same journal in which just such an approach to the Clevelandellida was later published (Pecina and Vdačný 2022). This practice has, by no means, been limited to protists and its application in entomology has also been disputed (Zamani *et al.* 2022).

From a conceptual standpoint, providing only molecular sequences, to the exclusion of other characters, as species diagnoses could be considered the antithesis of so-called 'integrative taxonomy'. This integrative approach embraces not only morphologic and molecular characters, but also ecologic, metabolic, and behavioural characters, among others, in the determination of species boundaries (Dayrat 2005, Clamp and Lynn 2017, Vdačný 2017, Dupérré 2020). The practice of diagnosing species solely on the basis of nucleotide substitutions and deposition of DNA extracted from individual cells as holotypes seems to contradict the recommendation that: '...delineation of units of life's diversity needs to be reciprocally illuminated by an integrative approach that takes into account and critically weights both morphological and molecular data' (Vdačný 2017, Pecina and Vdačný 2022). Furthermore, this practice ignores (or rejects) the existence of intraspecies and intragenomic rRNA gene sequence variability (Alverson and Kolnick 2005, Gribble and Anderson 2007, Lindner *et al.* 2013, Weber and Pawlowski 2014, Wang *et al.* 2017).

Shrinkage of protargol-impregnated Clevelandellidae

It is well established that the extent to which preparation changes the size and shape of ciliates varies with species, the fixative used, and staining method applied (Jerome *et al.* 1993). Ciliate cells impregnated by the same protargol method have been estimated to shrink by 20–30% in the case of *Fuscheria terricola* (Berger *et al.* 1983), 10% in the case of *Protospathidium serpens* (Xu and Foissner 2005a), 10–20% for *Arcuospithidium cultriforme* (Xu and Foissner 2005b), and 20–40% for *Dileptus sphagnicola* (Vdačný and Foissner 2012). Recently, a conversion value of 15% has been more frequently chosen (Foissner 2016, Vdačný and Foissner 2017a, b, 2019).

In recent studies of Clevelandellidae, the published *in vivo* cell size was calculated from combined morphometric data of protargol preparations considering 15% preparation shrinkage combined with *in vivo* measurements (Pecina and Vdačný 2020a, b). The difference between dimensions of directly measured live cells and protargol preparations in the current study shows significant and variable deviation from the popular 15% value (Supporting Information, Table S50). While the mean of shrinking for all the species combined is roughly close to constants used in aforementioned studies ($18.6 \pm 7.4\%$ for length, $16.6 \pm 10.9\%$ for width), the high standard deviation indicates there is a striking variability in shrinkage among different species, e.g. change in length from 4.2% in *R. hastula* to 29.2% in the long morph of *C. hromadkai*. Moreover, shrinkage is not necessarily symmetric, the most striking example being *C. elongata* in which length decreases by 22.9%, but its width increases by 12.5% in protargol preparations. Since the advent of affordable and widely available digital imaging, there has been no reason to substitute estimated dimensions for actual direct measurements of live cells. We recommend abandoning the practice of publishing

estimated *in vivo* cell sizes for ciliates, based on *in vivo* measurements mixed with measurements of fixed cells adjusted by arbitrary conversion factors, as numbers obtained in such a way are highly unreliable.

Comparison of newly described species with similar species

All dimensions mentioned are the mean of measurements from protargol preparations, unless indicated otherwise. In the case of multiple populations of one species, the range of means is provided.

Clevelandella ananiasi, *C. philipi*, *C. sidi*, and *C. fryntai* share a similar overall shape (spade-shaped with a conspicuous left-sided notch at the base of the peristomial projection) with *C. parapanesthiae* and *C. kidderi*.

Clevelandella ananiasi can be distinguished from *C. philipi* by: posterior protrusion of left lobe of anterior body part (overhanging no more than one-fifth of peristomial projection vs. overhanging about one-third of peristomial projection), number of adoral membranelles (23 vs. 30 or 32). It can be distinguished from *C. sidi* and *C. fryntai* by length (55 vs. 117 μm and 129 or 158 μm). It can be distinguished from *C. parapanesthiae* by: length (55 vs. 79–90 μm), macronucleus (teardrop-shaped to ellipsoidal vs. scimitar-shaped), and number of adoral membranelles (23 vs. 36–39). It can be distinguished from *C. kidderi* by: length (55 vs. 94 μm) and number of adoral membranelles (23 vs. 48).

Both *C. ananiasi* and *C. philipi* are of similar size as *R. nipponensis*, *Rhynchoclevelandella* sp. 2, and *R. hastula*. However, they can be distinguished from them by different body shape, with *Rhynchoclevelandella* species being more slender (L/W ratio in *C. ananiasi* and *C. philipi* 1.8–1.9 vs. 2.6 in *R. nipponensis*, 2.2 in *Rhynchoclevelandella* sp. 2, and 3.4 in *R. hastula*), outline (right and left margins of anterior body part straight or convex vs. more or less concave), and posterior protrusion of the left lobe of the anterior body part (overhanging vs. not overhanging).

Clevelandella philipi can be distinguished from *C. sidi* by length (63–75 vs. 117 μm). *Clevelandella philipi* can be distinguished from *C. parapanesthiae* by: length (63–75 vs. 79–90 μm), macronucleus (teardrop-shaped to ellipsoidal vs. long scimitar-shaped), and number of adoral membranelles (30–32 vs. about 36–39). *Clevelandella philipi* can be distinguished from *C. kidderi* by: length (63–75 vs. 94 μm), peristomial projection (24–28% vs. 32% of the body), number of adoral membranelles (30–32 vs. about 47), and posterior protrusion of the left lobe of the anterior body part (strongly overhanging vs. slightly overhanging).

Clevelandella sidi can be distinguished from the rest of spade-shaped species by morphology of the paroral (both files equal length vs. right file shorter than left). It can be distinguished from *C. parapanesthiae* by: length (117 vs. 79–90 μm), L/W ratio (2.5 vs. 1.8–1.9), and macronucleus (broad inverted teardrop-shaped vs. scimitar-shaped). It can be distinguished from *C. kidderi* by: length (117 vs. 94 μm) and L/W ratio (2.5 vs. 1.9). It can be distinguished from *C. fryntai* by: length (114 vs. 129–158 μm) and outline (right and left margins of anterior body part straight vs. convex).

Clevelandella fryntai is the largest of the spade-shaped Clevelandellida (see above). *Clevelandella fryntai* can be distinguished from *C. parapanesthiae* by: length (129–158 vs. 79–90 μm), number of adoral membranelles (62–67 vs. 36–39),

and macronucleus (inverted teardrop-shaped to lenticular vs. scimitar-shaped). It can be distinguished from *C. kidderi* by: length (129–158 vs. 94 μm) and number of adoral membranelles (62–67 vs. 46).

Clevelandella hromadkai in short morph can be easily distinguished from all other Clevelandellidae species due to its unique shape and appearance. A long morph of *C. hromadkai* can be distinguished from *C. elongata* by: length (132–155 vs. 220 μm), number of adoral membranelles (58–62 vs. 94), overall shape (broadest in the central third of the cell vs. more worm-like narrow appearance), and posterior protrusion of the left lobe of the anterior body part (present vs. absent).

Clevelandella klobasa can be distinguished from *C. panesthiae* by: length (135 vs. 105–121 μm), macronucleus (sausage-like vs. teardrop-shaped), peristomial projection (inconspicuous vs. conspicuous), adoral zone (markedly curved vs. slightly oblique), and number of adoral membranelles (59 vs. about 45–48).

Genetic variability and host/geographic specificity of Clevelandellidae

The current study samples Clevelandellidae from the broadest range of hosts to date, enabling at least some assessment of intra-specific genetic variability, host specificity, and biogeography. For most species, our isolates from different hosts and/or localities show some degree of genetic variability (Fig. 1). This is in stark contrast with recent publications (Pecina and Vďačný 2020b, 2022) where *Antecelelandella constricta*, *R. hastula*, *C. panesthiae* (referred to under a younger synonym *C. nova*), and *C. parapanesthiae* from different host populations and distant localities are genetically identical. While the current study is primarily based on material obtained directly from wild host populations and bred in controlled cultures at the Department of Zoology of Charles University, the aforementioned works included material exclusively from commercial breeders. It is, however, questionable whether the conditions in commercial cultures were sufficient to prevent contamination by symbionts. Since Clevelandellidae form cysts (Kidder 1937), they can very likely cross-contaminate different host populations when the hosts come into contact with each other's faeces. This may possibly lead to one dominant genotype among contaminated populations originating from different species and locations.

Genus *Rhynchoclevelandella* was, despite extensive host sampling (Pecina and Vďačný 2022; this study), never found in host genus *Salganea*, which is repeatedly retrieved as a sister-lineage to the rest of the Panesthiinae (including Geoscapheinae) (Lo *et al.* 2016, Beasley-Hall *et al.* 2021). Other than that, the host specificity does not seem to be an important factor for the Clevelandellidae symbionts. Although several species have so far been reported from a single host species, this most likely reflects under-sampling. The majority of species can be found in diverse hosts. However, there may be some degree of geographic specificity, both regarding species and intraspecific relationships. The *C. ananiasi*/*C. philipi* clade is so far exclusive to Papua New Guinea (PNG) and *Clevelandella* sp. 3 to Australia. Within *C. panesthiae*, two large clades were identified—one exclusive to PNG and the second comprising the remaining isolates from Vietnam (VN), Thailand (TH), and the Philippines (PH). Similarly, of the three *Rhynchoclevelandella* clades, one is exclusive to Australia, one to

PNG, and one to Asia. Interestingly, the exclusively STH clade of *Antecelelandella constricta* isolates from PNG branches together with a group from various hosts inhabiting other islands—Borneo (NB), Philippines (PH), and Halmahera (HA). A more confident assessment of Clevelandellidae biogeography and host specificity will require even broader sampling and a more robust phylogenetic analysis based on more molecular markers. However, it is possible that in such an evolutionarily young ciliate group with small genetic distances and high potential for spreading of cysts-contaminated faeces, the final picture will be mostly stochastic with the ciliates forming separate lineages not according to the host, but rather according to geographical isolation of a particular locality.

Interestingly it seems that in natural populations different genotypes of a single species can coexist at one locality. We have detected two sister-genotypes of *Antecelelandella constricta* in STH, two genotypes of *Paracelelandia brevis* in STH, two genotypes of *Paracelelandia brevis* in ASS, two sister-genotypes of *C. fryntai* in SRU, and, most interestingly, two distantly related genotypes of *Antecelelandella constricta* in one individual from PAC.

Diversity of Clevelandellidae

Although the family Clevelandellidae was erected more than 80 years ago (Kidder 1937), only two additional species have been described on the basis of the morphology until recently: *Metacelelandella termitis*, and *C. kidderi*. Recent works (using both morphological and molecular methods), excluding the current study, have surprisingly found no new morphologically distinct species (Pecina and Vďačný 2020a, b, 2022). There are two possible (and probably concurrent) reasons:

- (i) Low host diversity: the majority of all studies ever done on Clevelandellidae have dealt with symbionts exclusively from a few representatives of a single host genus *Panesthia* (mostly just subspecies of *Panesthia angustipennis*), which is the most common Panesthiinae in captivity. Although Pecina and Vďačný (2022) tried to explore more diverse hosts by including a few host individuals of the genera *Macropanesthia* and *Salganea*, no new morphologically distinct species were found. The subfamily Panesthiinae, however, comprise at least 169 species in 11 genera.
- (ii) The studies included hosts obtained exclusively from private breeders. It is possible that prolonged captivity of the hosts may have a negative impact on the diversity of symbionts, as mentioned above.

The fact that the same morphospecies of Clevelandellidae were found in hosts from Philippines (Kidder 1937), Japan (Yamasaki 1939), Andaman Islands (Mandal and Nair 1974), Australia (Lynn and Wright 2013, Pecina and Vďačný 2022), and also in Vietnam, Thailand, and Cambodia (Pecina and Vďačný 2020a, b) might give the misimpression that Clevelandellidae have low species diversity. The findings of the current study, however, show the opposite.

While we still chose to use five populations of genus *Panesthia* (PAA, PGW, PAC, PA, and PT), we broadened the sampling of hosts with genera *Ancaudellia* (ASS, AP, and AH), *Miopanesthia*

(MP), and *Salganea* (STH, STR, SRU, and SR). Six new species in genus *Clevelandella* were molecularly and morphologically characterized and one (*Clevelandella* sp. 4) has not yet been completely characterized. Six of them are found only in the newly included hosts. Lynn and Wright (2013) considered all the organisms they have found as identical to species described by Kidder (1937). But when we put their sequences into the context of broader molecular data, we see that they probably include two new species (*Rhynchoclevelandella* sp. 1 and *Clevelandella* sp. 3) with unknown morphology, possibly indigenous to Australia. It is thus anticipated that there is still a considerable diversity of Clevelandellidae to be found by exploring new host genera and populations from isolated localities.

Considerations for future studies

The Clevelandellidae provide a rich diversity of endocommensal ciliates for the study of biogeography, host specificity, ultrastructure, cell physiology, and evolution. Although the current study and previous studies (Pecina and Vďačný 2020a, b, 2022) shed further light on the biogeography and host specificity of Clevelandellidae, more remains to be learned necessitating even broader host sampling (e.g. wider sampling of Geoscapheinae). To date, there has been relatively little ultrastructural study of Clevelandellidae (Albaret 1975). The comparative ultrastructure of features such as the complex internalized ciliated excretory apparatuses of nyctotherids and Clevelandellidae would be of particular interest, especially with the advent of sophisticated techniques such as focused ion beam scanning electron microscopy (Kizilyaprak *et al.* 2014). More detailed morphological data will better inform possible evolutionary scenarios for the evolution of the ‘posteriorized’ Clevelandellidae from a *Nyctotherus*-like ancestor. In terms of cell physiology, the origin and composition of the cytoplasmic carbohydrate platelets and their contribution to cell metabolism require further study. Techniques such as Raman microscopy may provide specific information on the polysaccharide composition of these structures (Smith *et al.* 2016). Transcriptomic methods should provide information on metabolic pathways involved in the formation of these products and of their metabolic role at various stages of the cell cycle, and offer answers to the question, as to whether Clevelandellidae play any role in wood digestion. Such approaches may clarify the relative benefits in the symbiotic relationship of Clevelandellidae and cockroaches: is the relationship actually mutualistic or do Clevelandellidae enjoy a more one-sided benefit from the relationship?

Taxonomic summary

Zoobank registration of the publication: urn:lsid:zoobank.org:pub:58F980CB-B7DE-4877-9BE9-57607B5A1050.

Remark: The voucher material along with inventory numbers is summarized in Supporting Information, Table S51.

Taxonomic assignment: Ciliophora: Intramacronucleata: SAL clade: APM clade: Armophorea: Clevelandellida.

Family Clevelandellidae Kidder, 1938

Diagnosis: Small to large Armophorea with posteriorized oral structures. Adoral zone of membranelles on right and paroral

membrane on left side of peristomium. Somatic ciliature hemitrichous (possibly except in *Metaclevelandella*). Excretion via an internal ciliated excretory antrum.

Type genus: *Clevelandella* Kidder, 1938.

Included genera: *Anteclevelandella* Pecina and Vďačný, 2022; *Clevelandella* Kidder, 1938; *Metaclevelandella* Uttangi and Desai, 1963; *Paraclevelandia* Kidder, 1937; *Rhynchoclevelandella* Pecina and Vďačný, 2022.

Remarks: Although *Metaclevelandella termitis*, not reported since its original description, was described as holotrichously ciliated, the possibility that incomplete ciliation was overlooked (as was the case in Kidder’s descriptions of Clevelandellida) cannot be excluded. This question can only be resolved by a thorough redescription.

Genus *Anteclevelandella* Pecina and Vďačný, 2022

Diagnosis: Body elongate and nearly cylindrical, only slightly flattened dorsoventrally, constricted in the region of macronucleus. Macronucleus evenly ovoid, its long axis parallel to the transverse axis of the body. Peristomial projection inconspicuous, merges gradually with body proper.

Type species:

Clevelandia constricta Kidder, 1937.

Included species:

Anteclevelandella constricta (Kidder, 1937).

Anteclevelandella constricta (Kidder, 1937)

Synonyms: *Emmaninius plantiformis* Yamasaki, 1939; *Clevelandella plantiformis* (Yamasaki, 1939); *Anteclevelandella macropanesthia* Pecina and Vďačný, 2022; *Anteclevelandella salganeae* Pecina and Vďačný, 2022.

Genus *Clevelandella* Kidder, 1938

Amended diagnosis: Body broadly spade-shaped to elongate curved elliptical with posterior peristomial projection.

Type species: *Clevelandia panesthia* Kidder, 1937.

Included species: *Clevelandella ananiasi* sp. nov., *C. elongata* (Kidder, 1937); *C. fryntai* sp. nov.; *C. hromadkai* sp. nov.; *C. panesthia* (Kidder, 1937); *C. parapanesthia* (Kidder, 1937); *C. philipi* sp. nov.; *C. kidderi* Mandal and Nair, 1974; *C. klobasa* sp. nov., *C. sidi* sp. nov.

Clevelandella ananiasi sp. nov.

ZooBank registration: urn:lsid:zoobank.org:act:693D96F5-0E81-4648-BE2B-F5AC52FD31CB.

Diagnosis: Spade-shaped, dorsoventrally flattened *Clevelandella* with average length in protargol preparations 55 µm, mean 23 adoral membranelles, posterior protrusion of left lobe of anterior body part overhanging no more than one-fifth of peristomial projection, and with teardrop-shaped or ellipsoidal macronucleus.

Etymology: Named in honour of Mr Ananias Kamam, our collaborator from Papua New Guinea.

Type locality: Papua New Guinea, Wanang 3, S5.228, E145.080.

Type host: *Ancaudellia serratissima serratissima* (Brunner von Wattenwyl, 1865).

Type material: A protargol-impregnated holotype cell (Fig. 4D, E) marked in a black circle on a slide deposited in the collection of the National Museum of the Czech Republic, Prague, Czech Republic, inventory number P6E 5431.

Clevelandella fryntai sp. nov.

ZooBank registration: urn:lsid:zoobank.org:act:E84B29E8-A18E-44E3-92E3-663958980E9D.

Diagnosis: Spade-shaped, dorsoventrally flattened *Clevelandella* with average length in protargol preparations 143 µm, mean 65 adoral membranelles, and with teardrop-shaped or lenticular macronucleus.

Etymology: Named in honour of eccentric zoologist and ethologist Prof. Daniel Frynta who provided the material.

Type locality: Cambodia, near Mondulkiri province, N12.383, E107.176.

Type host: *Salganea rugulata* Saussure, 1895.

Type material: A protargol-impregnated holotype cell (Fig. 17H–J) marked in a black circle on a slide deposited in the collection of the National Museum of the Czech Republic, Prague, Czech Republic, inventory number P6E 5460.

Clevelandella hromadkai sp. nov.

ZooBank registration: urn:lsid:zoobank.org:act:EB15F99F-FD7D-49F0-9F63-6771F3697429.

Diagnosis: Dorsoventrally not flattened *Clevelandella* of cultriform shape, body proper curved in dorsal direction, with prominent left lobe and peristomial projection merging gradually with body proper. Average length in protargol preparations 127 µm in short form and 215 µm in long form.

Etymology: Named in honour of remarkable Czech cockroach enthusiast Mr Jiří Hromádka.

Type locality: Papua New Guinea, Wanang 3, N5.228, E145.080.

Type host: *Ancaudellia serratissima serratissima* (Brunner von Wattenwyl, 1865).

Type material: A protargol-impregnated holotype cell (Fig. 9D) marked in a black circle on a slide deposited in the collection of the National Museum of the Czech Republic, Prague, Czech Republic, inventory number P6E 5364.

Clevelandella klobasa sp. nov.

ZooBank registration: urn:lsid:zoobank.org:act:CC02115A-273A-43BA-9BCB-4F6783939788.

Diagnosis: Dorsoventrally flattened *Clevelandella*, broadly lanceolate, peristomial projection inconspicuous, peristomial opening broad. Macronucleus sausage-shaped. Average length in protargol preparations 170 µm.

Etymology: The species epithet is from *klobása* (n., feminine gender), the Czech word for sausage, referring to the sausage-shaped macronucleus.

Type locality: Papua New Guinea, Wanang 3, N5.228, E145.080.

Type host: *Salganea ternatensis hirsuta* Roth, 1979.

Type material: A protargol-impregnated holotype cell (Fig. 13D) marked by a black arrow on a slide deposited in the collection of the National Museum of the Czech Republic, Prague, Czech Republic, inventory number P6E 5380.

Clevelandella philipi sp. nov.

ZooBank registration: urn:lsid:zoobank.org:act:72561759-FBB1-4007-AF97-39630E48C436.

Diagnosis: Spade-shaped, dorsoventrally flattened *Clevelandella* with average length in protargol preparations 69 µm, mean 31 adoral membranelles, posterior protrusion of left lobe of anterior body part overhanging up to one-third of peristomial projection, and with teardrop-shaped or ellipsoidal macronucleus.

Etymology: Named in honour of Mr Philip Komong, our collaborator from Papua New Guinea.

Type locality: Papua New Guinea, Wanang 3, N5.228, E145.080.

Type host: *Salganea ternatensis hirsuta* Roth, 1979.

Type material: A protargol-impregnated holotype cell (Fig. 7C, D) marked in a black circle on a slide deposited in the collection of the National Museum of the Czech Republic, Prague, Czech Republic, inventory number P6E 5381.

Clevelandella sidi sp. nov.

ZooBank registration: urn:lsid:zoobank.org:act:312386D2-BE75-45F2-AEE7-E24D28C77719.

Diagnosis: Dorsoventrally flattened *Clevelandella* with average length in protargol preparations 142 µm, mean 52 adoral membranelles, broad, inverted teardrop-shaped macronucleus, and entirely diplostichomonad POM.

Etymology: Named in honour of exceptional terrain entomologist and leader of PNG expedition, Dr Petr 'Sidi' Stiblík.

Type locality: Cambodia, near Mondulkiri NP, N12.383, E107.176.

Type host: *Salganea rugulata* Saussure, 1895.

Type material: A protargol-impregnated holotype cell (Fig. 15C) marked in a black circle on a slide deposited in the collection of the National Museum of the Czech Republic, Prague, Czech Republic, inventory number P6E 5438.

***Clevelandella panesthiae* (Kidder, 1937)**

Synonyms: *Emmaninius papilloris* Yamasaki, 1939; *Clevelandella papilloris* (Yamasaki, 1939); *Clevelandella nova* Pecina and Vďačný, 2022.

***Clevelandella parapanesthiae* (Kidder, 1937)**

Synonyms: *Clevelandella bipanesthiae* Pecina and Vďačný, 2022; *C. biparapanesthiae* Pecina and Vďačný, 2022; *C. triparapanesthiae* Pecina and Vďačný, 2022.

***Clevelandella kidderi* Mandal and Nair, 1974**

Synonym: *Clevelandella lynni* Pecina and Vďačný, 2020

Genus *Paraclevelandia* Kidder, 1937

Diagnosis: As in Kidder (1937).

Type species: *Paraclevelandia brevis* Kidder, 1937.

***Paraclevelandia brevis* Kidder, 1937**

Synonym: *Paraclevelandia simplex* Kidder, 1937.

Genus *Metaclevelandella* Uttangi and Desai, 1963

Diagnosis: As in Uttangi and Desai (1963).

Type species: *Metaclevelandella termitis* Uttangi and Desai, 1963.

Genus *Rhynchoclevelandella* Pecina and Vďačný, 2022

Amended diagnosis: Clevelandellidae with slender, spade-shaped cells (L/W ratio >2), more closely related to *R. hastula* than to *Antelevelandella constricta*, *C. panesthiae*, and *Paraclevelandia brevis*.

Type species: *Clevelandella hastula* Kidder, 1937.

Included species: *Rhynchoclevelandella bihastula* Pecina and Vďačný, 2022; *R. hastula* (Kidder, 1937); *R. nipponensis* (Kidder, 1937) (syn. *Emmaninius longicollis* Yamasaki, 1939; *Clevelandella longicollis* (Yamasaki, 1939); *R. trihastula* Pecina and Vďačný, 2022).

SUPPLEMENTARY DATA

Supplementary data are available at *Zoological Journal of the Linnean Society* online.

ACKNOWLEDGEMENTS

The authors are grateful to the community of Wanang for permission to use their land and Binatang Research Centre for field assistance, in particular Ananias Kamam and Philip Komong; Joselin Marcus E. Fragada (CESO III, DENR 11 Regional Director) and Alma B. Mohagan (Central Mindanao University) for the material collected by Dominik Vondráček under the permit WGP No. XI-2016-13; Jiří Hromádka, who provided material and morphological identification of

Panesthiinae hosts; Daniel Frynta, Dominik Vondráček, Miloš Marek, Pavel Just, Petr Synek, and Petr Šípek, who provided material; Jan Šobotník and Petr Stiblík for help with obtaining the samples on PNG and Michal Vinkler who lent the inverted microscope. We also thank the Viničná Microscopy Core Facility (VMCF of the Faculty of Science, Charles University), a facility supported by MEYS CR (LM2023050 Czech-BioImaging), for their support and assistance with this work, the Oberösterreichisches Landesmuseum, Linz, Austria for making type material available and two anonymous reviewers for the time and effort they selflessly spent to improve our manuscript.

FUNDING

This work was supported by the Grant Agency of the Czech Republic (project 19-19297S), Charles University Grant Agency (project 1158119), and SVV 260686/2023 project of the Charles University.

CREDIT STATEMENT

Michael Kotyk: conceptualization, methodology, formal analysis, investigation, resources, writing—original draft, review and editing, visualization, project administration, funding acquisition. William A. Bourland: methodology, formal analysis, investigation, writing—original draft, review and editing, visualization. M. Soviš: investigation. Daniel Méndez-Sánchez: visualization. P. Škaloud: formal analysis, writing—original draft. Zuzana Kotyková Varadinová: formal analysis, resources, writing—original draft, review and editing. Ivan Čepička: formal analysis, funding acquisition, supervision, writing—original draft, review and editing.

CONFLICT OF INTEREST

None declared.

DATA AVAILABILITY

Sequence data underlying this article are available in GenBank at <https://www.ncbi.nlm.nih.gov/nucleotide/>, accession numbers OQ993372-OQ993504 (Supporting Information, Table S2). Permanent protargol slides are deposited in the collection of the National Museum of the Czech Republic, Prague, Czech Republic <https://www.nm.cz/en> with catalog numbers (Supporting Information, Table S51).

REFERENCES

- Albaret J-L. Etude systématique et cytologique sur les ciliés hétérotriches endocommensaux. *Mémoires du Muséum National d'Histoire Naturelle (Nouvelle Série)* 1975;89:1–114.
- Alverson AJ, Kolnick L. Intragenomic nucleotide polymorphism among small subunit (18S) rDNA paralogs in the diatom genus *Skeletonema* (Bacillariophyta). *Journal of Phycology* 2005;41:1248–57.
- Assunção P, Jaén-Molina R, Caujapé-Castells J *et al.* Molecular taxonomy of *Dunaliella* (Chlorophyceae), with a special focus on *D. salina*: ITS2 sequences revisited with an extensive geographical sampling. *Aquatic Biosystems* 2012;8:2–11.
- Beasley-Hall PG, Rose HA, Walker J *et al.* Digging deep: a revised phylogeny of Australian burrowing cockroaches (Blaberidae: Panesthiinae, Geoscaphaeinae) confirms extensive nonmonophyly and provides insights into biogeography and evolution of burrowing. *Systematic Entomology* 2021;46:767–83.
- Beccaloni GW. *Cockroach Species File Online, version 5.0/5.0*. World Wide Web Electronic Publication, 2014. <http://Cockroach.SpeciesFile.org> (1 March 2023, date last accessed).

- Bell WJ, Roth LM, Nalepa CA. *Cockroaches: Ecology, Behavior, and Natural History*. Baltimore: The Johns Hopkins University Press, 2007.
- Berger H, Foissner W, Adam H. Morphology and morphogenesis of *Fuscheria terricola* n. sp. and *Spathidium muscorum* (Ciliophora: Kinetofragminophora). *The Journal of Protozoology* 1983;**30**:529–35.
- Bottier M, Thomas KA, Dutcher SK et al. How does cilium length affect beating? *Biophysical Journal* 2019;**116**:1292–304.
- Bourland WA, Wendell L. Redescription of *Atopospira galeata* (Kahl, 1927) nov. comb. and *A. violacea* (Kahl, 1926) nov. comb. with redefinition of *Atopospira* Jankowski, 1964 nov. stat. and *Brachonella* Jankowski, 1964 (Ciliophora, Armophorida). *European Journal of Protistology* 2014;**50**:356–72.
- Bourland W, Rotterová J, Čepička I. Redescription and molecular phylogeny of the type species for two main metopid genera, *Metopus es* (Müller, 1776) Lauterborn, 1916 and *Brachonella contorta* (Levander, 1894) Jankowski, 1964 (Metopida, Ciliophora), based on broad geographic sampling. *European Journal of Protistology* 2017a;**59**:133–54.
- Bourland W, Rotterová J, Čepička I. Morphologic and molecular characterization of seven species of the remarkably diverse and widely distributed metopid genus *Urostomides* Jankowski, 1964 (Armophorea, Ciliophora). *European Journal of Protistology* 2017b;**61**:194–232.
- Bourland W, Rotterová J, Luo X et al. The little-known freshwater metopid ciliate, *Idiometopus turbo* (Dragesco and Dragesco-Kernéis, 1986) nov gen, nov comb, originally discovered in Africa, found on the Micronesian island of Guam. *Protist* 2018;**169**:494–506.
- Bourland W, Rotterová J, Čepička I. Description of three new genera of Metopidae (Metopida, Ciliophora): *Pileometopus* gen. nov., *Castula* gen. nov., and *Longitaenia* gen nov, with notes on the phylogeny and cryptic diversity of metopid ciliates. *Protist* 2020;**171**:125740.
- Brune A. Symbiotic digestion of lignocellulose in termite guts. *Nature Reviews Microbiology* 2014;**12**:168–80.
- Caisová L, Marin B, Melkonian M. A close-up view on ITS2 evolution and speciation—a case study in the Ulvophyceae (Chlorophyta, Viridiplantae). *BMC Evolutionary Biology* 2011;**11**:1–24.
- Caisová L, Marin B, Melkonian M. A consensus secondary structure of ITS2 in the Chlorophyta identified by phylogenetic reconstruction. *Protist* 2013;**164**:482–96.
- Čepička I, Hampl V, Kulda J. Critical taxonomic revision of parabasalids with description of one new genus and three new species. *Protist* 2010;**161**:400–33.
- Chatton E, Lwoff A. La constitution primitive de la strie ciliaire des infusoires La desmodexie. *Comptes Rendus Biologies et Science* 1935;**118**:1086–172.
- Chouvenec T, Šobotník J, Engel MS et al. Termite evolution: mutualistic associations, key innovations, and the rise of Termitidae. *Cellular and Molecular Life Sciences: CMLS* 2021;**78**:2749–69.
- Clamp JC, Lynn DH. Investigating the biodiversity of ciliates in the 'Age of Integration'. *European Journal of Protistology* 2017;**61**:314–22.
- Cochran DG. *Cockroaches: Their Biology, Distribution and Control*. Geneva: World Health Organization, 1999.
- Coleman AW. The significance of a coincidence between evolutionary landmarks found in mating affinity and a DNA sequence. *Protist* 2000;**151**:1–9.
- Coleman AW. *Paramecium aurelia* revisited. *The Journal of Eukaryotic Microbiology* 2005;**52**:68–77.
- Darriba D, Posada D, Kozlov AM et al. ModelTest-NG: a new and scalable tool for the selection of DNA and protein evolutionary models. *Molecular Biology and Evolution* 2020;**37**:291–4.
- Dayrat B. Towards integrative taxonomy. *Biological Journal of the Linnean Society* 2005;**85**:407–15.
- Djernæs M, Kotyková Varadinová Z, Kotyk M et al. Phylogeny and life history evolution of Blaberoidea (Blattodea). *Arthropod Systematics & Phylogeny* 2020;**78**:29–67.
- Dobell C, Laidlaw P. On the cultivation of *Entamoeba histolytica* and some other entozoic amoebae. *Parasitology* 1926;**18**:283–318.
- Dupérré N. Old and new challenges in taxonomy: what are taxonomists up against? *Megataxa* 2020;**1**:59–62.
- Engel MS, Ceriaco LM, Daniel GM et al. The taxonomic impediment: a shortage of taxonomists, not the lack of technical approaches. *Zoological Journal of the Linnean Society* 2021;**193**:381–7.
- Evangelista DA, Wipfler B, Béthoux O et al. An integrative phylogenomic approach illuminates the evolutionary history of cockroaches and termites (Blattodea). *Proceedings Biological Sciences* 2019;**286**:20182076.
- Foissner W. An update of 'basic light and scanning electron microscopic methods for taxonomic studies of ciliated protozoa'. *International Journal of Systematics and Evolutionary Microbiology* 2014;**64**:271–92.
- Foissner W. Protists as bioindicators in activated sludge: identification, ecology and future needs. *European Journal of Protistology* 2016;**55**:75–94.
- Foissner W, Xu K. Monograph of the Spathidiida (Ciliophora, Haptoria): Vol I: Protospathidiidae, Arcuospathidiidae, Apertospathulidae. *Monographiae Biologicae* 2007;**81**:1–485.
- Geiman QM, Wichterman R. Intestinal protozoa from Galapagos tortoises (with descriptions of three new species). *The Journal of Parasitology* 1937;**23**:331–47.
- Gore JC, Schal C. Expression, production and excretion of Bla g 1, a major human allergen, in relation to food intake in the German cockroach, *Blattella germanica*. *Medical and Veterinary Entomology* 2005;**19**:127–34.
- Govorushko S. Economic and ecological importance of termites: a global review. *Entomological Science* 2019;**22**:21–35.
- Grain J. Cinétosome, cil, systèmes fibrillaires en relation avec le cinétosome. In: Grassé P-P (ed.), *Traité de Zoologie, Anatomie, Systématique, Biologie, Tome II, Fascicule 1*. Paris: Masson, 1984, 35–179.
- Gribble KE, Anderson DM. High intraindividual, intraspecific, and interspecific variability in large-subunit ribosomal DNA in the heterotrophic dinoflagellates *Protoperidinium*, *Diplopsalis*, and *Preperidinium* (Dinophyceae). *Phycologia* 2007;**46**:315–24.
- Hall TA. BioEdit: a user-friendly biological sequence alignment editor and analysis program for Windows 95/98/NT. *Nucleic Acids Symposium Series* 1999;**41**:95–8.
- Hoyte HMD. The protozoa occurring in the hind-gut of cockroaches. II. Morphology of *Nyctotherus ovalis*. *Parasitology* 1961;**51**:437–63.
- Jankowski A. Phylum Ciliophora Doflein, 1901. In: Alimov AF (ed.), *Handbook on Zoology, Protista. Part 2*. St. Petersburg: Russian Academy of Sciences, Zoological Institute, 2007, 415–993.
- Jerome CA, Montagnes DJS, Taylor FJR. The effect of the quantitative protargol stain and Lugol's and Bouin's fixatives on cell size: a more accurate estimate of ciliate species biomass. *Journal of Eukaryotic Microbiology* 1993;**40**:254–9.
- Josse J, Husson F. missMDA: a package for handling missing values in multivariate data analysis. *Journal of Statistical Software* 2016;**70**:1–31.
- Katoh K, Standley DM. MAFFT Multiple sequence alignment software version 7: improvements in performance and usability. *Molecular Biology and Evolution* 2013;**30**:772–80.
- Katoh K, Misawa K, Kuma K et al. MAFFT: a novel method for rapid multiple sequence alignment based on fast Fourier transform. *Nucleic Acids Research* 2002;**30**:3059–66.
- Kidder GW. The intestinal protozoa of the wood-feeding roach *Panesthia*. *Parasitology* 1937;**29**:163–205.
- Kidder GW. Nuclear reorganization without cell division in *Paraclevelandia simplex* (family Clevelandellidae), an endocommensal ciliate of the woodfeeding roach *Panesthia*. *Archiv für Protistenkunde* 1938;**91**:69–77.
- Kizilyaprak C, Daraspe J, Humbel BM. Focused ion beam scanning electron microscopy in biology. *Journal of Microscopy* 2014;**254**:109–14.
- Kozlov AM, Darriba D, Flouri T et al. RAXML-NG: a fast, scalable and user-friendly tool for maximum likelihood phylogenetic inference. *Bioinformatics* 2019;**35**:4453–5.
- Li C, Zhao W, Zhang D et al. *Sicuophora* (syn. *Wichtermania*) *multigranularis* from *Quasipaa spinosa* (Anura): morphological and molecular study, with emphasis on validity of *Sicuophora* (Armophorea, Clevelandellida). *Parasite* 2018;**25**:38.
- Lindner DL, Carlsen T, Henrik Nilsson R et al. Employing 454 amplicon pyrosequencing to reveal intragenomic divergence in the internal transcribed spacer rDNA region in fungi. *Ecology and Evolution* 2013;**3**:1751–64.
- Lo N, Tong KJ, Rose HA et al. Multiple evolutionary origins of Australian soil-burrowing cockroaches driven by climate change in the Neogene. *Proceedings Biological Sciences* 2016;**283**:20152869.

- Lynn DH. *Woodruffia metabolica*: exception to the rule of desmodexy questioned. *Science* 1975;**188**:1040–1.
- Lynn DH. *The Ciliated Protozoa: Characterization, Classification, and Guide to the Literature*. Dordrecht: Springer, 2008.
- Lynn DH, Wright ADG. Biodiversity and molecular phylogeny of Australian *Clevelandella* species (Class Armophorea, Order Clevelandellida, Family Clevelandellidae), intestinal endosymbiotic ciliates in the wood-feeding roach *Panesthia cribrata* Saussure, 1864. *Journal of Eukaryotic Microbiology* 2013;**60**:335–41.
- Mandal AK, Nair KN. *Clevelandella kidderi* sp. n. (Clevelandellidae) new heterotrichous ciliate from wood-feeding roach (*Panesthia* sp) of Andaman Islands, India. *Acta Protozoologica* 1974;**12**:351–4.
- McKean G. A study of the ciliated protozoan *Nyctotherus ovalis*. Morphology: general and ultrastructural, life cycle: anisogamonty and division. D.Phil. Thesis, Ann Arbor, Michigan: University of Illinois at Urbana-Champaign, 1972.
- Medlin L, Elwood HJ, Stickel S *et al.* The characterization of enzymatically amplified eukaryotic 16S-like rRNA-coding regions. *Gene* 1988;**71**:491–9.
- Miao M, Warren A, Song W *et al.* Analysis of the internal transcribed spacer 2 (ITS2) region of scuticociliates and related taxa (Ciliophora, Oligohymenophorea) to infer their evolution and phylogeny. *Protist* 2008;**159**:519–33.
- Miller MA, Pfeiffer W, Schwartz T. 'Creating the CIPRES Science Gateway for inference of large phylogenetic trees'. In: *Proceedings of the Gateway Computing Environments Workshop (GCE), New Orleans, LA, 14 Nov. 2010*, pp. 1–8, 2010.
- Noda S, Kitade O, Inoue T *et al.* Cospeciation in the triplex symbiosis of termite gut protists (*Pseudotrichonympha* spp), their hosts, and their bacterial endosymbionts. *Molecular Ecology* 2007;**16**:1257–66.
- Oksanen J, Blanchet FG, Friendly M *et al.* *vegan: Community Ecology Package. R Package, version 2.5-7*, 2020. <https://CRAN.R-project.org/package=vegan>
- Patterson DJ. Contractile vacuoles and associated structures: their organization and function. *Biological Reviews* 1980;**55**:1–46.
- Pawlowski J. Introduction to the molecular systematics of foraminifera. *Micropaleontology* 2000;**46**:1–12.
- Pecina L, Vďačný P. Two new endozoic ciliates, *Clevelandella lynni* sp. n. and *Nyctotherus galerus* sp. n., isolated from the hindgut of the wood-feeding cockroach *Panesthia angustipennis* (Illiger, 1801). *Journal of Eukaryotic Microbiology* 2020a;**67**:436–49.
- Pecina L, Vďačný P. Morphological versus molecular delimitation of ciliate species: a case study of the family Clevelandellidae (Protista, Ciliophora, Armophorea). *European Journal of Taxonomy* 2020b;**697**:1–46.
- Pecina L, Vďačný P. DNA barcoding and coalescent-based delimitation of endosymbiotic clevelandellid ciliates (Ciliophora: Clevelandellida): a shift to molecular taxonomy in the inventory of ciliate diversity in panesthiine cockroaches. *Zoological Journal of the Linnean Society* 2022;**194**:1072–102.
- de Puytorac P, Grain J. Ultrastructure du cortex buccal et évolution chez les ciliés. *Protistologica* 1976;**12**:49–67.
- R Core Team. *R: A Language and Environment for Statistical Computing*. Vienna, Austria: R Foundation for Statistical Computing, 2023. <https://www.R-project.org> (20 October 2023, date last accessed).
- Ralton JE, Sernee MF, McConville MJ. Evolution and function of carbohydrate reserve biosynthesis in parasitic protists. *Trends in Parasitology* 2021;**37**:988–1001.
- Rotterová J, Bourland V, Čepička I. Tropidoactrididae fam nov, a deep branching lineage of Metopida (Armophorea, Ciliophora) found in diverse habitats and possessing prokaryotic symbionts. *Protist* 2018;**169**:362–405.
- Satir P, Sleight MA. The physiology of cilia and mucociliary interactions. *Annual Review of Physiology* 1990;**52**:137–55.
- Scrivener AM, Slaytor M, Rose HA. Symbiont-independent digestion of cellulose and starch in *Panesthia cribrata* Saussure, an Australian wood-eating cockroach. *Journal of Insect Physiology* 1989;**35**:935–41.
- da Silva-Neto ID, da Silva Paiva T, do Nascimento Borges B *et al.* Fine structure and molecular phylogeny of *Parametopidium circumlabens* (Ciliophora: Armophorea), endocommensal of sea urchins. *Journal of Eukaryotic Microbiology* 2016;**63**:46–61.
- Škaloud P, Rindi F. Ecological differentiation of cryptic species within an asexual protist morphospecies: a case study of filamentous green alga *Klebsormidium* (Streptophyta). *The Journal of Eukaryotic Microbiology* 2013;**60**:350–62.
- Slaytor M. Cellulose digestion in termites and cockroaches: what role do symbionts play? *Comparative Biochemistry and Physiology Part B: Comparative Biochemistry* 1992;**103**:775–84.
- Smith R, Wright KL, Ashton L. Raman spectroscopy: an evolving technique for live cell studies. *Analyst* 2016;**141**:3590–600.
- Taerum SJ, De Martini F, Liebig J *et al.* Incomplete co-cladogenesis between *Zootermopsis* termites and their associated protists. *Environmental Entomology* 2018;**47**:184–95.
- Takahashi E, Imai S. Light and scanning electron microscopy of *Nyctotherus kyphodes* (Ciliophora, Plagiotomidae) from the Galapagos giant tortoise, *Testudo* sp. *Bulletin of the Nippon Veterinary & Zootechnical College* 1989;**38**:9–15.
- Tuffrau M, Fleury A. Classe des Hypotriches Stein, 1859. In: De Puytorac P (ed.), *Traité de Zoologie. Anatomie, Systématique, Biologie, Tome II. Infusaires Ciliés, Fasc. 2 Systématique, Masson, Paris*. Paris: Masson, 1994, 83–151.
- Uttangi J, Desai R. *Metaclevelandella termitis*, a new genus and species of Heterotrichous ciliate (family Clevelandellidae) found in the Indian termite *Capritermes incola* Wasm. *Parasitology* 1963;**53**:39–43.
- Varadinová Z, Frynta D, Aulický R *et al.* Detection of cockroach faeces: consumption of fluorescent bait and production of UV-light-detectable faeces from German cockroach, *Blattella germanica*. *Entomologia Experimentalis et Applicata* 2015;**155**:167–75.
- Vďačný P. Integrative taxonomy of ciliates: assessment of molecular phylogenetic content and morphological homology testing. *European Journal of Protistology* 2017;**61**:388–98.
- Vďačný P, Foissner W. Monograph of the dileptids (Protista, Ciliophora, Rhynchostomatia). *Denisia* 2012;**31**:1–529.
- Vďačný P, Foissner W. A huge diversity of metopids (Ciliophora, Armophorea) in soil from the Murray River floodplain, Australia. I. Description of five new species and redescription of *Metopus setosus* Kahl, 1927. *European Journal of Protistology* 2017a;**58**:35–76.
- Vďačný P, Foissner W. A huge diversity of metopids (Ciliophora, Armophorea) in soil from the Murray River floodplain, Australia. II. Morphology and morphogenesis of *Lepidometopus platycephalus* nov gen, nov spec. *Acta Protozoologica* 2017b;**56**:39–57.
- Vďačný P, Foissner W. A huge diversity of metopids (Ciliophora, Armophorea) in soil from the Murray River floodplain, Australia. III. Morphology, ontogenesis and conjugation of *Metopus boletus* nov spec, with implications for the phylogeny of the SAL supercluster. *European Journal of Protistology* 2019;**69**:117–37.
- Venables WN, Ripley BD. *Modern Applied Statistics with S*, 4th edn. New York: Springer, 2022.
- Wang C, Zhang T, Wang Y *et al.* Disentangling sources of variation in SSU rDNA sequences from single cell analyses of ciliates: impact of copy number variation and experimental error. *Proceedings Biological Sciences* 2017;**284**:20170425.
- Warren DL, Geneva AJ, Lanfear R. RWTY (R We There Yet): an R package for examining convergence of Bayesian phylogenetic analyses. *Molecular Biology and Evolution* 2017;**34**:1016–20.
- Weber AA-T, Pawlowski J. Wide occurrence of SSU rDNA intragenomic polymorphism in foraminifera and its implications for molecular species identification. *Protist* 2014;**165**:645–61.
- Xu K, Foissner W. Descriptions of *Protospathidium serpens* (Kahl, 1930) and *P. fraterculum* n sp (Ciliophora, Haptoria), two species based on different resting cyst morphology. *The Journal of Eukaryotic Microbiology* 2005a;**52**:298–309.
- Xu K, Foissner W. Morphology, ontogenesis and encystment of a soil ciliate (Ciliophora, Haptorida), *Arcuospathidium cultrifforme* (Penard, 1922), with models for the formation of the oral bulge, the ciliary patterns, and the evolution of the spathidiids. *Protistology* 2005b;**4**:5–55.
- Yamasaki M. On some new ciliates living in the hind-gut of the roach *Panesthia angustipennis* Illiger. *Annotationes Zoologicae Japonenses* 1939;**18**:65–74.
- Zamani A, Fric ZF, Gante HF *et al.* DNA barcodes on their own are not enough to describe a species. *Systematic Entomology* 2022;**47**:385–9.